



Thèse de privat-docent

2020

Open Access

This version of the publication is provided by the author(s) and made available in accordance with the copyright holder(s).

---

## Pathogenesis of ovarian cancer

---

Labidi-Galy, Sana Intidhar

### How to cite

LABIDI-GALY, Sana Intidhar. Pathogenesis of ovarian cancer. 2020. doi: 10.13097/archive-ouverte/unige:136866

This publication URL: <https://archive-ouverte.unige.ch//unige:136866>

Publication DOI: [10.13097/archive-ouverte/unige:136866](https://doi.org/10.13097/archive-ouverte/unige:136866)



**UNIVERSITÉ  
DE GENÈVE**

**FACULTÉ DE MÉDECINE**

**Clinical medicine section**

Departement of medicine

---

## **"PATHOGENESIS OF OVARIAN CANCER"**

Thesis submitted to the Faculty of medicine of the  
University of Geneva

For the degree of Privat-Doctent

By Dr Sana Intidhar LABIDI-GALY

---

*Genève*

*2019*

## Summary

Epithelial ovarian cancer (EOC) is a heterogeneous disease with five histotypes: serous (high-grade and low-grade), endometrioid, clear cell and mucinous carcinomas. New evidences suggest that the majority of EOC are of extra-ovarian origin. We used next-generation sequencing to investigate the cell of origin of high-grade serous ovarian carcinomas (HGSOC) and mucinous ovarian carcinomas (MOC). We analyzed exome-wide sequence and structural analyses of multiple tumor samples from five individuals with advanced stage sporadic HGSOC. Our results suggest that ovarian cancer is a disease of the fallopian tubes, with the development of p53 signatures and serous tubal intraepithelial carcinoma as early events. The subsequent formation of a cancer in the ovaries represents a seeding event from a primary tumor in the fallopian tube that already contains sequence and structural alterations in key driver genes, including *TP53*, PI3K pathway, and *BRCA1/BRCA2* genes. Our work could have implication for screening and early diagnosis of HGSOC. In a separate work, we used unsupervised clustering of gene-expression profile of different histotype of ovarian tumors, their eutopic tissues (ovarian surface epithelium and fallopian tube) and single-cell RNA-sequencing of primordial germ cells (PGCs). We observed that mucinous ovarian tumors (borderline and carcinoma) cluster more closely to PGCs than their eutopic tissue of origin. Our work brings a new and plausible explanation of the clinical and epidemiologic characteristics of MOC and could help into developing new target therapies for this rare and chemoresistant tumor.

# Table of content

<b>Introduction</b> .....	4
<b>I. New understanding of the origin of epithelial ovarian carcinoma</b> .....	4
<b>II. The dualistic pathway</b> .....	5
<b>III. Cells of origin of ovarian carcinomas</b> .....	6
<b>III. A High-grade serous ovarian carcinoma</b> .....	6
<b>III. B Low-grade serous ovarian carcinoma</b> .....	8
<b>III. C Endometrioid and clear cell carcinoma</b> .....	9
<b>III. D Mucinous ovarian carcinoma</b> .....	9
<b>IV. Hypotheses of pathogenesis</b> .....	11
<b>IV. A. Incessant ovulation hypothesis</b> .....	11
<b>IV. B. Gonadotropin hypothesis</b> .....	13
<b>IV. C. Incessant menstruation hypothesis</b> .....	15
<b>Results</b> .....	18
<b>Article 1: High-grade serous ovarian carcinoma originate in the fallopian tube</b> .....	19
<b>Article 2: Primordial germ cells as a potential cell of origin for mucinous cystic neoplasms of the pancreas and mucinous ovarian tumors</b> .....	20
<b>Article 3: Dépistage du cancer de l’ovaire: ce n’est pas pour demain</b> .....	21
<b>Conclusions and perspectives</b> .....	22
<b>I. Implications of the fallopian tube as cell of origin of HGSOC</b> .....	22
<b>I.A Screening and early diagnosis</b> .....	23
<b>I.B Surgical prevention in high-risk women</b> .....	24
<b>II. Implications of PGCs as cell of origin of MOC</b> .....	25

## Introduction

Ovarian cancer is the leading cause of death from gynecological cancer, yet the physiopathology underlying epithelial ovarian carcinomas (EOC) is only partly understood. EOC are a highly heterogeneous group of diseases that include different histotypes with distinct clinicopathological and molecular features. Several hypotheses have been proposed for the pathogenesis of EOC, based on different etiopathological models: incessant ovulation (1, 2), incessant menstruation (3) and gonadotropins (4). Each of these theories has compelling evidence in their favor but has failed so far to provide a unified explanation. New evidences suggest that the majority of EOC are of extra-ovarian origin with high grade serous ovarian carcinomas originating from the fallopian tube epithelium (FTE) whereas clear cell and endometrioid carcinomas are related to endometriosis and mucinous ovarian carcinomas could originate from germ cells. Through a comprehensive review of the literature that integrates epidemiologic, histologic and molecular data, we review the pathophysiologic models of initiation and progression of EOC and discuss the results of two articles that we recently published where we used next-generation sequencing to investigate the cell of origin of high-grade serous ovarian carcinomas and mucinous ovarian carcinomas.

### I. New understanding of the origin of epithelial ovarian carcinoma

Ovarian cancer comprises a large array of histologic, biological and genetic features, and is usually divided into three groups: epithelial malignancies (EOC), which represent the most common type (90%), stromal tumors and germ cell tumors. EOC can be further subdivided into five major histotypes: serous (high-grade and low-grade), endometrioid, clear cell and mucinous carcinomas. The cell of origin of EOC has been controversial and the former paradigm was that EOC arise from the ovarian surface epithelium (OSE). OSE is composed of nondescript cells more closely resembling the mesothelium lining the peritoneal cavity with which it is continuous. As EOC has different histologic subtypes, it has been thought that OSE undergoes a process termed “metaplasia” and differentiate into different histotypes. However, clinicopathological and molecular studies have failed to support this hypothesis of OSE as the origin of all EOC, and rather provided new evidence that the majority of ovarian carcinomas arises from Müllerian-derived epithelial cells outside the ovary. Insights into the pathogenesis of HGSOC have emerged from investigating the prevalence of occult ovarian and fallopian tube carcinomas in women carrying germline mutations of *BRCA* genes (5-9). Potential precursor lesions of HGSOC, a *TP53* mutant single-cell epithelial layer (p53 signature) and serous tubal intraepithelial carcinoma (STIC) were identified in the fimbriae of the fallopian tubes (FT) removed as part of prophylactic surgery in *BRCA* carriers (5). Similar lesions were not detected in the ovary. STICs were consistently observed in the FT of the majority of patients

with advanced stage sporadic HGSOC (10-12) and harbor identical mutations of *TP53*. We recently reported whole exome-sequence and copy number analyses of microdissected paired samples of fallopian tube lesions (p53 signatures and STICs) and HGSOC in order to investigate the clonal relationship between fallopian and ovarian lesions. We showed through an evolutionary analysis that p53 signatures and STICs were the precursors of ovarian carcinomas which in turn gave rise to metastatic lesions (13).

Low-grade serous carcinomas have a distinct pathogenesis from HGSOC. They develop from serous borderline tumors, which may in turn develop from tubal epithelium shed from “papillary tubal hyperplasia” or tubal epithelium that had previously formed an ovarian cortical inclusion cyst or a cystadenoma (14). Ovarian endometrioid and clear cell carcinomas are likely to arise from ectopic endometrium implanted on the ovary (endometrioma) (15, 16). Clear cell carcinomas (CCOC) and contiguous atypical endometriosis had identical mutations of *ARID1A*, a tumor suppressor gene mutated in 50% of CCOC (15, 17), strongly suggesting a clonal relationship (15). For the rarest EOC, i.e mucinous ovarian carcinomas (MOC), the cell of origin is not clear. They are very likely to evolve in stepwise fashion from benign tumors (cystadenoma) to a preinvasive lesion (borderline) to carcinoma (18). Using unsupervised clustering of gene-expression profile of MOC and single-cell RNA-sequencing of primordial germ cells (PGCs), we recently showed that MOC are closer to PGCs than the eutopic tubal or ovarian surface epithelium (19).

Overall, it appears that the majority of EOC develop from implanted tumor precursors imported from either the fallopian tube or the endometrium rather than the OSE. If the hypothesis of extra-ovarian origin of “ovarian” cancer is validated, the true primary ovarian neoplasms, analogous to testicular neoplasms, should mainly include mucinous ovarian carcinomas and germ cell/ gonadal stromal tumors and represent no more than 15% of ovarian cancers. Of course, this model needs to be confirmed by several critical experiments. Nevertheless, the new paradigm of the extraovarian origin of EOC will have significant implications for clinical management and research.

## **II. The dualistic pathway**

A two-tier classification system has now been proposed for EOC (20-22). Such dualistic model of tumorigenesis, although not practically applicable to diagnosis, is useful for appreciating the pathogenesis of ovarian carcinomas in the light of recent availability of genome-wide analysis (17, 23-26). Type I represents approximately 25% of EOC and include low-grade serous, low-grade endometrioid, clear cell and mucinous carcinomas. Patients with type I EOC usually present an early stage, assume an indolent course and are responsible for a small proportion of ovarian cancer related deaths. Molecularly, these tumors tend to be chromosomally stable

and *TP53* mutations are unfrequent (17, 23, 25-27). In the case of low-grade serous and mucinous carcinomas, they are suggested to arise from the corresponding cystadenoma, often through a borderline (low malignant potential) tumor, supporting the classical paradigm of stepwise morphologic progression during tumorigenesis (28). Tumor progression of low-grade serous and mucinous carcinomas is characterized by sequence mutations in *KRAS*, *BRAF* and/or amplification of *ERBB2* oncogenes (24), resulting in constitutive activation of the MAPKinase pathway (29). Endometrioid and clear cell carcinomas originate from ovarian endometrioma (29). Common molecular alterations are frequent inactivating mutations of *ARID1A*, a tumor suppressor gene involved in chromatin remodeling and mutations of genes encoding components of the Wnt signaling pathway (*CTNNB1*, *PTEN* and *PIK3CA*).

Approximately 75% of EOC belong to the type II group, which is comprised of high-grade serous, carcinosarcoma (malignant Müllerian mixed tumors), high-grade endometrioid, and undifferentiated carcinomas. As compared to type I, type II EOC is highly aggressive, metastasize early, tend to present at advanced stages and contribute to 90% of EOC related deaths. HGSOC account for the majority of type II tumors. Molecularly, HGSOC show marked chromosomal disruption with remarkable genome-wide DNA copy number alterations and *TP53* mutations in virtually all cases (24). Germline mutations of *BRCA1/BRCA2* genes occur in up to 20% of HGSOC (30) and are accompanied by systematic somatic loss of the wild-type allele (loss of heterozygosity: LOH) (24, 31). Pathway analyses suggested that homologous recombination is defective in about half of the tumors. These observations paved the way for the development of PARP inhibitors as maintenance therapy in platinum-sensitive HGSOC, irrespective of *BRCA* status (32, 33). It appeared that platinum-sensitive was a sort of “*in vivo* functional test” for homologous recombination defects and the best predictor for response to PARP inhibitors (34).

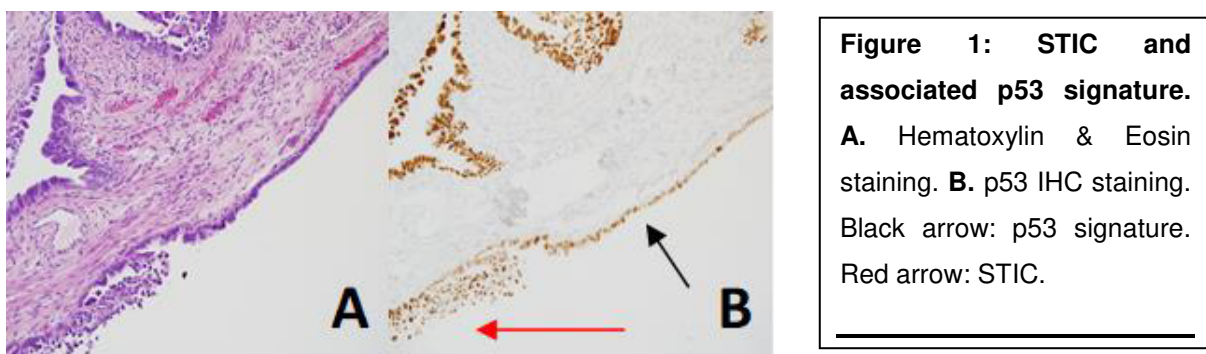
### **III. Cells of origin of ovarian carcinomas**

#### **III. A High-grade serous ovarian carcinoma**

HGSOC is the most frequent histotype of EOC, representing 70% of the cases. Until recently, the prevailing view of the origin of HGSOC was that it derived from OSE or cortical inclusion cysts which develop from OSE. The search for the cell of origin of HGSOC took a turn following the discovery of *BRCA1* and *BRCA2* as the genes predominantly responsible for high-risk (or hereditary) breast and ovarian cancer syndromes (35, 36). *BRCA* carriers have increased lifetime of 40-60% (*BRCA1*) and 11-27% (*BRCA2*) risk for EOC (37). Shortly after the discovery of *BRCA1/2* genes, salpingo-oophorectomy became standard practice for ovarian cancer risk reduction in *BRCA* mutation carriers (10).

---

The finding of dysplastic changes and early invasive cancers that resemble HGSOE within the fimbria of *BRCA* carriers, plus the failure to identify similar changes in OSE of such individuals, led to the realization that the fallopian tube could be the cell of origin of HGSOE in *BRCA* carriers (8, 9). The fimbria are in constant close proximity to ovarian surface. They literally rub against this surface at ovulation and can easily intermix with the coelomic epithelium as a result of tubo-ovarian adhesions (38). Based on the findings of occult early serous carcinoma in the fimbriae of fallopian tubes, Piek et al. proposed that occult tubal carcinomas might shed malignant cells that then implant and grow on the ovary, simulating primary ovarian cancer (8). A protocol for close examination of the fallopian tubes was developed, termed Sectioning and Extensive Examining of the FIMbria (SEE-FIM) (9). The first clearly defined step in the morphologic continuum of benign tubal transformation is "p53 signature," characterized by stretches of benign-appearing secretory cells that exhibit evidence of DNA damage, *TP53* mutations, and concomitant p53 protein stabilization (9). A p53 signature is defined as a discrete population of at least 12 secretory cells with intense nuclear p53 staining. They are most often found in the distal fallopian tube (9, 39). The frequency of p53 signatures in *BRCA* women is similar to that in normal controls. The next recognizable step is Serous Tubal Intraepithelial Carcinoma (STIC) (Figure 1). STICs are characterized by a multilayered epithelium that lacks polarity and are composed of malignant secretory cells with evidence of DNA damage and p53 protein stabilization as well as high proliferative index (5, 10, 40). STICs are characterized by a high nuclear-to cytoplasmic ratio, pleomorphism, hyperchromasia, a lack of ciliated cells, with or without epithelial stratification, and occasional mitotic figures (5). More than 90% of STICs harbor *TP53* mutations and their p53-staining patterns are compatible with *TP53* mutations. The most common mutations are missense and splice/frameshift mutations, but nonsense mutations also occur. Strong, diffuse staining correlates with a missense mutation, whereas complete absence of staining correlates with nonsense mutations (41, 42).



The emergence of STIC as potential precursor of HGSOE led to systematic and extensive analyses of the fimbriae of women undergoing debulking surgery for sporadic HGSOE and



resulted into identifying STIC lesions in more than half of the cases (11, 43). Laser-capture microdissection studies of STICs and concordant HGSOCS involving the ovary have shown that 92% of STICs harbor identical *TP53* mutations with the associated ovarian carcinomas (41). These results suggest a clonal relationship but do not exclude the possibility of fallopian tube lesions being metastases from primary ovarian carcinomas (42, 44). The temporal correlation between transformation and seeding to the ovary was largely unknown. Our genomic analysis of paired samples of STICs and HGSOCS revealed systematic LOH of *BRCA1*, *BRCA2* and *TP53*, and frequent LOH of *PTEN*, in addition to somatic mutations of these genes (13). These observations suggest that a combination of sequence changes in a few genes including *TP53* together with loss of the *TP53* wild-type allele as well as *BRCA1*, *BRCA2*, and *PTEN* are crucial early events needed for the initiation of STIC in *BRCA* carriers and sporadic HGSOCS (10).

In the last two decades, the shift of paradigm for the tissue of origin of HGSOCS revolutionizes the fundamental concepts of ovarian cancer pathogenesis. The role of the ovary changed from the organ of origin toward a metastatic site.

### **III. B Low-grade serous ovarian carcinoma**

---

About 5% of serous ovarian cancers are low-grade (45). The majority of low-grade serous tumors are presumed to originate from ectopic Müllerian epithelium, which is derived from embryonic Müllerian ducts and exhibits the same immunophenotype as the epithelium derived from the fallopian tube. This Müllerian epithelium is thought to arise in one of three possible ways: 1) transfer of salpingeal epithelium from the fallopian tube to the ovarian surface, leading to cortical inclusion cysts, 2) retrograde passage of endometrial epithelium, or 3) metaplasia of the ovarian surface epithelium (46).

Low-grade serous carcinomas (LGSCs) are phenotypically similar with serous borderline tumors (SBT), especially the micropapillary type. They share similar cytomorphology and it is often observed concomitant presence of borderline and low-grade invasive components. They have similar gene-expression profile and cluster together in unsupervised clustering (47). Identical mutations are found in SBT and associated LGSC (48) suggesting the existence of an adenoma-carcinoma sequence (14). Based on these similarities, the revised WHO classification (2014) defines micropapillary SBT as non-invasive LGSC. Unlike the other type I tumors, LGSCs are often bilateral and may be associated with extra-ovarian disease. Progression to HGSOCS occurs rarely (49). Studies have reported a better outcome for women whose tumors contain *BRAF* mutations than for women with *KRAS* mutations or wild-type *BRAF* and *KRAS*.

Women with low-grade carcinomas are diagnosed at younger age, on average, compared to women with high-grade carcinomas (55.5 years versus 62.6 years) (50). LGSC are paradoxically poor responders to conventional chemotherapy but sensitive to hormone therapy (51) and MEK inhibitors combined with PI3K inhibitors (52).

### **III. C Endometrioid and clear cell carcinoma**

Endometriosis is a chronic disease characterized by the presence of endometrial-like tissue (both glands and stroma) outside the uterine cavity. It causes a chronic inflammation, pelvic pain and infertility (53). Malignancies associated with endometriosis are mostly confined to the ovaries, evolving from an endometrioma, even though the disease frequently involves multiple sites in the pelvis and/or abdomen (22). Endometriomas present a 4-fold increased risk of transformation into clear-cell and endometrioid ovarian cancers. It is hypothesized that typical endometrioma would transform, through “atypical endometrioma”, into ovarian cancer. This process seems related to oxidative stress, inflammation and hyperestrogenism. “Atypical endometriomas” are considered as the precursor lesions of endometriosis-associated ovarian cancers (EAOC). Overall, it is estimated that 8% of endometriomas contain atypical endometriosis (54).

EAOC are mainly of type I and account for 20% of EOC: 10% are endometrioid and 10% are clear cell carcinomas. Recent exome sequencing studies reported frequent mutations of *ARID1A* and *PIK3CA* genes and recurrent mutations of *PPP2R1A* and *KRAS* in OCCC (15, 17) whereas endometrioid cancer had frequent mutations of *PTEN*, *CTNNB1* and *KRAS* (15, 55). Consistently, activation of the oncogenic *KRAS* and PI3K pathways and inactivation of the chromatin remodeling gene *ARID1A* are suggested pathogenic mechanisms for clear cell and endometrioid ovarian cancers (56, 57). Paired whole-genome sequencing of OCCC and synchronous endometriosis revealed ancestral mutations in both tumor-adjacent and -distant endometriotic lesions, regardless of any cytological atypia, strengthen the clonal evolution hypothesis (58). Intriguingly, 26% of non-ovarian deep infiltrating endometriosis, which are associated with virtually no risk of malignant transformation, harbor somatic cancer driver mutations such as *ARID1A* and *KRAS*. These observations suggest that the presence of driver mutations alone are not sufficient to drive the transformation of endometriosis (59). Other factors specific to ovarian microenvironment are necessary for transformation of endometriosis into cancer.

### **III. D Mucinous ovarian carcinoma**

---

Mucinous ovarian tumors (MOT) account for 10-15% of all ovarian tumors (45) and are the most frequent ovarian tumors in young patients eligible for fertility-sparing surgery (60). They

usually present as a large cyst confined to the ovary (stage I). Numerous milestones in the diagnosis and classification of MOT have been recently reached, including: 1) the finding of a morphological continuum and tumor progression from mucinous cystadenomas (80%) and borderline tumors (15%) to mucinous carcinomas (5%) (45) with *KRAS* mutation an early event in carcinogenesis (27, 61); 2) the understanding that virtually all cases of pseudomyxoma peritonei arise from the appendix (62); and 3) the requirement that a diagnosis of primary metastatic mucinous ovarian cancer exclude the possibility of metastases from gastrointestinal sources.

MOT are generally heterogeneous with a mix of benign appearing, borderline and invasive pattern within an individual neoplasm. They are occasionally associated with Brenner tumors or mature teratomas. Recent studies suggest that teratoma-associated MOT are of germ cell origin (63, 64). A clonal relationship has also been shown between Brenner tumors and associated MOT (65).

It has been suggested that MOT could originate from transitional cells or endocervical subtype foci of Mullerian metaplasia on the ovarian surface (66). Gene-expression profile of MOC is distinct from 1) other EOC (67-69); 2) from FT or OSE (68, 69) and 3) strongly correlate with those of normal colonic epithelium (68). However, the origin of the common MOT was yet to be defined, since no mucin-secreting epithelial cells have been described in the ovary. MOC are divided into two categories according to the growth pattern: the expansile (confluent) subtype without obvious stromal invasion and the infiltrative subtype with evident stromal invasion (45). The histologic classification has prognostic implication for stage I. The expansile pattern of growth has more favorable prognosis with lower metastatic potential than the invasive one (70).

Whole exome sequencing studies have revealed molecular similarities between MOT and a rare pancreatic tumor, mucinous cystic neoplasm (MCN), with mutations at similar frequencies in *RNF43* and *KRAS* (27, 71). Like MOT, MCN is a typically low-grade neoplasm. It develops mainly in young women who smoke and localize in the body and/or tail of the pancreas (72, 73). This tumor is characterized by the presence of a unique ovarian like-stroma that is mandatory for diagnosis (74). We observed that MOT and MCN have similar immunohistochemical pattern, more likely to be CK7+, CK7-, MUC2 and CDX2- (Table1), and distinct from appendiceal or colon mucinous carcinoma (75).

The clinical, pathologic and molecular similarities raise the question to whether MCN and MOT share a common cell of origin. To establish a possible biological relationship among ovarian and pancreatic mucinous tumors and their putative cell of origin, we analyzed the gene-expression pattern and/or single-cell RNA-sequencing of a large number of tumor and normal

tissue samples. Our data suggested that MOT and MCN may share PGCs as a common cell of origin (76).

	N	CK7*	CK20*	MUC2*	CDX2*	PAX8*	β-Cat**	SMAD4***
<b>MOT:</b>	<b>21</b>	<b>21</b>	<b>9 (43)</b>	<b>8 (38)</b>	<b>6 (29)</b>	<b>5 (24)</b>	<b>0 (0)</b>	<b>2 (10)</b>
<b>Total</b>		<b>(100)</b>	4 (19)	1 (5)	2 (10)	2 (10)		
<b>Pos #</b>		20	3 (14)	0 (0)	1 (5)	2 (10)		
<b>(%)</b>		(95)	2 (10)	7 (33)	3 (14)	1 (5)		
<b>4+</b>		0 (0)	6 (29)	6 (29)	5 (24)	2 (10)		
<b>3+</b>		1 (5)	6 (29)	7 (33)	10	14 (67)		
<b>2+</b>		0 (0)	0 (0)		(48)			
<b>1+</b>	0 (0)							
<b>0</b>								
<b>MCN:</b>	<b>16</b>	<b>16</b>	<b>2 (13)</b>	<b>1 (6)</b>	<b>4 (25)</b>	<b>1 (6)</b>	<b>0 (0)</b>	<b>0 (0)</b>
<b>Total</b>		<b>(100)</b>	1 (6)	0 (0)	1 (6)	0 (0)		
<b>Pos #</b>		16	0 (0)	1 (6)	2 (13)	0 (0)		
<b>(%)</b>		(100)	1 (6)	0 (0)	1 (6)	1 (6)		
<b>4+</b>		0 (0)	6 (38)	0 (0)	1 (6)	0 (0)		
<b>3+</b>		0 (0)	8 (50)	15 (94)	11	15 (94)		
<b>2+</b>		0 (0)	0 (0)		(69)			
<b>1+</b>	0 (0)							
<b>0</b>								

MOT, mucinous ovarian tumor; MCN, mucinous cystic neoplasm;  
 \* Total Positive defined as ≥2+  
 \*\* β-Catenin (β-Cat) evaluated for nuclear expression only  
 \*\*\* SMAD positive = complete loss of nuclear staining in tumor cells

**Table 1: Expression of immunohistochemical markers in mucinous ovarian and pancreatic tumors.**

#### IV. Hypotheses of pathogenesis

##### IV. A. Incessant ovulation hypothesis

In the human females, ovulatory cycles are almost continuous from menarche to menopause. Social conditions of modern life render the majority of ovulations purposeless. The drastic reduction in the total numbers of pregnancies and cumulative lactation time, as well as the absence of starvation periods, all of which would normally suppress the ovulatory activity, result in maximizing the number of lifetime ovulations women experience today. In other mammals, ovulation may be limited to a breeding season, and the reproductive potential is generally exercised to the full (77). Comparative ovarian oncology showed the rarity of epithelial tumors in these animals.

A long-standing hypothesis, called the “incessant ovulation” was proposed by Fathalla in 1971 from the observation that human females are unique from other mammals in their persistent ovulation (1). Fathalla proposed that repetitive disruption of the OSE with subsequent exposure to a surge of estrogen from the follicular fluid (FF) during ovulation, damages and traumatizes the OSE (1, 2). Thus, two aspects of ovulation (disruption of OSE and exposure to FF) are linked to ovarian cancer pathogenesis. Over time, this process of continuous damage and subsequent healing of the OSE and adjacent tubal epithelium increases cell proliferation, DNA replication and the likelihood of genomic instability, which could lead to carcinogenesis (78).

The theory of “incessant ovulation” maintains that destruction and repair of OSE at ovulation are accompanied by inflammation that plays a role in ovarian carcinogenesis (1). In fact, ovulation is the result of an acute inflammatory response to gonadotropin stimulation at the level of the preovulatory ovarian follicle (79). Agents that inhibit acute inflammatory reactions such as non-steroidal anti-inflammatory drugs (NSAID) suppress ovulation in rabbits (80) and reduce ovulation rate in women (81).

Increasing experimental evidence supports the “incessant ovulation” hypothesis. Mature human follicles reach approximately 23 mm in diameter, yielding upwards of 5 mL of follicular fluid (FF) (82). During ovulation, FF is released and bathes the surrounding tissue, including the OSE and the fallopian tube fimbria proximal to the ovary. FTE exposure to human FF lead to DNA double strand breaks (DSBs) and stabilization of the DNA damage checkpoint p53 (83). FF components include hormones, fatty acids, inflammatory cytokines, reactive oxygen species (ROS) and growth factors, all of them having potential anti-apoptotic and mutagenic effect. Estradiol (E2) is one of the prominent components; its concentration in FF can reach 1,000 fold that of serum levels (84). Estrogens are considered as genotoxic carcinogens, generating free-radicals that induce DNA damage (85). In breast cells, estradiol can induce DNA DSBs and BRCA1 is required for repairing these breaks and preventing genomic instability. *BRCA1* haploinsufficiency, as observed in *BRCA1* carriers, exacerbates DSBs and genomic instability in breast cells (86). A plausible hypothesis for pathogenesis of HGSOE is repeated exposure to high levels of estradiol during ovulation inducing DNA DSBs in the FTE. Defect in DNA repair in *BRCA* carriers would accelerate malignant transformation of epithelial cells.

Apart from estradiol, progesterone is the most abundant hormonal component of FF. Progesterone is the hormone of pregnancy and luteal phase of the menstrual cycle. Progesterone has extensive immunomodulatory properties (87) (88). This hormone is critical for the end stages of follicle development and for ovulation. *Pgr*-null mice fail to ovulate in response to gonadotrophin surge (89), uncovering the essential role of progesterone-dependent pathways in the regulation of ovulation. Gene-expression profile (GEP) of the ovary identified several key molecules and signaling pathways implicated in inflammation, such as EDN2, PPAR $\gamma$  and IL-6. These factors are regulated by progesterone receptors (PR) during the ovulatory process (90). Evidence of the role of progesterone in cancer development in *BRCA* carriers was revealed by the high serum levels of this hormone, up to +121%, during the luteal phase in premenopausal *BRCA* carriers, compared to non carriers (91). Compiling evidence point to progesterone as a key player in breast tumorigenesis (92-94). In ovarian cancer, several alterations in the FTE of *BRCA* carriers were observed during the luteal phase suggesting that progesterone could be involved in HGSOE tumorigenesis: 1) GEP of FTE

removed at the luteal phase from *BRCA* carriers more closely resembled HGSOC samples, compared to FTE removed during from the follicular phase (95); 2) FTE samples of the luteal phase are more infiltrated by immune cells than those of follicular phase (96) and 3) they express inflammation related and NF- $\kappa$ B-responsive genes (97), suggesting an altered response to ovulation-associated cytokines.

The “incessant ovulation” hypothesis is supported by strong epidemiologic data. There is a clear reduction in the risk of EOC when ovulation is suppressed through pregnancy and/or lactation and use of OCPs (98-101). Parity is a well-established protective factor for ovarian cancer. Women with at least one full-term pregnancy have 40% risk reduction compared with nulliparous women, and each additional full-term pregnancy lowered the risk further (102). This protective effect is observed in all histotypes (103, 104). Similarly, lactation has a protective effect against EOC (105, 106). Recent data suggest a link between the duration of lactation and reduced risk of EOC (105, 107). The overall risk reduction appeared greatest for endometrioid and clear cell subtypes (108). For OCPs, there is a significant duration-response relationship, with reduction in incidence of more than 50% among women using it for 10 years or more (101, 109). The reduction persisted for more than 30 years after oral contraceptive use had ceased, but became somewhat attenuated over time. OCPs have protective effect against all EOC except mucinous carcinoma (101, 104). The extensive use of OCPs since the 1970’s account for the overall declined incidence of EOC (110).

Similarly to the general population, protective effects of reproductive factors, i.e. parity and OCPs, were observed in *BRCA* carriers (111-114). Other situations where women are exposed to high levels of reproductive hormones have been linked to increased risks for EOC. Long durations (> 10 years) use of unopposed estrogen or use of estrogen plus progestin as part of menopausal hormone replacement therapy (HRT), are associated with increased EOC risk (115-117), with the highest risk for endometrioid tumors (117). In contrast, a correlation has been shown between a marked reduction in HRT use around 2002 and an accelerated decline in EOC incidence rates, with the largest changes for, again, endometrioid carcinomas (118).

Given the increasing number of women treated with ovulation-inducing drugs, the potential increased risk for EOC is an important issue. Clomiphene is the most widely prescribed drug for ovulation induction to reverse anovulation or oligoovulation. There is an increased risk of borderline ovarian tumors, but not EOC, in subfertile women treated with clomiphene alone or clomiphene plus gonadotrophin for *in vitro* fertilization (119, 120). A link has also been reported between exposure to progesterone as a fertility drug and increased risk of SBT (121).

#### **IV. B. Gonadotropin hypothesis**

---

Gonadotropins, follicle-stimulating hormone (FSH) and luteinizing hormone (LH), are produced in the anterior pituitary gland. They play a key role in regulating steroidogenesis and gametogenesis (122). Excessive exposure to gonadotropins, related to menopause, ovulation or infertility therapy raised the question whether these hormones could be involved in ovarian cancer pathogenesis. The “gonadotropin hypothesis”, implicates excessive direct and indirect stimulation of OSE by FSH and/or LH, leading to proliferation and ultimately malignant transformation (4). According to Cramer and Welch, the critical steps in the transformation to EOC are the entrapment of OSE in inclusion cysts with continued stimulation of the entrapped epithelium by gonadotropins, estrogen, or estrogen precursors, leading to subsequent malignant transformation (4).

Several lines of evidence suggest that gonadotropins could be involved in pathogenesis of SBT and granulosa cell tumors. In the normal ovary, FSH receptors (FSHR) and LH receptors (LHR) are predominately expressed in the ovarian granulosa cells (122, 123) theca cells (for LHR) and OSE (122). In EOC, FSHR and LHR levels are more frequently expressed by serous borderline cystadenoma, low-grade serous carcinomas and granulosa cell tumors (124, 125) than HGSOC (126, 127). Mice with FSH receptor knockout (*FSHRKO*) develop, after a long delay of 12-15 months, sex-cord tumors and/or serous papillary cystadenoma (128, 129). These *FSHRKO* mice are anovulatory, sterile, have atrophic ovaries and display high levels of circulating FSH and LH whereas estradiol levels are low because they (129). Serous papillary cystadenoma were preceded by changes in OSE with formation of cysts. These results reinforce the hypothesis that gonadotropins can drive malignant transformation of OSE independently from estradiol and ovulation. It is also possible that gonadotropins favor tumorigenesis indirectly through androgens. Indeed, high levels of testosterone were observed in these *FSHRKO* mice. In humans, doubling of testosterone circulating levels during pregnancy is associated with about 2-fold higher risk of sex-cord tumors (130) and serous borderline tumors (131).

Polycystic ovarian syndrome (PCOS), a common reproductive and endocrinologic disorder found in 6-10% of the female population is frequently associated with high levels of LH (increased ratio LH/FSH). Women with PCOS have hirsutism due to hyperandrogenism (132). The association between PCOS and EOC is not clear but an increased risk of SBT was reported by two studies (133). Irregular menstrual cycles, another condition that is accompanied with increased androgens, has been associated with increased risk of SBT (134). These observations are consistent with the *FSHRKO* mouse model and point to the potential role of LH and/or testosterone in pathogenesis of SBT (131).

---

Inhibin is expressed by luteal and granulosa cells and acts as a negative regulator of pituitary FSH synthesis and secretion (135). *De novo* germline mutation of *INHA* gene encoding the  $\alpha$ -subunit of inhibin has been reported in a patient with early onset serous borderline ovarian tumor (136). Mutations in *INHA* led to a dramatic reduced production of inhibins A and B by HEK-293F transfected cells. Inhibin downregulation potentially increases the release of FSH from the anterior pituitary, thus participating to ovarian oncogenesis. These data are corroborated by inhibin- $\alpha$  subunit knockout (*Inha*<sup>-/-</sup>) mice which are infertile, as determined by their inability to ovulate, develop mixed and granulosa cell tumors (GCT) as early as 4 weeks of age and exhibit a 2- to 3-fold increase in FSH levels (137). Mice with *Inha*<sup>-/-</sup> and mutated *Gnrh* gene (resulting in reduced levels of FSH and LH) did not develop gonadal tumors (138). Surprisingly, when *Inha*<sup>-/-</sup> mice were crossed with *Fshb*<sup>-/-</sup> (FSH  $\beta$ -subunit knockout) mice, females developed slow growing and less hemorrhagic sex cord-stromal tumors after 12 weeks of age, later than seen in the *inha*<sup>-/-</sup> mice (139). Double knockout *Inha*<sup>-/-</sup> *Lhb*<sup>-/-</sup> have increased survival and delayed tumor progression, and these observations correlate with lower serum FSH and estradiol levels compared to *Inha*<sup>-/-</sup> controls (140). Together, these results suggest that LH is not required for GCT formation in the absence of inhibin but promotes tumor progression (135). Epidemiologic data in support of the gonadotropin theory are the increased risk of developing GCT in women exposed to ovulation-inducing drugs or high concentrations of pituitary gonadotropins in the context of treatment for infertility (141, 142). This is also consistent with the molecular profile GCT which resemble FSH-responsive granulosa cells of the late preovulatory follicle (125).

Overall, it seems that gonadotropins are involved in pathogenesis of SBT and GCT in premenopausal women. These two histotypes develop mainly in perimenopausal women with a median age at diagnosis of 50-55 years. Menopause is accompanied with a dramatic increase in gonadotropins serum levels that reach a peak of 10-20 times for FSH and 3-4 times for LH, compared to values during the follicular phase of menstrual cycle (143). Thus, it is possible that permanent increase of gonadotropins in perimenopausal women accelerate the development of already initiated SBT and GCT.

#### **IV. C. Incessant menstruation hypothesis**

A third hypothesis, previously named “retrograde transportation” (144, 145), and now called “incessant menstruation” has recently emerged. It suggests that repeated exposure to retrograde menstruation exposes the ovary and the FTE to ROS and oxidative iron from the blood (3). ROS induce oxidative stress resulting into carcinogenic DNA mutations or loss. Retrograde menstruation into the peritoneal cavity is a very common physiologic event in all menstruating women. It is also a pathogenesis model of endometriosis (146), an estrogen-



dependent chronic pelvic inflammatory condition that affects women during their reproductive period. The two most frequent pain symptoms caused by endometriosis are dysmenorrhea (80%) and deep dyspareunia (30%). According to the retrograde menstruation hypothesis, endometrial fragments would reach the pelvis via transtubal retrograde flow, implant primarily on the pelvic peritoneum, ovaries and rectovaginal septum, proliferate and cause chronic inflammation.

Endometriosis is characterized by the ectopic presence of normal-appearing, functional endometrial tissue composed of glands and stroma outside the uterus (147) and these benign lesions can harbor mutations in cancer-associated genes (59). It frequently involves multiple sites in the pelvis. However, the risk of developing EOC is 10 times higher in patients with a history of pathology proven ovarian endometrioma (ectopic endometrium implanted on the ovary) than women with recalled endometriosis (148) (14) (15, 16, 58). Blocking ovulation with oral contraceptive pills (OCPs) reduces the risk of endometrioma's recurrence after conservative surgery by 90% (149). In women with a history of endometriosis, factors that suppress ovulations such as OCPs use or parity reduce the risk of EOC by 80%, whereas factors that abrogate retrograde menstruation (a plausible hypothesis for pathogenesis of endometriosis) such as hysterectomy or tubal ligation reduce the risk of EOC by 30% only (150). Together, these observations suggest that endometriosis is necessary but not sufficient for malignant transformation and point to the particular microenvironment of the ovary. They suggest that repeated ovulation combined with endometriosis participate to ovarian carcinogenesis.

Epidemiologic data suggested an association between endometriosis and increased risk of type I EOC : clear cell (OR=3.05, 95%CI 2.43-3.84), low-grade serous (OR=2.11, 95%CI 1.39-3.20) and endometrioid carcinomas (OR=2.04, 95%CI 1.67-2.48)(151). Pathologic and molecular studies further linked endometriosis with these histotypes (15, 152, 153). Inflammation is a typical feature of endometriosis, as the presence of ectopic tissue in the peritoneal cavity is associated with overproduction of prostaglandins, cytokines and chemokines (154-156). As discussed above, the risk of EOC is higher only in women with endometrioma (ovarian endometriosis).

Epidemiological arguments in favor of the "incessant menstruation" hypothesis are the protective role hysterectomy without oophorectomy and tubal ligation against EOC (157-161). The younger the woman was when she got her tubal ligation, the greater was the protective effect against EOC, supporting the role of chronic exposure to inflammation in promoting EOC (158, 161). Disruption of the genital tract impeaches retrograde menstruation to access to the ovary and fallopian tube. The magnitude of risk reduction with tubal ligation is greater for

endometriosis-associated EOC, i.e. endometrioid and clear cell carcinomas (50%) than HGSOC (20%) (160). On the other hand, bilateral salpingectomy performed as a contraceptive method reduced the risk of EOC by 61%, compared to 28% for tubal ligation (159). The significant risk reduction observed with bilateral salpingectomy is consistent with the possible tubal origin of HGSOC.

---

## **Results**

**Article 1: High-grade serous ovarian carcinoma originate in the fallopian tube**

**Article 2: Primordial germ cells as a potential cell of origin for mucinous cystic neoplasms of the pancreas and mucinous ovarian tumors**

**Article 3: Screening of ovarian cancer: not for tomorrow**

## **High-grade serous ovarian carcinoma originate in the fallopian tube**



High-grade serous ovarian carcinoma (HGSOC) is the most frequent histotype of ovarian cancer. It is diagnosed at advanced stages in the majority of cases and is responsible for the majority of deaths from ovarian cancer. A better comprehension of the pathogenesis would help into developing new screening tools. In the current study, we used laser-capture microdissection and whole-exome sequencing of multiple lesions of HGSOC from several patients. Evolutionary analyses revealed that pre-invasive tumors in the fallopian tube (p53 signatures and serous tubal intraepithelial carcinoma) are the early lesions of ovarian cancers. Our work bring new insights into pathogenesis of HGSOC and could have implications for future development of screening and early diagnosis tools.

ARTICLE

DOI: 10.1038/s41467-017-00962-1

OPEN

# High grade serous ovarian carcinomas originate in the fallopian tube

S. Intidhar Labidi-Galy<sup>1,13</sup>, Eniko Papp<sup>2,14</sup>, Dorothy Hallberg<sup>2</sup>, Noushin Niknafs<sup>2,3</sup>, Vilmos Adleff<sup>2</sup>, Michael Noe<sup>2</sup>, Rohit Bhattacharya<sup>2,4</sup>, Marian Novak<sup>1,14</sup>, Siân Jones<sup>5</sup>, Jillian Phallen<sup>2</sup>, Carolyn A. Hruban<sup>2</sup>, Michelle S. Hirsch<sup>6</sup>, Douglas I. Lin<sup>6,15</sup>, Lauren Schwartz<sup>7</sup>, Cecile L. Maire<sup>1</sup>, Jean-Christophe Tille<sup>8</sup>, Michaela Bowden<sup>6</sup>, Ayse Ayhan<sup>9,10,11,12</sup>, Laura D. Wood<sup>2</sup>, Robert B. Scharpf<sup>2</sup>, Robert Kurman<sup>2,12</sup>, Tian-Li Wang<sup>2,12</sup>, le-Ming Shih<sup>2,12</sup>, Rachel Karchin<sup>2,3</sup>, Ronny Drapkin<sup>1,6,16</sup> & Victor E. Velculescu<sup>1,6,16</sup>  

High-grade serous ovarian carcinoma (HGSOC) is the most frequent type of ovarian cancer and has a poor outcome. It has been proposed that fallopian tube cancers may be precursors of HGSOC but evolutionary evidence for this hypothesis has been limited. Here, we perform whole-exome sequence and copy number analyses of laser capture microdissected fallopian tube lesions (p53 signatures, serous tubal intraepithelial carcinomas (STICs), and fallopian tube carcinomas), ovarian cancers, and metastases from nine patients. The majority of tumor-specific alterations in ovarian cancers were present in STICs, including those affecting *TP53*, *BRCA1*, *BRCA2* or *PTEN*. Evolutionary analyses reveal that p53 signatures and STICs are precursors of ovarian carcinoma and identify a window of 7 years between development of a STIC and initiation of ovarian carcinoma, with metastases following rapidly thereafter. Our results provide insights into the etiology of ovarian cancer and have implications for prevention, early detection and therapeutic intervention of this disease.

<sup>1</sup>Department of Medical Oncology, Dana-Farber Cancer Institute and Harvard Medical School, Boston, MA 02215, USA. <sup>2</sup>Sidney Kimmel Comprehensive Cancer Center, Johns Hopkins University School of Medicine, Baltimore, MD 21287, USA. <sup>3</sup>Department of Biomedical Engineering, Institute for Computational Medicine, Johns Hopkins University, Baltimore, MD 21218, USA. <sup>4</sup>Department of Computer Science, Institute for Computational Medicine, Johns Hopkins University, Baltimore, MD 21218, USA. <sup>5</sup>Personal Genome Diagnostics, Baltimore, MD 21224, USA. <sup>6</sup>Department of Pathology, Brigham and Women's hospital and Harvard Medical School, Boston, MA 02115, USA. <sup>7</sup>Department of Pathology, University of Pennsylvania Perelman School of Medicine, Philadelphia, PA 19104, USA. <sup>8</sup>Division of Clinical Pathology, Faculty of Medicine, Geneva University Hospital, 1205 Geneva, Switzerland. <sup>9</sup>Department of Pathology, Seirei Mikatahara Hospital, Hamamatsu 433-8558, Japan. <sup>10</sup>Department of Tumor Pathology, Hamamatsu University School of Medicine, Hamamatsu 431-3192, Japan. <sup>11</sup>Department of Molecular Pathology, Hiroshima University School of Medicine, Hiroshima 739-0046, Japan. <sup>12</sup>Departments of Gynecology and Obstetrics and Pathology, Johns Hopkins University School of Medicine, Baltimore, MD 21287, USA. <sup>13</sup>Present address: Department of Oncology, Geneva University Hospitals, Geneva 1205, Switzerland. <sup>14</sup>Present address: Personal Genome Diagnostics, Baltimore, MD 21224, USA. <sup>15</sup>Present address: Department of Pathology, Beth Israel Deaconess Medical Center, Boston, MA 02215, USA. <sup>16</sup>Present address: Department of Obstetrics and Gynecology, Penn Ovarian Cancer Research Center, University of Pennsylvania Perelman School of Medicine, Philadelphia, PA 19104, USA. S. Intidhar Labidi-Galy and Eniko Papp contributed equally to this work. Ronny Drapkin and Victor E. Velculescu jointly supervised this work. Correspondence and requests for materials should be addressed to R.D. (email: [rdrapkin@penmedicine.upenn.edu](mailto:rdrapkin@penmedicine.upenn.edu)) or to V.E.V. (email: [velculescu@jhmi.edu](mailto:velculescu@jhmi.edu))

Ovarian cancer is the leading cause of death from gynecologic cancers<sup>1,2</sup>. The 10-year survival is < 30% and has not improved significantly over the last 30 years<sup>3</sup>. Despite significant efforts, various screening and therapeutic strategies have generally not led to improved overall survival<sup>4,5</sup>. One of the major challenges to improved diagnostic and therapeutic intervention in ovarian cancer has been a limited understanding of the natural history of the disease. Ovarian carcinoma is a highly heterogeneous group of diseases including different histological subtypes with distinct clinicopathological and molecular genetic features that can be generally classified as Type I and Type II tumors<sup>6</sup>. Among them, high-grade serous ovarian carcinoma (HGSOC, the major Type II tumor) is the most common histologic subtype of ovarian cancer, accounting for three quarters of ovarian carcinoma<sup>7–10</sup>. Genomic analyses of HGSOC have identified genetic alterations in *TP53*, *BRCA1*, *BRCA2*, *PTEN*, and other genes although few of these discoveries have affected clinical care<sup>11,12</sup>. HGSOC is diagnosed at advanced stages in ~70% of cases, and these women have a significantly worse outcome than those with early stage disease. Until recently, the prevailing view of HGSOC was that it developed from the ovarian surface epithelium. However, early in situ lesions that arise from the ovarian surface epithelium and progress to invasive HGSOC have never been reproducibly identified.

Insights into the pathogenesis of HGSOC have emerged from investigating the prevalence of occult ovarian and fallopian tube (FT) carcinomas in women with germline mutations of *BRCA1/BRCA2* genes<sup>13–17</sup>. Potential precursor lesions of HGSOC were identified in the fimbriae of the FTs removed as part of prophylactic surgery<sup>16</sup>. Such lesions, including a *TP53* mutant single-cell epithelial layer (p53 signature) and serous tubal intraepithelial carcinoma (STIC)<sup>17,18</sup>, have been identified in patients with advanced stage sporadic HGSOC of the ovary, FT and peritoneum<sup>18</sup>. Immunohistochemical as well as targeted sequencing analyses have shown that FT lesions harbor the same *TP53* mutation as surrounding invasive carcinomas<sup>17–21</sup>. These analyses suggest a clonal relationship among such tumors but given the limited number of genes analyzed do not conclusively identify the initiating lesions nor exclude the possibility of FT metastases from primary ovarian carcinomas<sup>21,22</sup>. Yet additional studies have evaluated clonal intraperitoneal spread of ovarian cancer using whole genome analyses, but these efforts did not analyze precursor lesions such as STICs that may give rise to this disease<sup>23</sup>.

In this study, we use exome-wide sequence and structural analyses of multiple tumor samples from the same individual to examine the origins of HGSOC. We have previously shown that the acquisition of somatic alterations can be used as a molecular marker in the development of human cancer<sup>24</sup>. Here, we examine whether the compendium of somatic alterations identified in different lesions may provide insights into the evolutionary relationship between primary FT lesions, including p53 signatures and STIC lesions, ovarian carcinomas, and intraperitoneal metastases.

## Results

**Overall approach.** To elucidate the relationship among tumors in patients with HGSOC, we performed whole-exome sequencing of 37 samples from five patients diagnosed with sporadic HGSOC who underwent upfront debulking (Supplementary Data 1). This included STIC lesions, FT carcinomas, and ovarian cancers in all five patients; appendiceal, omental, or rectal metastases in three of patients (CGOV62, CGOV280, CGOV278); p53 signatures in two patients (CGOV62, CGOV63); and a STIC lesion in the contralateral FT from the affected ovarian cancer (CGOV280).

In addition, we analyzed isolated STIC lesions from four patients (CGOV64, CGOV65, CGOV303, and CGOV304), three of whom had germline pathogenic *BRCA* alterations and underwent prophylactic bilateral salpingo-oophorectomy, and a fourth who had bilateral salpingo-oophorectomy and hysterectomy in the context of a pelvic mass (Supplementary Data 1). For all patients, laser capture microdissection (LCM) was used to isolate lesions after immunohistochemistry (IHC) staining of p53 in STICs and p53 signatures if these contained a *TP53* missense mutation or after hematoxylin staining if the samples contained a *TP53* nonsense mutation (Fig. 1). All other samples were microdissected after hematoxylin staining. Whole blood, normal ovarian stroma, normal FT stroma, or normal cervix were used as control samples.

To identify genetic alterations in the coding regions of these cancers, we used next-generation sequencing platforms to examine entire exomes in matched tumor and normal specimens of all patients (Fig. 1). This approach allowed us to identify non-synonymous and synonymous sequence changes, including single base and small insertion or deletion mutations, as well as copy number alterations in coding genes. Given the challenges of exome-wide analyses of small tumor samples observed in STICs and p53 signature lesions, we developed experimental and bioinformatic approaches for detection of somatic alterations from laser capture microdissected tissue. These included optimized approaches for microdissection of STICs and p53 signatures after immunohistochemical staining, improved DNA recovery from laser captured material, library construction from limited and stained tissue samples, and error correction methods in next-generation sequence analyses (Methods section). The analyses of p53 signatures were particularly challenging because these are extremely small lesions, representing 10–30 cells per section and less than several hundred cells total that result in minute amounts (less than a few ng) of isolated DNA. We optimized these approaches using a targeted next-generation sequencing approach analyzing 120 genes in a subset of samples from patient CGOV62, and then used whole-exome analyses to evaluate coding sequence alterations in all samples (Supplementary Data 2–4). We obtained a total of 719 Gb of sequence data, resulting in an average per-base sequence ~178-fold total coverage (~112-fold distinct coverage) for each tumor analyzed by whole-exome sequencing (Supplementary Data 2).

**Analysis of sequence and structural changes.** Whole-exome sequence analyses of the tumor samples from each patient identified somatic mutations that were present in all neoplastic samples analyzed as well as specific changes that were present in individual or subsets of tumors (Fig. 2). As expected, we identified sequence changes in the *TP53* tumor suppressor gene, a well-known driver gene in HGSOC, in all cases. The *TP53* alterations were identical in all samples analyzed for each patient including in the p53 signatures, the STIC lesions, and other carcinomas. These data suggest that mutation of *TP53* was among the earliest initiating events for HGSOC development as all lesions harbored this alteration.

IHC staining for p53 did not identify any nuclear positive staining of p53 on the ovarian surface epithelium in any of the cases that had *TP53* missense mutation, whereas all carcinomas, STICs, and p53 signatures in the FT were positive. Whole-exome sequence analyses of normal ovarian stroma (no p53 staining) microdissected from three patients (CGOV64, CGOV65, CGOV280) did not find any genomic abnormalities. Analysis of the resected tissues revealed that none of the nine cases had ovarian inclusion cysts.

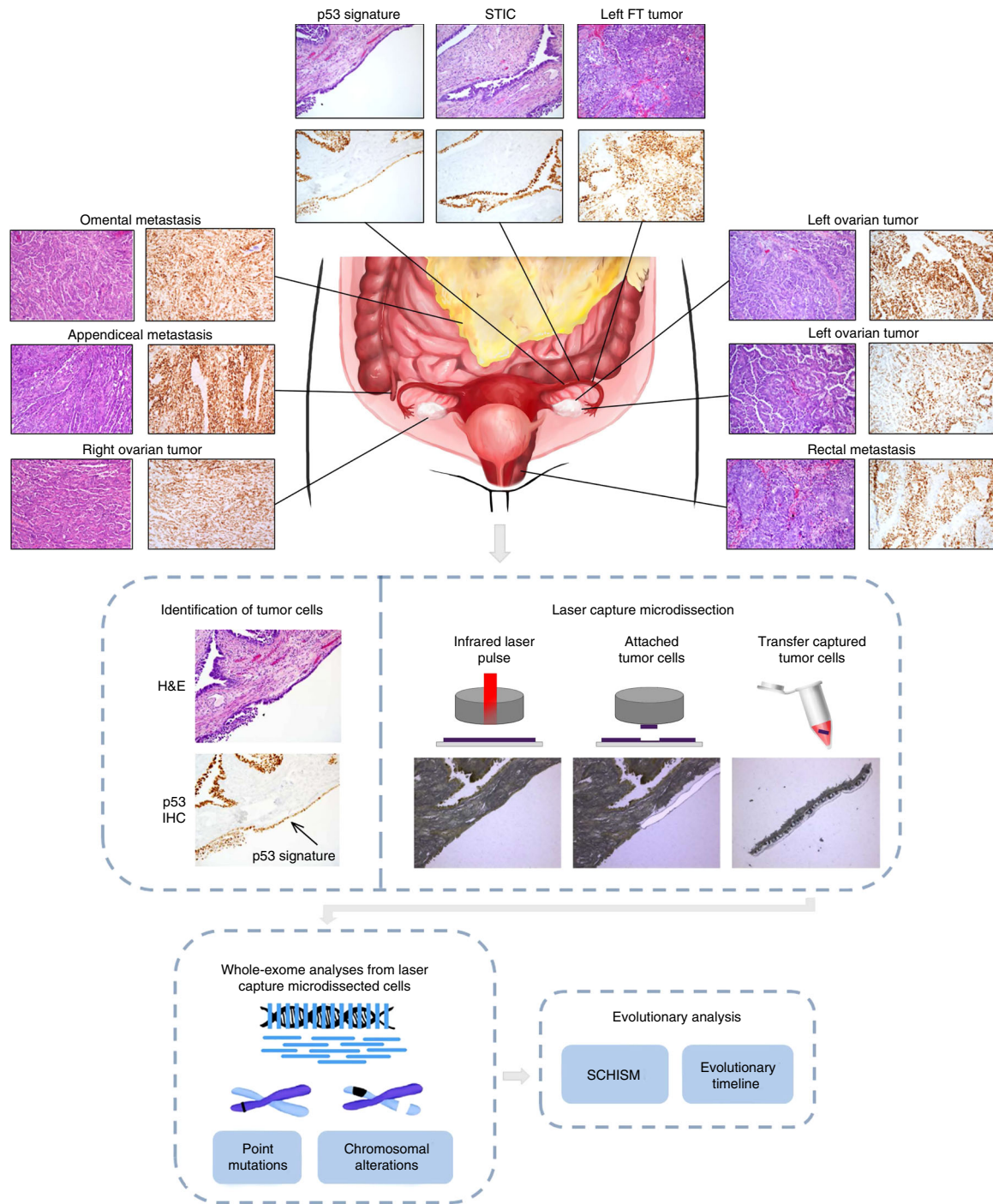


**Fig. 1** Schematic of sample isolation and next-generation sequencing analyses. (Top panel) Tumor sites analyzed from CGOV62 with stage III HGSOC. For each sample, slides were stained with hematoxylin and eosin as well as analyzed by immunohistochemical staining of p53. (Middle panel) Tumor samples were microdissected for genomic analyses. For microdissection for STIC and p53 signature lesions, tumor cells were identified using immunohistochemical staining of p53 and isolated through laser capture microdissection. (Bottom panel, left) Next-generation sequencing analyses were performed for tumor specimens using either whole-exome or targeted analyses. (Bottom panel, right) Somatic mutations and chromosomal alterations were used to evaluate tumor evolution using the tumor subclonality phylogenetic reconstruction algorithm SCHISM and to determine a timeline for tumor progression

These observations suggest that there is no early lesion with *TP53* mutation in the surface epithelium or other normal regions within the ovary.

Because *TP53* mutations are expected to be clonal and were all homozygous due to loss of heterozygosity (LOH) of the remaining wild-type allele (as determined in our subsequent allelic imbalance analyses), we used the mutant allele fraction of *TP53* in each sample to estimate tumor purity. We further

analyzed sequence alterations in all samples with estimated tumor purities > 50%, while four samples with tumor cellularities below this threshold (omental metastasis from CGOV279 and right ovarian tumor from CGOV278) or that were miliary carcinomas (rectal and sigmoidal metastases from CGOV63) were only analyzed for structural changes.

Using a high-sensitivity mutation detection pipeline, we identified an average of 33 non-synonymous and synonymous



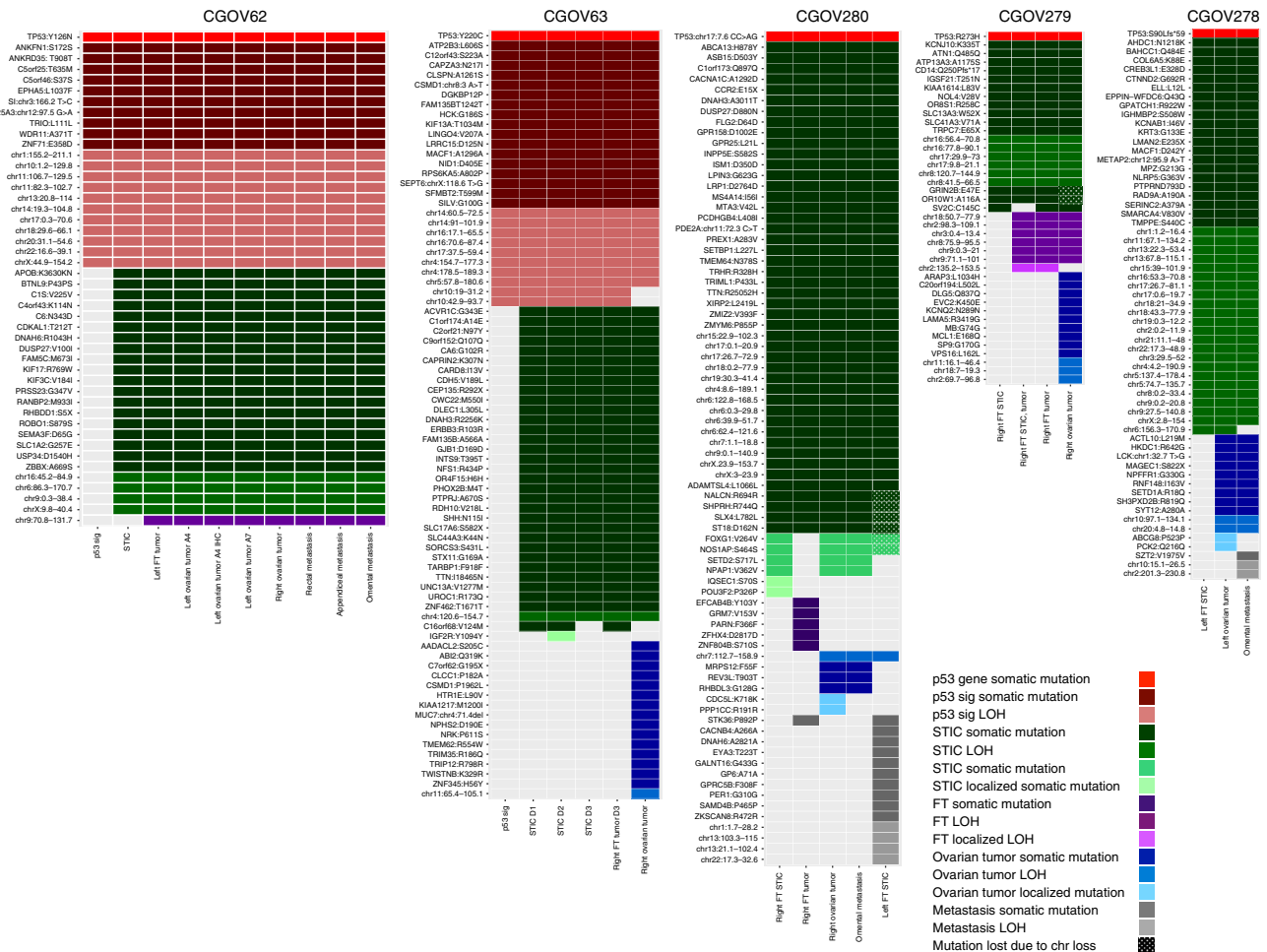


**Fig. 2** Somatic mutation and allelic imbalance profiles among different tumor lesions. Somatic mutations and segments of allelic imbalance detected by whole-exome analyses are indicated as colored cells in rows for all patients. Darker shades of each color indicate somatic mutations while lighter shades indicate allelic imbalances. The tumor samples analyzed for each patient are indicated in columns (p53 sig, p53 signature; STIC, serous tubal intraepithelial carcinoma). For ovarian tumors in CGOV62 and STIC lesions in CGOV63 multiple blocks are indicated, including one ovarian tumor where multiple sections were analyzed after hematoxylin and eosin staining or after immunohistochemistry (IHC) staining of p53. These analyses indicated that staining methods did not affect detection of somatic alterations. The color of mutations indicates the degree of relatedness among tumor samples: red, shared among all tumor samples with TP53 highlighted at the top row; green, shared among all tumor samples except p53 signature lesion; purple, shared among fallopian tube tumor and omental metastasis; blue indicates mutations that were first detected in the ovarian tumors; and gray indicates mutations that were only detected in metastatic lesions. Additional color shades or patterns indicate mutations that are localized to specific lesions or lost due to chromosome loss as shown in the legend

sequence alterations per tumor sample. Candidate alterations were evaluated across samples in an individual to determine if they were present in multiple neoplastic lesions or were unique to a particular sample. To allow for the possibility that a subclone may have developed in a tumor lesion prior to becoming a dominant clone at another location, we determined if genetic alterations that were present in one tumor were also present in a low fraction of neoplastic cells of other lesions. This method required high coverage of analyzed alterations in all samples and excluded potential artifacts related to mapping, sequencing or PCR errors, allowing specific detection of alterations present in  $\geq 1\%$  of sequence reads (see Methods section for additional information).

The composition of sequence alterations was relatively similar among the affected lesions of each patient. For example, for CGOV62, the STIC lesion, FT carcinomas, left and right ovarian cancers, and all three metastatic lesions harbored a common set of somatic mutations (Fig. 2). In CGOV63, CGOV279, and CGOV278, while most of the sequence alterations were the same among the tumors of each patient, a subset of mutations could

distinguish the STIC lesions and FT carcinomas from ovarian cancers or intraperitoneal metastases.

Given the importance of chromosomal instability in HGSO<sup>11</sup>, we extended our analyses to examine structural variation in the multiple tumors of each patient. We focused on regions of allelic imbalance that can result from the complete loss of an allele (LOH) or from an increase in copy number of one allele relative to the other. We divided the genome into chromosome segments and for each segment compared the minor allele (B-allele) frequency values in tumor and normal samples using the ~17,000 whole-exome germline heterozygous single-nucleotide polymorphisms (SNPs) observed (Fig. 3, Supplementary Figs. 1–9 and Supplementary Data 7–11). Overall, we observed that an average of ~26% (range 12–39%) of the genome had chromosomal imbalances in the samples analyzed (Fig. 3).

Integration of sequence and structural alterations identified an average of 47 alterations per sample (range 21–74) (Fig. 2). The combination of both types of alterations allowed robust genomic differentiation between STICs and ovarian cancers or metastatic



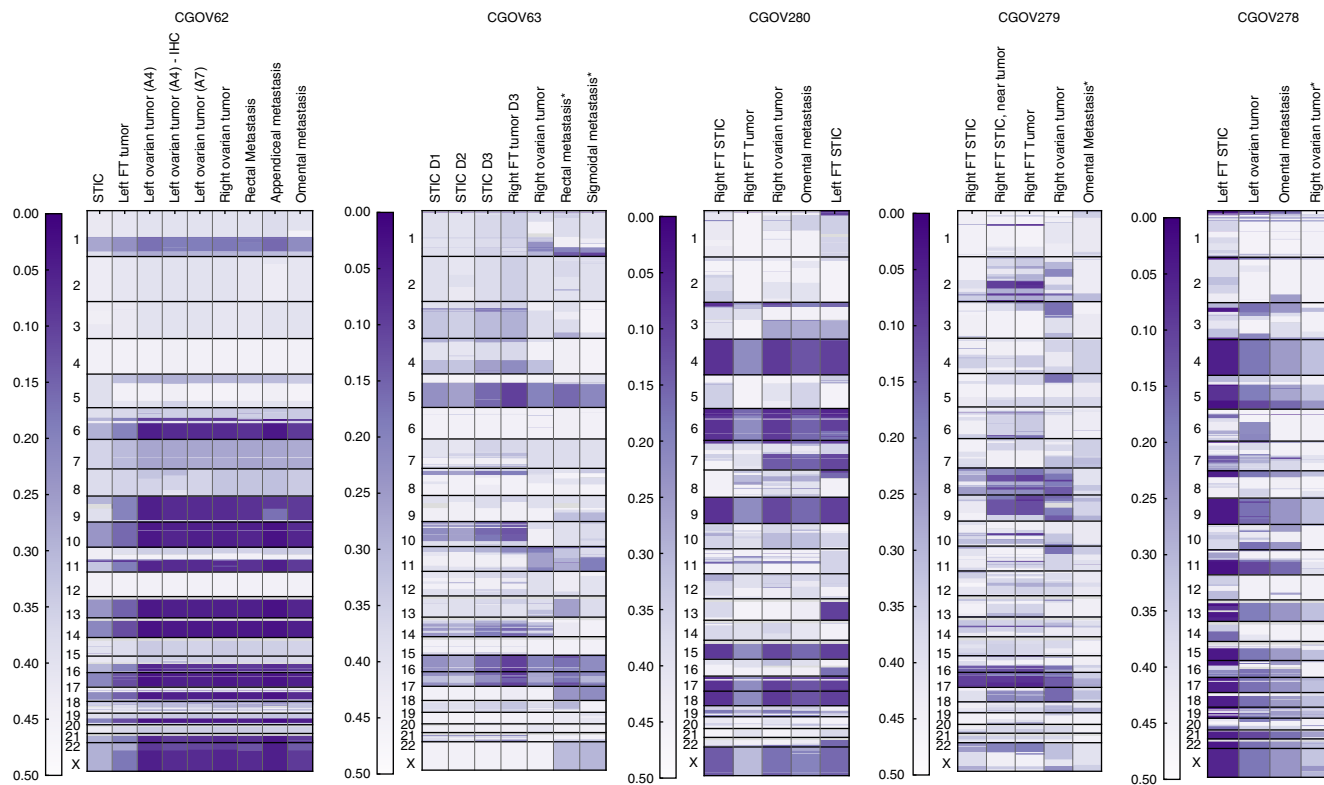


**Fig. 3** Genome-wide allelic imbalance profile. Minor allele frequency of heterozygous SNPs identified from normal tissue in each patient are derived in each tumor sample, enabling assessment of allelic imbalance in ~17,000 loci across the exome. Circular binary segmentation (CBS) is applied to minor allele frequencies of SNPs with minimum coverage of 10 $\times$  in each tumor sample, and the resulting segment means are shown as a heatmap. Asterisks indicate samples where corresponding mutation analyses were not performed due to low tumor purity (omental metastasis of CGOV279, right ovarian tumor of CGOV278) or military pattern of tumor samples (peritoneal metastases of CGOV63). Given the relatively lower number of distinct DNA molecules available from the p53 signature samples from CGOV62 and CGOV63, these samples were subjected to a more sensitive LOH analysis (Methods, Genome-wide imbalance analysis) and are not shown here

lesions in all patients analyzed. In patient CGOV62, a LOH of 9q (70.8–131.7 Mb) provided a clear difference between the STIC and all other carcinomas analyzed (Figs. 2 and 3). Likewise, chromosomal changes in 7q represented a distinguishing feature between the right STIC or right FT tumors and the remaining lesions (ovarian cancers, omental metastasis, and left STIC) in CGOV280 (Figs. 2 and 3). In patient CGOV279, multiple regions of allelic imbalance were present in a STIC near the FT carcinoma, while these were absent in a STIC that was not adjacent to this lesion.

**Evolutionary relationship of neoplastic lesions.** As somatic genetic alterations can be used to recreate the evolutionary history of tumor clones, we used the somatic sequence mutations and chromosomal alterations observed in each patient to determine the history of tumor clonal evolution. We employed a subclone hierarchy inference tool called SCHISM (SubClonal Hierarchy Inference from Somatic Mutations) which enables improved phylogenetic reconstruction by incorporating estimates of the fraction of neoplastic cells in which a mutation occurs (mutation cellularity)<sup>25</sup>. We estimated the cellularity of each mutation by correcting the observed allele frequencies for tumor purity and copy number levels (Methods section). In addition to the observed structural alterations, this approach allowed us to use 213 synonymous and non-synonymous somatic sequence alterations to construct the phylogenetic trees illustrated in Fig. 4 and Supplementary Data 5.

A SCHISM tree node represents cells harboring a unique compartment of mutations defining a subclone whereas an edge represents a set of mutations acquired by the cells in the progeny nodes that distinguish them from the cells in the parental node. By definition, for an individual cancer there could only be one parental clone, although there could be many different progeny subclones representing invasive or metastatic lesions or further evolution of the primary tumor. The optimal hierarchy among subclones is determined by examining all possible pairwise relationships between somatic alterations, and performing a heuristic search over the space of phylogenetic trees to identify a model that best explains the observed alterations.

In all samples, the SCHISM analysis of sequence and structural alterations suggested that the p53 signature or STIC lesions contained the ancestral clone for the observed cancers (Fig. 4). This evolutionary relationship was strengthened by the observation that nearly all of the alterations within the p53 signature and STIC lesions were shared by all other lesions. For example, the ovarian tumors of all cases displayed alterations that were shared in FT lesions but also contained additional changes, suggesting that these represented daughter clones of the latter tumors (Fig. 2). Likewise, the ovarian cancers or their immediate precursors were likely the direct parental clones for the metastases in CGOV62, CGOV278, and CGOV280 as demonstrated by the shared alterations that were not contained in earlier FT lesions. Overall, the phylogenetic model generated by these data suggests a progression from FT epithelium to p53 signatures and to STIC lesions which are then precursors of FT carcinoma, ovarian

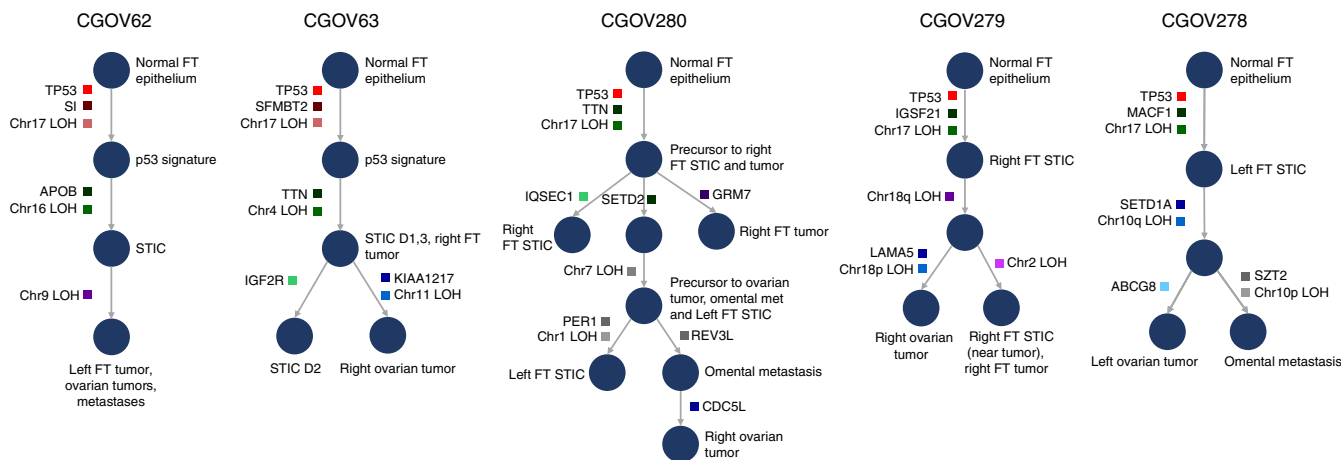


**Fig. 4** Schematic of tumor evolution. The history of tumor evolution in each patient is modeled as a subclonal hierarchy inferred from the somatic mutations and large scale genomic regions harboring loss of heterozygosity (LOH features) using the SCHISM framework, and is depicted as a tree. Each tree starts from a root node corresponding to the normal fallopian tube epithelium (germline). In all patients, mutations in *TP53* (red boxes) are among the earliest somatic alterations and are ubiquitously present in all tumor samples. Somatic alterations (boxes) are acquired along edges (arrows) of the tree, and example alterations are indicated in each case. Nodes of the tree represent cells whose genotype is described by the presence of somatic mutations and LOH features on the path connecting the node to the root of the tree. Each node is labeled with tumor samples harboring all upstream and lacking any downstream alterations. The trees inferred for all patients support a pattern of evolution with p53 signatures and STIC lesions as early events in tumorigenesis. Mutation clusters and LOH feature groups follow the same color code as Fig. 2

carcinoma, and metastatic lesions. In addition to the sequential accumulation of alterations in this linear evolution, we also observed branching phylogenetic trees due to continued evolution within STIC lesions as well as FT carcinomas and ovarian carcinomas (Fig. 4). We compared evolutionary trees resulting from SCHISM analysis with those derived by maximum parsimony phylogeny using PHYLIP and the results were similar in all cases (Fig. 4 and Supplementary Fig. 11).

Interestingly, patient CGOV280 had a right STIC, a right fallopian carcinoma, and a right ovarian cancer but also had a STIC in the left FT (Supplementary Fig. 5). In this case the SCHISM analysis suggested that the lesion in the left FT which was pathologically determined to be a STIC actually represented a metastatic lesion of the right ovarian cancer (Fig. 4). This lesion shared nearly all the alterations of the ovarian cancer but contained 10 single base substitutions and four additional regions of allelic imbalance on chromosomes 1, 13, and 22, and both the left STIC and right ovarian cancer had an additional region of allelic imbalance on chromosome 7 that was absent in the right STIC (Figs. 2 and 3). These observations are consistent with the above model of STIC to ovarian cancer progression, but suggest that in advanced disease ovarian cancers may also seed metastatic deposits throughout the peritoneum, including to the FT on the contralateral side.

**Genomic alterations in isolated STICs.** Neoplastic cells observed in the FTs rather than the ovaries removed from carriers of germline mutation of *BRCA1* and *BRCA2* provided the first indication of the FT as a potential cell of origin of HGSOc<sup>15, 26</sup>. Since <1.25% of HGSOc are diagnosed with stage I disease<sup>22</sup>, *BRCA* carriers provide a unique opportunity to analyze genomic alterations in isolated STICs without associated HGSOc. We examined neoplastic samples from three individuals with germline *BRCA* alterations where STIC lesions were incidentally identified after prophylactic bilateral salpingo-oophorectomy, and one patient where two STICs were identified after resection of a pelvic mass (Supplementary Data 1). We identified *BRCA1* or *BRCA2* sequence alterations or deletions in the germline of three

of these patients (*BRCA1* Q1200X, *BRCA2* L2653P, and a *BRCA2* 55 kb hemizygous deletion in CGOV65, CGOV64, and CGOV304, respectively), as well as somatic mutations in *TP53*, and LOH of both chromosome 13 and 17, encompassing the *BRCA1*, *BRCA2*, and *TP53* loci in all of these cases (Supplementary Figs. 6, 7, 8, and 9). Whole-exome analyses showed that the STIC lesions contained a total of 91, 23, 34, and 46 non-synonymous and synonymous somatic mutations, in CGOV65, CGOV64, CGOV303, and CGOV304, respectively. Overall, these analyses revealed that STICs in isolation in patients with or without germline *BRCA* changes have a roughly similar number of sequence changes to STICs in patients with sporadic tumors. These observations provide evidence that isolated STICs may act as precursors in the same manner as those identified in patients with sporadic advanced stages HGSOc analyzed in this study.

**Recurrent molecular alterations.** We examined tumors from the nine patients to identify recurrent non-silent sequence or chromosomal changes. Although no genes other than *TP53* were mutated in all patients analyzed, we identified mutations in ten genes that were altered in two or more patients (Supplementary Data 6). These included mutations in the tumors of two patients of the *PIK3R5* gene that encodes a regulatory subunit of the PI3-kinase complex. CGOV64 also had a somatic alteration in *PTEN* that together with changes in *PIK3R5* highlight the importance of the PI3K pathway in ovarian cancer<sup>11</sup>. Additional genes that were observed to be altered in other ovarian cancers through other large scale sequencing efforts such as TCGA<sup>11</sup> are indicated in Supplementary Data 6.

In addition to recurrent sequence changes, we found alterations in regions of allelic imbalances encompassing several tumor suppressor genes involved in ovarian cancer. Remarkably, these included losses of *BRCA1*, *BRCA2*, and *TP53* in all nine patients, and loss of *PTEN* for CGOV62, CGOV63, CGOV280, and CGOV64 (in addition to the somatic sequence alterations of these genes) (Supplementary Figs. 1–9). In all cases, the LOH observed in the metastatic lesions and ovarian tumor lesions for regions encompassing these genes were already present in the FT tumor

and STIC lesions. Considering the evolutionary model above, these data suggest that a combination of sequence changes in a few genes including *TP53* together with loss of the *TP53* wild-type allele as well as *BRCA1*, *BRCA2*, and *PTEN* may be crucial early events that are needed for the initiation of STICs<sup>27, 28</sup>.

**Evolutionary timeline of ovarian cancer development.** To estimate the time between the development of the earliest neoplastic clones in the FT and the development of ovarian and other metastatic lesions we used a mathematical model for comparative lesion analysis<sup>24, 29</sup>. This model estimates the time interval between a founder cell of a tumor of interest and the ancestral precursor cell assuming that mutation rates and cell division times are constant throughout a patient's life (Methods section). In patient CGOV62, this model would suggest ~1.9 years between the development of the STIC lesion and the ovarian cancer (90% CI, 0.5–4.2 years). For other patients this transition appears to have been slower as the average time between STICs and ovarian cancer among all patients was 6.5 years (1.4–10.7 years). Importantly, in patients with metastatic lesions, the time between the initiation of the ovarian carcinoma and development of metastases appears to have been rapid (average 2 years). There were either no additional mutations in metastatic lesions (e.g., CGOV62 omental, rectal or appendiceal metastasis or CGOV280 omental metastasis) or the number of additional changes was small (e.g., three changes in CGOV278 omental metastasis), reflecting the ease with which cancer cells located on the ovaries can subsequently seed additional peritoneal sites. Although the precise timing of this progression depends on assumptions related to mutation rates, which may change during tumor progression, models employing different rates all showed longer timeline from STIC lesions to ovarian tumors followed by rapid development of metastatic lesions (Methods section).

## Discussion

These results provide a comprehensive evolutionary analysis of sporadic HGSOC in five patients. Given the unique nature of the multiple samples we examined from each patient, our study may have certain limitations not typical of genome-wide efforts. First, the small size of the tumor samples compared to surrounding non-neoplastic tissue could potentially lead to low tumor purity. The high mutant allele fraction of *TP53* among cancer samples (average of 56–85%) indicates that this issue was largely overcome through LCM. Second, the small number of cells in p53 signature samples may have limited our genomic analyses for these lesions. The observation that all sequence changes in p53 signatures were also present in STIC and other carcinomas of multiple sites is consistent with our evolutionary model and suggests that these cells are likely to represent a parental clone of other neoplastic lesions. Third, our analysis was limited to ovarian cancers where STICs and other concomitant lesions were identified, and may therefore not be representative of all HGOCS. The absence of STIC lesions in ~40% of sporadic HGSOCs is likely due to an incomplete sampling of the FT or the overgrowth of the STIC by the carcinoma in the context of bulky disease, but may also reflect another site of origin that has yet to be determined for these cancers<sup>30</sup>. Fourth, this study did not intend to address the intra-tumoral heterogeneity within the carcinomas but rather focused on clonal changes within each tumor. Fifth, as in any evolutionary analyses, the genomic alterations we observed provide the most likely model of tumor development but do not exclude the possibility of other relationships. Nevertheless, our analyses of somatic alterations suggest that models where the ovarian cancer or metastatic lesions seed the FT tumors<sup>20, 21</sup>

(including STICs or p53 signatures) are infrequent and unlikely to be the source of most FT lesions.

Despite these potential limitations, the data we have obtained provide new insights into the etiology of ovarian Type II carcinoma and have significant implications for the prevention, early detection and therapeutic intervention of this disease. The results suggest that ovarian cancer is a disease of the FTs, with the development of p53 signatures and STICs as early events. The subsequent formation of a cancer in the ovaries represents a seeding event from a primary tumor in the FT that already contains sequence and structural alterations in key driver genes, including those in *TP53*, PI3K pathway, and *BRCA1/BRCA2* genes. The recurrent allelic imbalances observed in chromosomes 1, 6, 16, 18, 20, and 22 may suggest additional genes that are involved in this process. The timing of the progression from STICs to ovarian cancer in the cases we analyzed was on average 6.5 years, but seeding of metastatic lesions in these patients occurred rapidly thereafter. This timing is consistent with recent reports showing a difference of 7.7 years in the age of *BRCA* carriers with localized vs. advanced adnexal lesions<sup>31</sup>. This evolutionary timeline can help explain why most HGSOC patients are diagnosed at advanced stage (III/IV) with pelvic and peritoneal spread of disease, and why among asymptomatic *BRCA* germline mutation carriers half of the cases diagnosed with asymptomatic adnexal neoplasia have already seeded to pelvis or peritoneum (> IA)<sup>31</sup>. These observations are largely similar to other genomic analyses of the evolution of ovarian cancer<sup>19, 20, 23, 32</sup> as well as the recent analyses of STIC lesions that were reported while this study was under review<sup>33</sup>. Our study highlights the role of p53 signatures as early lesions in this evolutionary paradigm.

Our genomic analyses are consistent with population-based studies of the effects of salpingectomy on the risk of ovarian cancer. Prophylactic bilateral salpingo-oophorectomy has been shown to reduce the risk of developing ovarian cancer in *BRCA* mutation carriers to below 5%<sup>34, 35</sup>. Likewise, bilateral salpingectomy, performed as a contraceptive method instead of tubal sterilization, reduced the risk of ovarian cancer by 61% at 10 years<sup>36</sup>. Our study provides a mechanistic basis for these observations and has implications for clinical management in prevention of ovarian cancer. In high risk *BRCA* carriers, bilateral salpingectomy with delayed oophorectomy should be considered<sup>37</sup> through participation in ongoing clinical trials (NCT02321228; NCT01907789). In non-carriers, our work implies that for women who undergo surgery for benign uterine causes, total abdominal hysterectomy and bilateral salpingectomy with sparing of the ovaries should be considered<sup>38</sup>, and that bilateral salpingectomy may be a preferred contraceptive alternative to tubal ligation. The dual concepts in these recommendations for *BRCA* carriers and non-carriers are that removal of the FTs (rather than the ovaries) may be curative as it eliminates the underlying cellular precursors of ovarian cancer, and that preservation of the ovaries provides long term benefits due to decreased risk and fatalities from coronary heart disease and other illnesses<sup>39</sup>. A limitation of this approach is that as the precise timing of when potentially malignant cells shed from the FT and microscopically seed the ovary is unknown, removal of the tubes may not provide optimal risk-reduction.

Our observations also have implications for improved detection of ovarian cancer. Unfortunately, <1.25% of HGSOC are confined to the ovary at diagnosis<sup>22</sup>. Earlier detection of this disease is likely to benefit from the identification of a precursor lesion, as has been the case for many other tumor types. Our data suggest that FT neoplasia is the origin of ovarian serous carcinogenesis, and can directly lead to cancer of the ovaries and of other sites. Currently, the typical histopathologic evaluation of FTs typically involves a cursory evaluation of one or two

representative sections. Our study suggests that systematic sectioning and extensive examination of total FTs<sup>16</sup> should become common practice in pathology, and not confined to academic tertiary care centers. Depending on whether the FTs are removed for benign conditions, risk-reducing bilateral salpingectomy, or gynecological cancers, specific examination protocols should be applied<sup>16, 40</sup>. Given the window of time that appears to exist between the formation of FT lesions and development of ovarian cancer, these insights open the prospect of novel approaches for screening. Such approaches may be especially important given the limited therapeutic options currently available for ovarian cancer<sup>4, 5</sup>. Recent advances for ultrasensitive detection of genetic alterations in blood-based liquid biopsies, pap smears, and other bodily fluids<sup>41, 42</sup>, or imaging approaches may provide opportunities in early diagnosis and intervention.

## Methods

**Specimens obtained for sequencing analysis.** The study was approved by the Institutional Review Board at Brigham and Women's Hospital and the Johns Hopkins Hospital and all patients gave informed consent before inclusion. Five sequential patients with stage III sporadic HGSO, in whom a STIC was identified in their FTs (FT), were included. In addition, we included isolated STICs from three patients with germline *BRCA* deleterious alterations who underwent prophylactic bilateral salpingo-oophorectomy as well as a fourth patient who had bilateral salpingo-oophorectomy and hysterectomy in the context of a pelvic mass. All cases underwent complete tubal examination using the SEE-FIM protocol<sup>16</sup>. Formalin-fixed paraffin embedded (FFPE) blocks were retrieved from the pathology files at Brigham and Women's Hospital and Johns Hopkins Hospital within the 3 months following surgical diagnosis and stored at 4 °C to slow down nucleic acids degradation. All the cases were reviewed by a gynecologic pathologist (M.S.H., D.I.L., L.S.) that confirmed the diagnosis of STIC and/or p53 signature in the FT. Slides from each FFPE block, including early lesions, invasive carcinomas and metastases, were stained with hematoxylin and eosin, and analyzed by p53 IHC staining. In each FT, at least one STIC and/or p53 signature was identified and microdissected separately. Importantly, STICs were not pooled together if they were in the same section and were considered separate STICs.

**Immunohistochemistry and laser capture microdissection.** For accurate microdissection of early lesions including STIC and p53 signature, IHC staining of p53 was specifically adapted for LCM as previously described<sup>43</sup>. PEN membrane frame slides Arcturus (Life technologies, Carlsbad, CA) were used. Each slide was coated with 350  $\mu$ l of undiluted poly-L-lysine 0.1% w/v (Sigma, St. Louis, MO). For drying, the slides were placed in a slide holder for 60 min at room temperature. Tissue sections were cut and mounted on the pretreated membrane slides. Deparaffinization was performed in fresh xylene for 5 min twice, followed by 100% ethanol for 2 min, 95% for ethanol 2 min, and 70% ethanol for 2 min. Subsequently, the slides were transferred into distilled water for 5 min. Heat-epitope antigen retrieval (AR) was performed in Citrate Buffer (Dako, Carpinteria, CA) at low temperature (60 °C) for 44 h instead of 120 °C for 10 min to reduce tissue and DNA damage by high temperature. Retrieval solution was pre-warmed to 60 °C before usage. After incubation in the oven, the AR solution was left to cool down to room temperature and the slides were rinsed for 30 seconds in fresh 1 $\times$ PBS then incubated for 40 min with primary antibody anti-p53 (Epitomics, Burlingame) at 1:100 in a humidifying chamber. Before adding the secondary antibody, slides were washed twice for 1 min in fresh 1 $\times$ PBS. The secondary antibody, labeled polymer-HRP anti-mouse (Dako EnVision System-HRP (DAB), Carpinteria, CA) was applied for 30 min. Then, slides were washed twice for 1 min in fresh 1 $\times$ PBS. Chromogenic labeling was performed with 3,3-DAB substrate buffer and DAB chromogen (Dako EnVision System-HRP (DAB), Carpinteria, CA) for 5 min. Slides were washed again for 30 s in fresh distilled water. Dehydration was performed as follows: 70% ethanol for 30 s, 95% ethanol for 30 s, 100% ethanol for 30 s, and xylene for 30 s. The stained slides were microdissected within 2 h with the Arcturus XT LCM system (Life technologies, Carlsbad, CA).

**Hematoxylin staining for laser capture microdissection.** Invasive carcinomas from the ovaries, the FTs and intraperitoneal metastases or STICs from patients with negative p53 IHC staining were microdissected after Hematoxylin staining. Briefly, deparaffinization was performed in fresh xylene for 1 min twice followed by 100% ethanol for 1 min, 95% for ethanol 1 min, and 70% ethanol for 1 min. The slides were transferred into distilled water for 2 min before staining with Hematoxylin for 2 min. Subsequently, slides were rinsed in distilled water until they became clear before undergoing dehydration in 70% ethanol for 1 min, 95% ethanol for 1 min, 100% ethanol for 1 min, and xylene for 1 min. The stained slides were microdissected within 2 h.

**Sample preparation and next-generation sequencing.** DNA was extracted from patient whole blood using a QIAamp DNA Blood Mini QIAcube Kit (Qiagen Valencia, CA). Genomic DNA from FFPE blocks was extracted from the microdissected tissues using the QIAamp DNA FFPE Tissue kit (Qiagen, Valencia, CA). In brief, the samples were incubated in proteinase K for 16 h before DNA extraction. The digested mixture was transferred to a microtube for DNA fragmentation using the truXTRAC™ FFPE DNA Kit with 10 min shearing time as per the manufacturer's instructions (Covaris, Woburn, MA). Following fragmentation, the sample was further digested for 24 h followed by 1 h incubation at 80 °C. DNA purification was performed using the QIAamp DNA FFPE Tissue kit following the manufacturer's instructions (Qiagen, Valencia, CA). Fragmented genomic DNA from tumor and normal samples were used for Illumina TruSeq library construction (Illumina, San Diego, CA) according to the manufacturer's instructions or as previously described<sup>44</sup>. Exonic or targeted regions were captured in solution using the Agilent SureSelect v.4 kit or a custom targeted panel according to the manufacturer's instructions (Agilent, Santa Clara, CA). Paired-end sequencing, resulting in 100 bases from each end of the fragments for exome libraries and 150 bases from each end of the fragment for targeted libraries, was performed using Illumina HiSeq 2000/2500 and Illumina MiSeq instrumentation (Illumina, San Diego, CA).

## Next-generation sequencing data and identification of somatic mutations.

Somatic mutations were identified using VariantDx<sup>45</sup> custom software for identifying mutations in matched tumor and normal samples. Prior to mutation calling, primary processing of sequence data for both tumor and normal samples were performed using Illumina CASAVA software (v1.8), including masking of adapter sequences. Sequence reads were aligned against the human reference genome (version hg18 or hg19) using ELAND. Candidate somatic mutations, consisting of point mutations, insertions, and deletions were then identified using VariantDx across either the whole exome or regions of interest<sup>44</sup>. For samples analyzed using targeted sequencing, we identified candidate mutations that were altered in > 10% of distinct reads. For samples analyzed using whole-exome sequencing, we identified candidate mutations that were altered in > 10% of distinct reads with  $\geq 5$  altered reads in at least one sample, where coverage at the altered base was at least as high as the *TP53* alteration in that sample, and where the ratio of the coverage of the mutated base to the overall sequence coverage of that sample was > 20%. Identified mutations were reported as present in other samples of the same patient if the mutation was present in at least two distinct altered reads. Mutations present in polyN tract  $\geq 5$  bases, or those with an average distinct coverage below 50 $\times$  were removed from the analysis.

An analysis of each candidate mutated region was performed using BLAT. For each mutation, 101 bases including 50 bases 5' and 3' flanking the mutated base was used as query sequence (<http://genome.ucsc.edu/cgi-bin/hgBlat>). Candidate mutations were removed from further analysis, if the analyzed region resulted in > 1 BLAT hits with 90% identity over 70 SCORE sequence length. All candidate alterations were verified by visual inspection.

**Genome-wide allelic imbalance analysis.** We performed comparative analysis of LOH across the tumor samples from each patient to identify copy number alterations occurring in the course of tumor evolution. Minor allele frequency (MAF) of germline heterozygous SNPs with minimum coverage of 10 $\times$  in each tumor sample were segmented using circular binary segmentation algorithm (CBS)<sup>46</sup>. Genomic segments where the difference between tumor and normal MAF exceeded a threshold of 0.10 were labeled as harboring LOH. In each tumor sample, the minimum MAF across segments with minimum size of 10 Mb was calculated to provide a measure of sample purity. Each segment marked as LOH was assigned to one of the three confidence categories: (1) high confidence, segment MAF within 0.1 of the minimum sample MAF. (2) Intermediate confidence, segment MAF within 0.1–0.2 of the minimum sample MAF. (3) Low confidence, segment MAF exceeding the minimum sample MAF by > 0.2.

Next, sample level segments were intersected across the entire set of samples from each patient to derive patient level segments while accounting for the possibility of variable segment break points in different samples (Supplementary Data 7–11). Patient level segments were filtered to keep those covering a minimum of 20 SNPs and with minimum length of 10 Mb. The resulting segments were further narrowed down to only include those with high confidence LOH in at least one of the samples. Genomic segments with LOH in a subset of samples can serve as informative markers to track tumor evolution similar to somatic mutations. To increase the specificity in identifying this class of genomic segments, we required a minimum distance of 0.1 between the MAF of samples with and without LOH. To minimize the possibility of over-segmentation which could result in inflated estimates of the number independent structural alterations, we evaluated patient level segments with boundaries within a 5 Mb window. In cases where the LOH calls were identical and the difference of segment MAFs were  $\leq 0.05$  in all tumor samples, the segments were merged.

For CGOV62 and CGOV63, the number of germline heterozygous SNPs meeting the coverage criteria in p53 signature samples was significantly lower than the other samples from the same patient. Thus, we modified the approach above in these two patients to enable sensitive analysis of LOH in p53 signature samples. Initially, the patient level genomic segments of interest were defined excluding



p53 signature samples. Next, in each genomic segment, the minor allele of each overlapping germline SNP was determined by taking a majority vote over their minor alleles in the other samples. The coverage and minor allele read count for each SNP was derived using samtools (v0.1.19) mpileup module<sup>47</sup>. The segment MAF in p53 signature samples were calculated by dividing the sum of minor allele read counts across all SNPs by the total coverage of SNPs, circumventing the variance resulting from low coverage at individual SNPs. In each p53 signature sample, segments with MAF lower than that of the normal by at least 0.1 were marked as LOH.

**Copy number analysis.** The genome-wide copy number profiles were determined by analysis of the ratio of read counts in the tumor and matched normal whole-exome sequenced samples. In each sample, the number of reads mapping to genomic bins located in target and off-target regions were corrected for biases arising from GC-content, repetitive sequences, and target capture process using CNVKit (v.0.7.6) (<https://doi.org/10.1371/journal.pcbi.1004873>). The log ratio of the processed tumor to normal read counts provides a measure of copy number in each bin, and was segmented to yield genomic intervals at constant copy number levels. The difference in sequencing library size between the tumor and normal samples is another factor that needs to be accounted for when analyzing reads ratios in NGS-based copy number pipelines. In CNVKit, the log ratio values in each sample are adjusted by setting the median of autosomal bins to 0 in log space, assuming a median ploidy of 2 for the genome. Given the high prevalence of copy number aberrations in ovarian cancer and the high frequency of allelic imbalance in the present cohort, this assumption may not be accurate, and will manifest itself as a genome-wide bias or shift of log ratio values.

Therefore, an alternative approach for normalization of log ratio values was adopted, which takes into account the level of allelic imbalance in each genomic region. Briefly, genomic regions with the least degree of allelic imbalance were identified in each tumor sample, and used in a normalization process based on the notion that these regions can only be present in an even number of copies. The distribution of log ratio values among these regions was inspected to ensure that they belong to the same copy number level. Otherwise, a subset of regions at a common log ratio (and thus copy number) level were selected. By fixing the copy number of these segments at a specified level, one can solve for the genome-wide bias of log ratio values as follows, and thus identify the genome-wide integer copy number profile.

$$R = \log_2 \left( \frac{\alpha CN_T + (1 - \alpha) CN_N}{2} \right) - \delta$$

In the equation above,  $R$  represents the observed log ratio of read counts,  $\alpha$  is the purity of the tumor sample,  $CN_T$  and  $CN_N$  are the integer copy number of tumor and normal samples at a locus, and  $\delta$  is the genome-wide bias term. Given the value of tumor purity and copy number,  $\delta$  is the only unknown in the equation. To favor solutions with less complex genomes, the copy number of regions with complete allelic balance was initially set to 2. If the resulting solution was deemed implausible (e.g., by implying chromosome or chromosome arm scale homozygous deletions), the copy number of regions with complete allelic balance was assigned to 4 and an alternative solution was found (Supplementary Fig. 10).

Details of the genomic segments selected to solve for the genome-wide bias term  $\delta$  are as follows. In CGOV62, chromosomes 4 and 12 did not have allelic imbalance in any tumor samples. The solution assigning copy number two to these regions implied homozygous deletion of the p-arm of chrX in multiple samples; therefore, the simplest plausible solution assigned them to four copies. In CGOV63, chromosomes 6 and 15 did not have allelic imbalance in any of the tumor samples, and were assigned to two copies. No complete chromosome with absence of allelic imbalance across all tumor samples could be found in CGOV278. Therefore, four genomic regions with no allelic imbalance were selected for the normalization process above. These regions were chr8:38–69 Mb, chr12:62–85 Mb, chr18:7–19 Mb, chr20:23–35 Mb. The solution assigning these regions to two copies resulted in an implausible assignment of homozygous deletion to chr5:50–136 Mb. Therefore, assignment of four copies to the selected regions results in the simplest solution. In CGOV279, two genomic regions were selected for the normalization procedure: chr5: 64–131 Mb, chr20:17–36 Mb. Evaluation of log ratio values suggested that the two regions are present at different copy levels, as evidenced by a difference of ~0.60 in the log ratio values. The region on chr5, which had the lower log ratio level, was assigned to copy number 2. In CGOV280, chr16q had no allelic imbalance in any samples excluding the left FT STIC. Examination of log ratio values of chr16q in the left FT STIC supports a copy loss in that sample. The genome-wide bias term  $\delta$  was determined by assignment of two copies to chr16q in the four samples with no allelic imbalance, and one copy in the left FT STIC.

**Subclonal hierarchy analysis.** The tumor subclonality phylogenetic reconstruction algorithm SCHISM<sup>25</sup> was used to infer tumor subclonal hierarchies from the set of confidently called somatic mutations in each patient. Given the estimates of genome-wide copy number profile, most copy number aberrations seem to occur early in the evolution of disease and are common across the lesions analyzed from each patient. Thus, the majority of somatic mutations can be assumed to occur following the acquisition of copy number aberrations, and can be present in cancer cells with multiplicity of one (one mutated copy per cell). Using this assumption,

we can estimate mutation cellularity (or cancer cell fraction) from the observed reference and alternate read counts, and estimates of copy number, and tumor purity as follows.

$$V_{\text{exp}} = \frac{m\alpha C}{\alpha CN_T + (1 - \alpha) CN_N}$$

In the equation above,  $V_{\text{exp}}$  is the expected variant allele frequency of the mutation,  $m$  is the multiplicity of the mutation which is set to 1,  $\alpha$  is the purity of the tumor sample,  $C$  is the cellularity of the mutation, and  $CN_T$  and  $CN_N$  are the integer copy number of tumor and normal sample at the locus of the mutation. The observed alternate read count of the mutation can be modeled as a binomial random variable drawn from a distribution with probability parameter equal to  $V_{\text{exp}}$  and number of trials equal to the total sequence coverage of the mutation. We calculated the likelihood for observation of the alternate read counts for cellularity values spanning the range of 0–1 in increments of 0.01, and derived the maximum likelihood estimate and confidence interval for the mutation cellularity.

To obtain reliable estimates of mutation cellularity, we clustered mutations by joint presence or absence across the available tumor samples. This approach makes phylogenetic reconstruction more tractable and the cellularity of the resulting clusters can be estimated with higher accuracy than that of individual mutations. For each patient, a mutation was called as present or absent in each of the available tumor samples (10 samples from CGOV62, 6 samples from CGOV63, 5 samples from CGOV280, 4 samples from CGOV279, and 3 samples from CGOV278). To call the mutation present, we used a minimum allele frequency of 2% and 2 distinct mutant reads. Mutation clustering was performed by a greedy algorithm. Tumor purity in each tumor sample was estimated as the read count fraction of  $TP53$  mutation in each patient. Each patient harbored a single distinct  $TP53$  mutation that was present in all tumor samples, and we assumed the wild-type allele was lost, as supported by the ubiquitous LOH of chromosome 17. To derive a more comprehensive view of the evolution of these samples, we extended the original SCHISM framework to model acquisition of large scale somatic copy number alterations, which can be detected by analysis of allelic imbalance (including LOH). First, we extracted a set of high confidence genomic regions with ubiquitous, partially shared, or private LOH in tumor samples of each patient (Methods section). These regions of LOH served as binary features that could be used for evolutionary analysis, and were clustered into LOH feature groups with identical patterns of presence or absence across samples (Fig. 2). Each LOH feature group was compared to the somatic mutation clusters in each patient, with respect to its pattern of presence or absence across samples. In cases where a mutation cluster with the identical pattern could be found, the cluster and the LOH feature group were assumed to have occurred together in the course of tumor evolution. Otherwise, the LOH feature groups were modeled as distinct features, and added in post-hoc analysis by application of the lineage precedence rule from SCHISM; which requires cellularity of ancestor alterations to be greater than or equal to cellularity of descendant alterations in all tumor samples.

SCHISM was run with the above inputs and default parameter settings to infer the order of somatic alterations and thus define subclonal hierarchy in each patient. SCHISM software is freely available for non-profit use at <http://karchinlab.org/appSchism>.

Evolutionary trees resulting from SCHISM analysis were compared with those derived by maximum parsimony phylogeny using PHYLIP (Phylip-3.695, PARS method). For CGOV280, an adjustment to the tree was applied to account for multiple subclones in Right FT STIC.

**Estimating an evolutionary timeline.** Following the approach of Jones et al.<sup>29</sup>, the observed data are the number of somatic mutations in the STIC ( $n_j$ ), the number of mutations in the metastasis ( $n_k$ ), and the age at which the patient was diagnosed ( $t_k$ ), where somatic mutations include both sequence and structural alterations. Unknown is the birthdate ( $t_j$ ) of the cell that was the last common ancestor of the STIC and the metastasis. Assuming the mutation rate of somatic passenger mutations and the length of the cell cycle is constant, the number of somatic mutations in the metastasis cell that were present in the STIC follows a binomial distribution with parameters  $n_k$  and probability  $t_j/t_k$ . As  $t_j$  is unknown, we posit a conjugate beta probability distribution on the rate  $t_j/t_k$  with shape parameters  $a$  and  $b$  estimated from previous studies as described below. The posterior distribution of  $t_j/t_k$  is  $\beta(a + n_j, b + n_k - n_j)$  from which 90% highest posterior density intervals can be constructed with point estimates for the birthdate reported as the posterior mean. For simplicity, we refer to the highest posterior density as a confidence interval. To construct a prior for  $t_j/t_k$ , we draw on a previous study of four colorectal cancer patients<sup>29</sup> where a small number of additional passenger mutations were acquired by the cell that gave birth to the metastasis. On average, 95% of the mutations in the original adenocarcinoma were present in the metastases. We center the mean for the beta prior at 0.95 using shape parameters  $a = 34$  and  $b = 1.6$ . Our prior is equivalent to one patient having 34 passenger somatic mutations in the original lesion and 1.6 additional mutations to be acquired by cells that gave birth to the metastases. For patients with three samples in a linear tree as determined by evolutionary analyses (say, samples  $j$ ,  $k$ , and  $l$  where sample  $j$  is the STIC,  $l$  is the metastasis, and  $k$  is an intermediate sample), we first derived the posterior distribution for  $t_k$  comparing mutations in samples  $k$  and  $l$ . Next, we derived the posterior distribution of  $t_j$  integrating over all possible values of  $t_k$ , thereby fully

incorporating the uncertainty of the intermediate timepoint in the estimate of  $t_j$ . We evaluated three additional prior models, and found that that posterior inference under these alternative models given by 90% credible intervals for  $t_k - t_j$ , results in qualitatively similar timelines among different lesions in tumor progression.

**Data availability.** Sequence data have been deposited at the European Genome-phenome Archive, which is hosted at the European Bioinformatics Institute, under study accession EGAS00001002589.

Received: 26 January 2017 Accepted: 9 August 2017

Published online: 23 October 2017

## References

- Ferlay, J. et al. Cancer incidence and mortality patterns in Europe: estimates for 40 countries in 2012. *Eur. J. Cancer* **49**, 1374–1403 (2013).
- Siegel, R. L., Miller, K. D. & Jemal, A. Cancer statistics, 2015. *CA Cancer J. Clin.* **65**, 5–29 (2015).
- Cress, R. D., Chen, Y. S., Morris, C. R., Petersen, M. & Leiserowitz, G. S. Characteristics of long-term survivors of epithelial ovarian cancer. *Obstet. Gynecol.* **126**, 491–497 (2015).
- Menon, U., Griffin, M. & Gentry-Maharaj, A. Ovarian cancer screening—current status, future directions. *Gynecol. Oncol.* **132**, 490–495 (2014).
- Jacobs, I. J. et al. Ovarian cancer screening and mortality in the UK Collaborative Trial of Ovarian Cancer Screening (UKCTOCS): a randomised controlled trial. *Lancet* **387**, 945–956 (2016).
- Kurman, R. J. & Shih Ie, M. The dualistic model of ovarian carcinogenesis: revisited, revised, and expanded. *Am. J. Pathol.* **186**, 733–747 (2016).
- Kurman, R. J. & Shih Ie, M. The origin and pathogenesis of epithelial ovarian cancer: a proposed unifying theory. *Am. J. Surg. Pathol.* **34**, 433–443 (2010).
- Karst, A. M. & Drapkin, R. Ovarian cancer pathogenesis: a model in evolution. *J. Oncol.* **2010**, 932371 (2010).
- Levanon, K., Crum, C. & Drapkin, R. New insights into the pathogenesis of serous ovarian cancer and its clinical impact. *J. Clin. Oncol.* **26**, 5284–5293 (2008).
- Bowtell, D. D. et al. Rethinking ovarian cancer II: reducing mortality from high-grade serous ovarian cancer. *Nat. Rev. Cancer* **15**, 668–679 (2015).
- Cancer Genome Atlas Research Network. Integrated genomic analyses of ovarian carcinoma. *Nature* **474**, 609–615 (2011).
- Patch, A. M. et al. Whole-genome characterization of chemoresistant ovarian cancer. *Nature* **521**, 489–494 (2015).
- Cass, I. et al. BRCA-mutation-associated fallopian tube carcinoma: a distinct clinical phenotype? *Obstet. Gynecol.* **106**, 1327–1334 (2005).
- Piek, J. M. et al. BRCA1/2-related ovarian cancers are of tubal origin: a hypothesis. *Gynecol. Oncol.* **90**, 491 (2003).
- Piek, J. M. et al. Dysplastic changes in prophylactically removed Fallopian tubes of women predisposed to developing ovarian cancer. *J. Pathol.* **195**, 451–456 (2001).
- Medeiros, F. et al. The tubal fimbria is a preferred site for early adenocarcinoma in women with familial ovarian cancer syndrome. *Am. J. Surg. Pathol.* **30**, 230–236 (2006).
- Lee, Y. et al. A candidate precursor to serous carcinoma that originates in the distal fallopian tube. *J. Pathol.* **211**, 26–35 (2007).
- Kindelberger, D. W. et al. Intraepithelial carcinoma of the fimbria and pelvic serous carcinoma: evidence for a causal relationship. *Am. J. Surg. Pathol.* **31**, 161–169 (2007).
- Kuhn, E. et al. TP53 mutations in serous tubal intraepithelial carcinoma and concurrent pelvic high-grade serous carcinoma—evidence supporting the clonal relationship of the two lesions. *J. Pathol.* **226**, 421–426 (2012).
- McDaniel, A. S. et al. Next-generation sequencing of tubal intraepithelial carcinomas. *JAMA Oncol.* **1**, 1128–1132 (2015).
- Bashashati, A. et al. Distinct evolutionary trajectories of primary high-grade serous ovarian cancers revealed through spatial mutational profiling. *J. Pathol.* **231**, 21–34 (2013).
- Nik, N. N., Vang, R., Shih Ie, M. & Kurman, R. J. Origin and pathogenesis of pelvic (ovarian, tubal, and primary peritoneal) serous carcinoma. *Annu. Rev. Pathol.* **9**, 27–45 (2014).
- McPherson, A. et al. Divergent modes of clonal spread and intraperitoneal mixing in high-grade serous ovarian cancer. *Nat. Genet.* **48**, 758–767 (2016).
- Yachida, S. et al. Distant metastasis occurs late during the genetic evolution of pancreatic cancer. *Nature* **467**, 1114–1117 (2010).
- Niknafs, N., Beleva-Guthrie, V., Naiman, D. Q. & Karchin, R. SubClonal hierarchy inference from somatic mutations: automatic reconstruction of cancer evolutionary trees from multi-region next generation sequencing. *PLoS Comput. Biol.* **11**, e1004416 (2015).
- Leeper, K. et al. Pathologic findings in prophylactic oophorectomy specimens in high-risk women. *Gynecol. Oncol.* **87**, 52–56 (2002).
- Roh, M. H. et al. High-grade fimbrial-ovarian carcinomas are unified by altered p53, PTEN and PAX2 expression. *Mod. Pathol.* **23**, 1316–1324 (2010).
- Perets, R. et al. Transformation of the fallopian tube secretory epithelium leads to high-grade serous ovarian cancer in Brca;Tp53;Pten models. *Cancer Cell* **24**, 751–765 (2013).
- Jones, S. et al. Comparative lesion sequencing provides insights into tumor evolution. *Proc. Natl Acad. Sci. USA* **105**, 4283–4288 (2008).
- Perets, R. & Drapkin, R. It's totally tubular...riding the new wave of ovarian cancer research. *Cancer Res.* **76**, 10–17 (2016).
- Conner, J. R. et al. Outcome of unexpected adnexal neoplasia discovered during risk reduction salpingo-oophorectomy in women with germ-line BRCA1 or BRCA2 mutations. *Gynecol. Oncol.* **132**, 280–286 (2014).
- Karnezis, A. N. & Cho, K. R. Of mice and women - non-ovarian origins of "ovarian" cancer. *Gynecol. Oncol.* **144**, 5–7 (2016).
- Eckert, M. A. et al. Genomics of ovarian cancer progression reveals diverse metastatic trajectories including intraepithelial metastasis to the fallopian tube. *Cancer Discov.* **6**, 1342–1351 (2016).
- Rebbeck, T. R. et al. Prophylactic oophorectomy in carriers of BRCA1 or BRCA2 mutations. *N. Engl. J. Med.* **346**, 1616–1622 (2002).
- Kauff, N. D. et al. Risk-reducing salpingo-oophorectomy in women with a BRCA1 or BRCA2 mutation. *N. Engl. J. Med.* **346**, 1609–1615 (2002).
- Falconer, H., Yin, L., Gronberg, H. & Altman, D. Ovarian cancer risk after salpingectomy: a nationwide population-based study. *J. Natl. Cancer. Inst.* **107**, dju410 (2015).
- Kwon, J. S. et al. Prophylactic salpingectomy and delayed oophorectomy as an alternative for BRCA mutation carriers. *Obstet. Gynecol.* **121**, 14–24 (2013).
- McAlpine, J. N. et al. Opportunistic salpingectomy: uptake, risks, and complications of a regional initiative for ovarian cancer prevention. *Am. J. Obstet. Gynecol.* **210**, 471.e1–471.e11 (2014).
- Parker, W. H. et al. Ovarian conservation at the time of hysterectomy and long-term health outcomes in the nurses' health study. *Obstet. Gynecol.* **113**, 1027–1037 (2009).
- Longacre, T. A., Oliva, E., Soslow, R. A. Association of directors of, A. & Surgical, P. Recommendations for the reporting of fallopian tube neoplasms. *Hum. Pathol.* **38**, 1160–1163 (2007).
- Haber, D. A. & Velculescu, V. E. Blood-based analyses of cancer: circulating tumor cells and circulating tumor DNA. *Cancer Discov.* **4**, 650–661 (2014).
- Kinde, I. et al. Evaluation of DNA from the Papanicolaou test to detect ovarian and endometrial cancers. *Sci. Transl. Med.* **5**, 167ra4 (2013).
- Eberle, F. C. et al. Immunoguided laser assisted microdissection techniques for DNA methylation analysis of archival tissue specimens. *J. Mol. Diagn.* **12**, 394–401 (2010).
- Bertotti, A. et al. The genomic landscape of response to EGFR blockade in colorectal cancer. *Nature* **526**, 263–267 (2015).
- Jones, S. et al. Personalized genomic analyses for cancer mutation discovery and interpretation. *Sci. Transl. Med.* **7**, 283ra53 (2015).
- Olshen, A. B., Venkatraman, E. S., Lucito, R. & Wigler, M. Circular binary segmentation for the analysis of array-based DNA copy number data. *Biostatistics* **5**, 557–572 (2004).
- Li, H. et al. The sequence alignment/map format and SAMtools. *Bioinformatics* **25**, 2078–2079 (2009).

## Acknowledgements

We thank members of our laboratories for critical review of the manuscript. This work was supported by the Dr Miriam and Sheldon G. Adelson Medical Research Foundation (R.D. and V.E.V.), Commonwealth Foundation (V.E.V.), US National Institutes of Health grants CA121113 (V.E.V.), CA006973 (V.E.V.), CA083636 (R.D.), CA152990 (R.D.), CA200469 (I.S.), US Department of Defense grant OCRP-OC-100517 (R.J.K. and I.S.), the Honorable Tina Brozman Foundation for Ovarian Cancer Research (R.D.), the SU2C-DCS International Translational Cancer Research Dream Team Grant (SU2C-AACR-DT1415; V.E.V.), the Foundation for Women's Wellness (R.D.), and the Richard W. TeLinde Gynecologic Pathology Laboratory Endowment (I.S.). Stand Up To Cancer is a program of the Entertainment Industry Foundation administered by the American Association for Cancer Research. S.I.L.-G. is a recipient of grants from Arthur Sachs/Fulbright/Harvard, La Fondation Philippe et La Fondation de France—"Recherche clinique en cancérologie—Aide à la mobilité des chercheurs".

## Author contributions

S.I.L.-G., E.P., R.D., and V.E.V. were involved in the conception and design of this project. S.I.L.-G., E.P., V.A., N.N., R.K., R.D., and V.E.V. developed the methodology. S.I.L.-G., E.P., V.A., M.N., M.N., M.S.H., D.I.L., L.S., C.L.M., J.-C.T., M.B., A.A., L.D.W., R.K., T.-L.W., I.-M.S., R.D., and V.E.V. were involved in the acquisition of data, acquiring and managing patients, providing facilities and ect. S.I.L.-G., E.P., D.H., R.B., N.N., S.J., J.P., C. A.H., R.B.S., R.K., R.D., and V.E.V. were involved in the analysis and interpretation of data through statistical analysis, biostatistics and computational analysis. S.I.L.-G., E.P.,

D.H., R.D., and V.E.V. were involved in the writing, review and revision of the manuscript. S.I.L.-G, E.P., D.H., R.B., N.N., S.J., J.P., R.B.S., R.K., R.D., and V.E.V. were involved with administrative, technical or material support by reporting or organizing data or construction databases. R.K., R.D., and V.E.V supervised the study.

## Additional information

**Supplementary Information** accompanies this paper at doi:[10.1038/s41467-017-00962-1](https://doi.org/10.1038/s41467-017-00962-1).

**Competing interests:** V.E.V. is a founder of Personal Genome Diagnostics and is a member of its Scientific Advisory Board and Board of Directors. V.E.V. owns Personal Genome Diagnostics stock, which is subject to certain restrictions under university policy. The terms of this arrangement is managed by the Johns Hopkins University in accordance with its conflict of interest policies. The remaining authors declare no competing financial interests.

**Reprints and permission** information is available online at <http://npg.nature.com/reprintsandpermissions/>

**Publisher's note:** Springer Nature remains neutral with regard to jurisdictional claims in published maps and institutional affiliations.



**Open Access** This article is licensed under a Creative Commons Attribution 4.0 International License, which permits use, sharing, adaptation, distribution and reproduction in any medium or format, as long as you give appropriate credit to the original author(s) and the source, provide a link to the Creative Commons license, and indicate if changes were made. The images or other third party material in this article are included in the article's Creative Commons license, unless indicated otherwise in a credit line to the material. If material is not included in the article's Creative Commons license and your intended use is not permitted by statutory regulation or exceeds the permitted use, you will need to obtain permission directly from the copyright holder. To view a copy of this license, visit <http://creativecommons.org/licenses/by/4.0/>.

© The Author(s) 2017

## **Primordial germ cells as a potential cell of origin for mucinous cystic neoplasms of the pancreas and mucinous ovarian tumors**

Mucinous cystic neoplasms of the pancreas (MCN) and mucinous ovarian tumors (MOT) are rare tumors that occur only in women, mainly young who smoke. They have similar pathological and molecular features. So far the cell of origin of these rare tumors is not clearly identified. We hypothesize that MOT and MCN would share the cell of origin, i.e. primordial germ cells (PGCs) that would stop in the pancreas during their migration to gonadal ridges in early embryo. To test our hypothesis, we used unsupervised clustering of gene-expression profile of pancreatic and ovarian tumors and tissues, and single-cell RNA sequencing of PGCs. We found that MCN and MOT are closer to PGCs than their eutopic tissue. Our work could have implications for developing new therapies in these chemoresistant tumors.

---



# Primordial germ cells as a potential shared cell of origin for mucinous cystic neoplasms of the pancreas and mucinous ovarian tumors

Kevin M Elias<sup>1,2,3</sup>, Petros Tsantoulis<sup>4,5</sup>, Jean-Christophe Tille<sup>6</sup>, Allison Vitonis<sup>7</sup>, Leona A Doyle<sup>3,8</sup>, Jason L Hornick<sup>3,8</sup>, Gurkan Kaya<sup>4,9</sup>, Laurent Barnes<sup>9</sup>, Daniel W Cramer<sup>3,7</sup>, Giacomo Puppa<sup>6</sup>, Sarah Stuckelberger<sup>10</sup> , Jagmohan Hooda<sup>10</sup>, Pierre-Yves Dietrich<sup>4,5</sup>, Michael Goggins<sup>11</sup> , Candace L Kerr<sup>12</sup>, Michael Birrer<sup>13</sup>, Michelle S Hirsch<sup>3,8</sup>, Ronny Drapkin<sup>10</sup>  and Sana Intidhar Labidi-Galy<sup>4,5\*</sup> 

<sup>1</sup> Division of Gynecologic Oncology, Department of Obstetrics and Gynecology and Reproductive Biology, Brigham and Women's Hospital, Boston, MA, USA

<sup>2</sup> Division of Gynecologic Oncology, Dana-Farber Cancer Institute, Boston, MA, USA

<sup>3</sup> Harvard Medical School, Boston, MA, USA

<sup>4</sup> Department of internal medicine specialties, Faculty of Medicine, Université de Genève, Geneva, Switzerland

<sup>5</sup> Department of Oncology, Hôpitaux Universitaires de Genève, Geneva, Switzerland

<sup>6</sup> Division of Pathology, Hôpitaux Universitaires de Genève, Geneva, Switzerland

<sup>7</sup> Department of Obstetrics and Gynecology, Epidemiology Center, Brigham and Women's Hospital, Boston, MA, USA

<sup>8</sup> Department of Pathology, Brigham and Women's Hospital, Boston, MA, USA

<sup>9</sup> Division of Dermatology, Hôpitaux Universitaires de Genève, Geneva, Switzerland

<sup>10</sup> Penn Ovarian Cancer Research Center, Department of Obstetrics and Gynecology, University of Pennsylvania, Philadelphia, PA, USA

<sup>11</sup> Department of Pathology, Johns Hopkins Hospital, Baltimore, MD, USA

<sup>12</sup> Department of Biochemistry and Molecular Biology, University of Maryland, Baltimore, MD, USA

<sup>13</sup> Division of Hematology–Oncology, University of Alabama at Birmingham Comprehensive Cancer Center, Birmingham, AL, USA

\*Correspondence to: S Labidi-Galy, Department of Oncology, Hôpitaux Universitaires de Genève, Rue Gabrielle Perret-Gentil 4, 1204, Geneva, Switzerland. E-mail: intidhar.labidi-galy@hcuge.ch

## Abstract

Mucinous ovarian tumors (MOTs) morphologically and epidemiologically resemble mucinous cystic neoplasms (MCNs) of the pancreas, sharing a similar stroma and both occurring disproportionately among young females. Additionally, MOTs and MCNs share similar clinical characteristics and immunohistochemical phenotypes. Exome sequencing has revealed frequent recurrent mutations in *KRAS* and *RNF43* in both MOTs and MCNs. The cell of origin for these tumors remains unclear, but MOTs sometimes arise in the context of mature cystic teratomas and other primordial germ cell (PGC) tumors. We undertook the present study to investigate whether non-teratoma-associated MOTs and MCNs share a common cell of origin. Comparisons of the gene expression profiles of MOTs [including both the mucinous borderline ovarian tumors (MBOTs) and invasive mucinous ovarian carcinomas (MOCs)], high-grade serous ovarian carcinomas, ovarian surface epithelium, Fallopian tube epithelium, normal pancreatic tissue, pancreatic duct adenocarcinomas, MCNs, and single-cell RNA-sequencing of PGCs revealed that both MOTs and MCNs are more closely related to PGCs than to either eutopic epithelial tumors or normal epithelia. We hypothesize that MCNs may arise from PGCs that stopped in the dorsal pancreas during their descent to the gonads during early human embryogenesis, while MOTs arise from PGCs in the ovary. Together, these data suggest a common pathway for the development of MCNs and MOTs, and suggest that these tumors may be more properly classified as germ cell tumor variants.

Copyright © 2018 Pathological Society of Great Britain and Ireland. Published by John Wiley & Sons, Ltd.

**Keywords:** mucinous ovarian tumor; mucinous cystic neoplasm; primordial germ cells; pathogenesis; RHOB

Received 20 December 2017; Revised 13 August 2018; Accepted 25 August 2018

No conflicts of interest were declared.

## Introduction

Epithelial ovarian cancers (EOCs) are the leading cause of gynecologic cancer death in the developed world [1]. EOC are histologically classified into four major subtypes: serous, clear cell, endometrioid, and mucinous. Of these, the mucinous type has been the least

studied, probably because of its less frequent incidence, comprising about 3% or less of EOCs [2]. Mucinous tumors are morphologically distinct from all other epithelial ovarian cancers. They tend to be borderline or low grade, have an indolent course and a favorable prognosis, and occur in young female smokers. Some mucinous ovarian tumors (MOTs) have been shown to

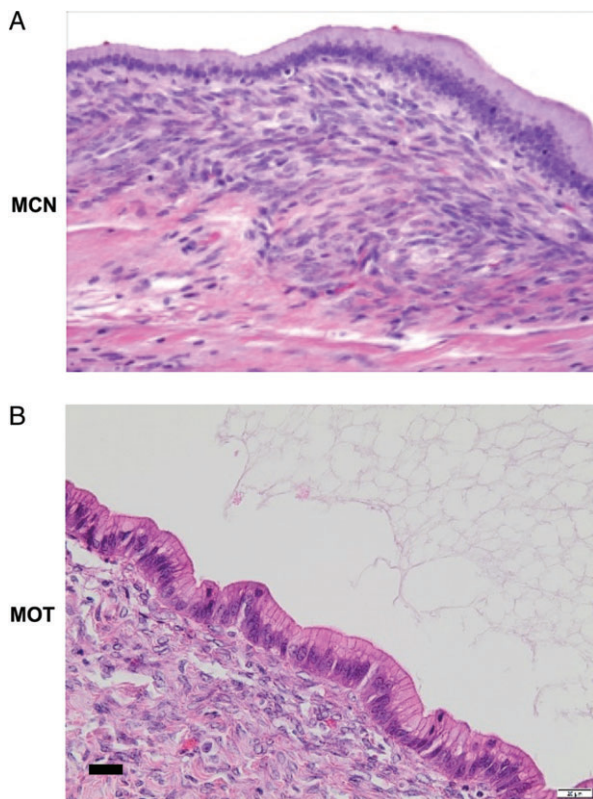


**Figure 1.** Hematoxylin and eosin sections of a mucinous cystic neoplasm (MCN) of the pancreas (A) and a mucinous ovarian tumor (MOT) (B). Note the similar morphology of the overlying, mucin-filled epithelium and dense underlying stroma. Scale bar = 20  $\mu$ m.

arise from germ cell tumors [3]. This has raised the hypothesis that these tumors might arise from a different cell of origin than other EOCs.

Morphologically, MOTs closely resemble a rare pancreatic tumor, mucinous cystic neoplasm (MCN) (Figure 1). MCN is distinct among pancreatic lesions by the presence of a unique ovarian-like stroma [4]. MCN, like MOT, is typically a low-grade neoplasm that occurs mainly in young women. Like MOTs, MCNs tend to be indolent, usually localized to the body and/or tail of the pancreas [5,6]. Whole-exome sequencing studies have revealed molecular similarities between MOT and MCN, with mutations at similar frequencies in *RNF43* and *KRAS* [7,8]. However, if MOT and MCN are somehow related, why do MCNs arise mainly in women (sex ratio 1:10), in the pancreas (a non-gynecologic organ), and why do they have such specific anatomic localization in the body/tail of the pancreas?

In human embryos, the precursors of gametes, termed primordial germ cells (PGCs), are initially located in extragonadal regions (yolk sac) at the third week of development and migrate caudally [9]. In the 5-week-old embryo, PGCs reach the dorsal mesentery, which becomes the body, tail, and isthmus of the pancreas. PGCs then continue to move laterally around both sides of the coelomic angle, pass beyond the primitive mesonephros bodies, and eventually enter the gonadal ridges at the ninth week [9]. This raises the possibility

that MOT and MCN could derive from a common embryologic precursor, PGCs that stopped in the body or tail of the pancreas during their migration to the gonads.

Here, we consider the possibility of a biological relationship among ovarian and pancreatic mucinous tumors based on the gene expression patterns of tumor and normal tissue samples. We demonstrate that the closest normal cell type to either of these tumors is in fact the PGC, rather than either pancreatic or gynecologic epithelia. We suggest that MOT and MCN may be related tumors and more properly be classified as unusual germ cell tumor variants.

## Materials and methods

### Ethics approval

Review of patient medical records and use of archival specimens were approved by the Brigham and Women's Hospital Institutional Review Board Protocols 2013P000553 and 2016P002742.

### Isolation and gene expression profile of human PGCs

Data were pooled from two published gene expression datasets [10,11]. We used gene expression profiles from 8- to 11-week human PGCs (one male and one female) [10] (E-MTAB-6851). As described by the authors, PGCs had been isolated using magnetic cell sorting technology (MACS) and indirect labeling of cells with magnetically tagged goat anti-mouse IgM antibodies toward a mouse anti-SSEA1 antibody [Miltenyi Biotec, Bergisch Gladbach, Germany, clone REA321; diluted (1:5)] [10]. To analyze gene expression profiles, the Affymetrix<sup>®</sup> Human U133 Plus 2.0 GeneChip (Affymetrix, Santa Clara, CA, USA) was used. In addition, single-cell RNA-sequencing data were obtained from five samples of human female PGCs from week 4 to week 11 (GSE63818) (see supplementary material, Table S1) [11]. For that study, human gonads from 7- to 11-week embryos were dissected in Dulbecco's phosphate buffered saline (DPBS) (plus 1% fetal bovine serum). The gonads were washed in DPBS twice before digestion in 250  $\mu$ l of Accutase Cell Detachment Solution (Millipore #SCR005; Merck KGaA, Darmstadt, Germany) for 5 min at 37  $^{\circ}$ C. For the isolation of pure human PGCs from 7- to 11-week embryos, 100  $\mu$ l of FcR Blocking Reagent and 100  $\mu$ l of CD117 MicroBeads (#130-091-332; Miltenyi Biotec) were added to the 300  $\mu$ l of gonad cell suspension and mixed well by gently pipetting. After magnetic enrichment, the fraction containing PGCs (CD117-positive cells) was further sorted by BD FACSAria (BD Biosciences, Franklin Lakes, NJ, USA), and CD117-positive cells were collected for downstream analysis. The purity of PGCs was assayed by immunostaining for OCT4 and single-cell RT-qPCR for human *OCT4* transcripts.

For 4-week embryos, the aorta–gonads–mesonephros regions were dissected and a single-cell suspension was obtained by digestion with Accutase. Then the cell suspension was inspected under the microscope carefully and the large cells (less than 0.1%) were manually picked out with a mouth pipette. For RNA sequencing, a DNA library prep kit for Illumina® (New England Biolabs Inc, Ipswich, MA, USA) was used to prepare the sequencing library following the manufacturer's protocol. Libraries were pooled and sequenced on Illumina® HiSeq2500 (Illumina Inc, San Diego, CA, USA) sequencers using 100-bp paired-end sequencing, as previously described [11].

### Gene expression profile of pancreatic and ovarian samples

Data were pooled from several published gene expression datasets [12–16] (see supplementary material, Table S1). We compiled gene expression data from 16 samples of normal pancreatic tissue (GSE16515) [16], 36 pancreatic ductal adenocarcinomas (PDACs) (GSE16515) [16], the epithelial component of seven microdissected MCNs of the pancreas (E-MTAB-6853) [13] (two distinct samples from MCN4 were analyzed), the epithelial component of eight microdissected mucinous borderline ovarian tumors (MBOTs) and nine microdissected invasive mucinous ovarian carcinomas (MOCs) (E-MTAB-6844) [12], 24 microdissected samples of Fallopian tube epithelium (FT) (GSE10971) [14], the epithelial component of 13 microdissected high-grade serous ovarian carcinomas (HGSOCs) (GSE10971) [14], and six microdissected samples of ovarian surface epithelium (OSE) (GSE40595) [15]. All array expression data were generated with Affymetrix® microarrays (Affymetrix, Santa Clara, CA, USA). Our raw data are available at ArrayExpress (<https://www.ebi.ac.uk/arrayexpress/>): E-MTAB-6844, E-MTAB-685, and E-MTAB-6853.

### Data processing

For all array expression datasets, we recovered the raw data in the form of .CEL files, which were imported and processed in the R language and environment for statistical computing [17]. Raw data from each dataset was treated with the Robust Multi-array Average (RMA) algorithm [18], from the 'Affy' BioConductor package [19] using default settings. For genes mapping to multiple probes, the mean expression was used as a gene-level summary. Batch effects were attenuated by using a previously published list of endogenous control genes [20] to correct for unwanted variation [21].

The single-cell RNAseq data (GSE63818) were obtained as RPKM estimates and then filtered to exclude genes with extremely low expression (< 0.3 RPKM) or extremely low variance (bottom 1%). For every sample, the gene expression estimates were aggregated by calculating the mean expression in the isolated single cells. The RNAseq expression estimates were mean-centered

against the microarray datasets to obtain a similar distribution of values. The mean-variance plot for all common genes from both platforms was used as a quality control and confirms that the results have comparable distributions for most of the expression range.

### Class comparison

Differentially expressed genes between groups were identified using the *limma* package with default options, with gene expression ordered by absolute log fold-change (FC) using a false discovery rate (FDR) of 0.05 or less [22]. These comparisons identified genes whose expression was significantly altered between PGCs, MCN specimens, PDACs, and normal pancreatic tissue. Similarly, we identified genes whose expression was different between PGCs, MBOT, HGSOC, OSE, and FT specimens. Dendrograms were created using hierarchical clustering (hclust) and a Euclidean distance metric on genes expressed by all samples ( $N = 9626$ ). The most discriminative and statistically significant genes were ordered by log FC and summarized in heatmaps. During the revision of the manuscript, the MOC samples were added and a second distinct analysis was done in order to identify genes whose expression was different between PGCs, MBOT, MOC, HGSOC, OSE and FT specimens. A new gene list was also generated ( $N = 9626$ ).

### Gene set enrichment analysis

Common biologic pathways for the 1000 most similarly expressed genes (as measured by absolute log FC) between PGCs and MCN or PGCs and MBOT were examined by gene set enrichment analysis using DAVID v.6.8 [23]. The top ten gene ontology terms most over-represented by adjusted  $P$  value after a Bonferroni correction are shown.

### Laser capture microdissection and RNA extraction for RT-qPCR

New samples were selected for validation of gene expression profiles by RT-qPCR. Sections were cut at 4  $\mu\text{m}$  thickness from each sample and stained with hematoxylin and eosin (H&E) for review to ensure proper tissue orientation and histology (JCT and GP). Fresh-frozen samples of HGSOC ( $n = 5$ ), PDAC ( $n = 5$ ), and normal pancreatic tissue ( $n = 5$ ) were macrodissected. The epithelium component from frozen samples of MCNs ( $n = 4$ ) and MBOTs ( $n = 4$ ) were laser capture-microdissected using a Leica LMD7000 instrument (Leica Microsystems, Wetzlar, Germany) (see supplementary material, Figure S1). Shortly before microdissection, 10  $\mu\text{m}$  sections were cut, adhered onto frame slides, immediately fixed in ethanol 75% for 2 min, stained with hematoxylin, washed in water, dehydrated in graded alcohols, then xylene, and microdissected. RNA was also isolated from immortalized OSE cell lines ( $n = 2$ ) and immortalized FT cell lines ( $n = 4$ ) [24]. Total RNA was extracted from



tissues or cell lines using a QIAGEN® RNeasy kit (#74104; QIAGEN, Valencia, CA, USA) following the manufacturer's protocol. Measurement of total RNA concentration was performed with a Qubit fluorimeter (Thermo Fisher Scientific, Waltham, MA, USA) and quality assessed with an Agilent Bioanalyzer (Agilent Technologies, Lexington, MA, USA).

### RT-qPCR

To confirm expression of identified genes, cDNA was synthesized from 150 ng of total RNA using a mix of random hexamers – oligo d(T) primers and Primer-Script reverse transcriptase enzyme (Takara Bio, Inc, Kusatsu, Japan), following the supplier's instructions. SYBR Green assays were designed using the program Primer Express v 2.0 (Applied Biosystems, Waltham, MA, USA) with default parameters. Amplicon sequences were aligned against the human genome by BLAST to ensure that they were specific for the gene being tested. Oligonucleotides were obtained from Thermo Fisher Scientific (Waltham, MA, USA). The efficiency of each design was tested with serial dilutions of cDNA. PCR reactions (10 µl volume) contained diluted cDNA, 2× Power Up SYBR Green Master Mix (Thermo Fisher Scientific), and 300 nM of forward and reverse primers. PCR primers are listed in the supplementary material, Table S2. PCR reactions were performed on an SDS 7900 HT instrument (Applied Biosystems) with the following parameters: 50 °C for 2 min, 95 °C for 10 min, and 45 cycles of 95 °C for 15 s and 60 °C for 1 min. Each reaction was performed in three replicates on a 384-well plate. Raw  $C_T$  values obtained with SDS 2.2 (Applied Biosystems) were imported in Excel (Microsoft, Redmond, WA, USA). Normalization factor and fold-changes were calculated using the GeNorm method [25]. Target gene  $C_T$  values were normalized to  $\beta$ -tubulin (*TUBB*) and  $\beta$ -actin (*ACTB*) transcripts.

### Chart review of MCN and MOT

Twenty-three cases of MCNs were identified by querying the Brigham and Women's Hospital (BWH) pathology database. All cases were confirmed by a staff GI pathologist (JLH or LAD) to be MCN and not an intraductal pancreatic mucinous neoplasm (IPMN), mucinous adenocarcinoma, or other form of pancreatic neoplasm. Medical charts for the cases were reviewed to extract clinical data after approval by the BWH Institutional Review Board (Protocol 2013P000553). MOT cases were identified from the New England Case Control (NECC) study as previously described [26]. In brief, cases were enrolled from July 1984 to September 1987 (NECC2), May 1992 to March 1997 (NECC3), August 1998 to April 2003 (NECC4), and October 2003 to November 2008 (NECC5). The four phases enrolled 2475 cases including 2274 with epithelial ovarian cancers, of which 287 were mucinous. Controls for NECC3 were identified by random-digit dialing supplemented

Table 1. Patient clinical characteristics

	Mucinous ovarian tumors N = 287N (%)	Mucinous cystic neoplasms N = 23N (%)	P value
Sex			
Female	287 (100)	23 (100)	1.0
Male	0 (0)	0 (0)	
Age, years			
< 44	128 (44.6)	6 (26)	0.12
44–53	69 (24.0)	6 (26)	
54–62	46 (16.0)	8 (35)	
> 62	44 (15.3)	3 (13)	
Race			
White	273 (95.1)	18 (78.2)	0.008
Non-white	14 (4.9)	5 (21.7)	
Ever-smoker			
No	123 (42.9)	12 (63.1)	0.10
Yes	164 (57.1)	7 (36.8)	
Unknown		4	
Stage*			
I	213 (88.8)	23 (100)	
II–IV	27 (11.3)	0 (0)	0.14

\*Missing for 47 cases.

with residents' lists for older controls. About 10% of households contacted had an eligible control and of these, 421 (72%) agreed to participate.

### Statistical methods

Unless specified otherwise, all statistical tests were performed in R v.3.4.3 using *P* value correction for multiple comparisons to account for the false discovery rate (FDR) [17]. Clinical characteristics of patients with MCN and MOT were compared using a *z*-test for population proportions. Median fold-changes of gene expression from RT-qPCR data were compared using a pairwise Student's *t*-test.

## Results

### Clinical presentation for patients with mucinous ovarian tumors or mucinous cystic neoplasms

We performed a chart review to investigate clinical similarities between patients with MOTs or MCNs. From BWH, we identified 23 cases of MCNs. Tumors occurred exclusively in women (Table 1). Compared with the cases in the NECC study, women with MCNs were similar in terms of age, smoking history, and stage at diagnosis. The only notable difference appeared to be in racial distribution, as a larger proportion of MCNs than MOTs were diagnosed among non-white women.

### Similar gene expression profiles for MCNs of the pancreas and PGCs

Unsupervised hierarchical clustering was performed for gene expression profiles from seven MCNs and 36 PDACs, 16 normal pancreatic tissues, and seven human

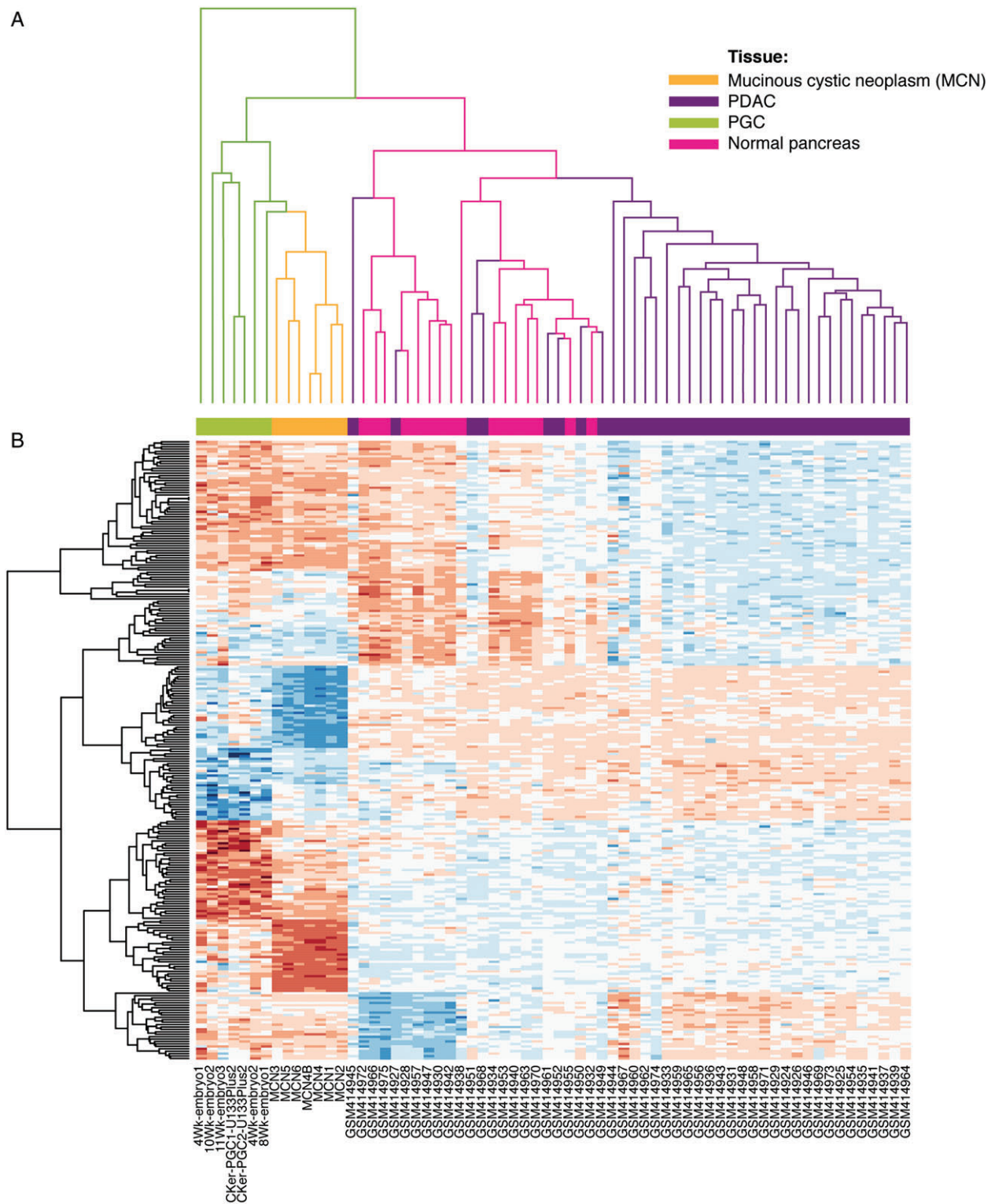


Figure 2. Unsupervised hierarchical clustering of PGCs and pancreatic and MCN samples. (A) Expression of 9626 genes in MCNs, PGCs, PDACs, and normal pancreatic tissue. Dendrogram of the 66 experimental samples. Hierarchical clustering illustrates that MCN specimens are closely associated with PGCs (left branch), whereas pancreatic ductal adenocarcinomas (PDACs) group together with normal pancreatic tissue (right branch). (B) Heatmap of the differentially expressed genes in MCNs, PGCs, PDACs, and normal pancreatic tissue. Blue = high expression; brown = low expression.

PGC samples. The dendrogram in Figure 2A shows the unsupervised hierarchical clustering of all 66 samples based on the expression of 9626 genes (the intersection of available genes over all datasets). The samples separated into two main branches. The left branch

contains PGCs and MCNs. The right branch includes PDACs and normal pancreatic tissues. This dendrogram suggests that PGCs are more closely related to MCNs and PDACs are more closely associated with normal pancreatic tissue. Importantly, a small number

of PDAC samples clustered together with normal pancreatic samples, but all MCN samples were clearly distinct. The heatmap displays the most differentially expressed, statistically significant genes per sample type (Figure 2B). It clearly demonstrates important similarities between PGC and MCN samples, compared with normal pancreas and PDAC. Importantly, the single-cell PGC RNA sequencing dataset and array expression PGC dataset are highly concordant, emphasizing the consistency of these gene expression profiles. Together, these data suggest that global gene expression in MCNs more closely resembles that of PGCs rather than normal pancreatic tissue or other pancreatic tumors.

We used *limma* and a cut-off at a FDR of 0.05 to identify common differentially expressed genes between the MCN and PGCs samples on the one hand and the PDAC and normal pancreatic tissue samples on the other hand. The list of 1000 top differentially expressed genes are listed in the supplementary material, Dataset S1. Gene set enrichment analysis of the shared gene sets between MCNs and PGCs showed overrepresentation of genes related to phosphoproteins (see supplementary material, Table S3).

#### Similar gene expression profiles for MOTs and PGCs

Unsupervised hierarchical clustering was performed from microarrays of eight MBOTs, 24 FT and six OSE samples, 13 HGSOCs, and seven PGCs. The dendrogram in the supplementary material, Figure S2A represents the unsupervised hierarchical clustering of all 58 samples. MBOT samples were aligned more closely with PGCs than OSE, whereas HGSOCs grouped with either OSE or FT samples. The heatmap summarizes differentially expressed genes in each sub-group of samples (see supplementary material, Figure S2B). It indicates that MBOT and PGC samples have important similarities and are more distantly related to OSE, HGSOCs, and FT, respectively. MBOTs are closely related to MOCs and a continuum appears to be present from borderline to carcinoma, which is different from other epithelial EOCs [27]. Thus, we questioned whether MOCs resemble PGCs. Unsupervised hierarchical clustering was performed from microarrays of eight MBOTs, nine MOCs, 24 FT and six OSE samples, 13 HGSOCs, and seven PGCs. MBOT and MOC samples clustered together and were aligned more closely with PGCs than OSE (Figure 3A,B). These data suggest that global gene expression in MOTs more closely resembles that of PGCs than Müllerian epithelia. The normal FT cells clustered closely with HGSOCs, adding further evidence to the theory that FT cells give rise to most HGSOCs [24,28,29]. Genes similarly expressed among MBOTs, MOCs, and PGCs versus HGSOCs, OSE, and FT were selected using *limma* at a FDR of 0.05. A complete list of the 1000 top genes is shown in the supplementary material, Dataset S2. Gene set enrichment analysis again showed a high percentage of phosphoproteins (see supplementary material, Table S4).

#### Shared gene expression among PGCs, MCNs, and MOTs

By comparing the lists of genes generated in the supplementary material, Datasets S1 and S2, we observed that many genes had similar expression patterns shared among the MOTs, PGCs, and MCN samples. Genes differentially expressed between MOTs (MBOTs and MOCs), MCNs, and PGCs, and the pancreatic and adnexal eutopic normal and tumor samples were selected and ordered by log FC (see supplementary material, Figure S3). A complete list of the 411 most differentially expressed genes among all the mucinous tumor types and PGCs versus other tissue types is shown in the supplementary material, Dataset S3. Three genes highly expressed and common among MOTs (MBOTs and MOCs), MCNs, and PGCs were *CPM*, *RHOB*, and *ASPN*. To validate the microarray results, these three genes were selected for RT-qPCR analysis. Expression levels for the three genes were determined on independent samples, not included in the microarray analyses. In agreement with our microarray data, MCNs were found to express higher levels of *ASPN*, *RHOB*, and *CPM* compared with normal pancreatic tissue or PDAC, although only *RHOB* compared with PDAC reached statistical significance ( $p = 7.2 \times 10^{-3}$ ) (Figure 4A). Consistent with our profiling data, MBOT samples expressed much higher levels of *ASPN* compared with OSE ( $p = 10^{-5}$ ), FT ( $p = 4.3 \times 10^{-5}$ ) or HGSOC ( $p = 3.14 \times 10^{-3}$ ). *RHOB* was also strongly expressed by MBOTs and this was statistically significant compared with OSE ( $p = 3.8 \times 10^{-4}$ ), FT ( $p = 1.3 \times 10^{-4}$ ) or HGSOC ( $p = 0.01$ ). *CPM* was not tissue-specific (Figure 4B). Since our RT-qPCR data were obtained on specimens distinct from those of the microarray data, our observations suggest that *RHOB* and *ASPN* could be specific new markers for these mucinous neoplasms.

#### Discussion

MOTs and MCNs are both rare, indolent mucinous neoplasms with a propensity to develop in young women who smoke. They share common epidemiologic, clinical, morphologic, and genomic features. The histological presence of a unique ovarian-type stroma is mandatory to diagnose MCNs and distinguishes MCNs from other pancreatic neoplasms [30]. MCNs nearly always occur in the body or tail of the pancreas, and unlike PDAC, do not communicate with the pancreatic ducts. Likewise, MOTs are unique among ovarian tumors in that they usually arise within large parenchymal cysts, not along the Fallopian tube–ovarian interface. The tumors share expression of CK7, and unlike gastrointestinal tumors, have only variable expression of CK20 and do not express MUC2 [31]. The stroma of MOTs and MCNs also show similar expression patterns for sex hormone receptors [32]. Here, we consider the possibility that MOTs and MCNs could derive from a



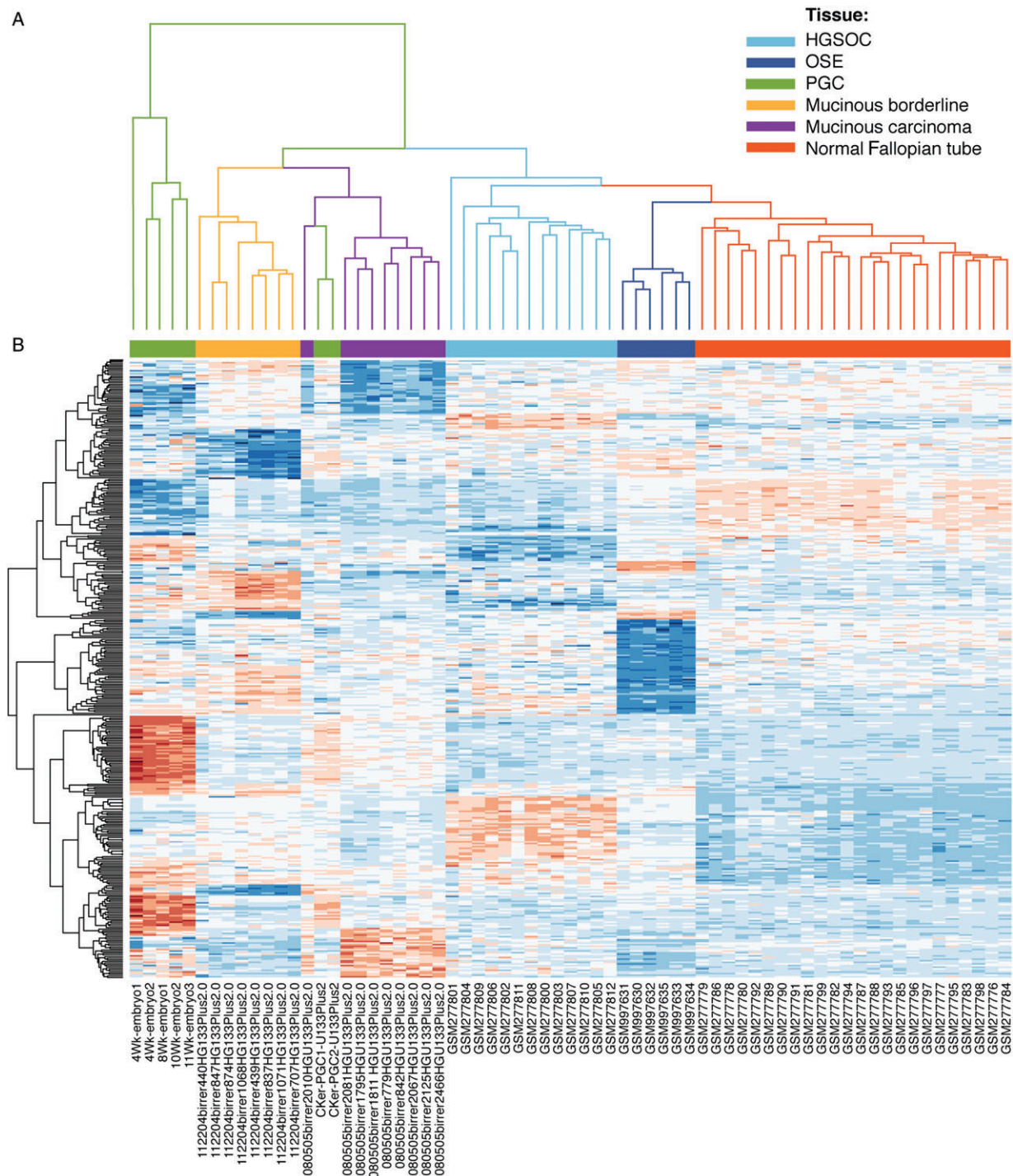
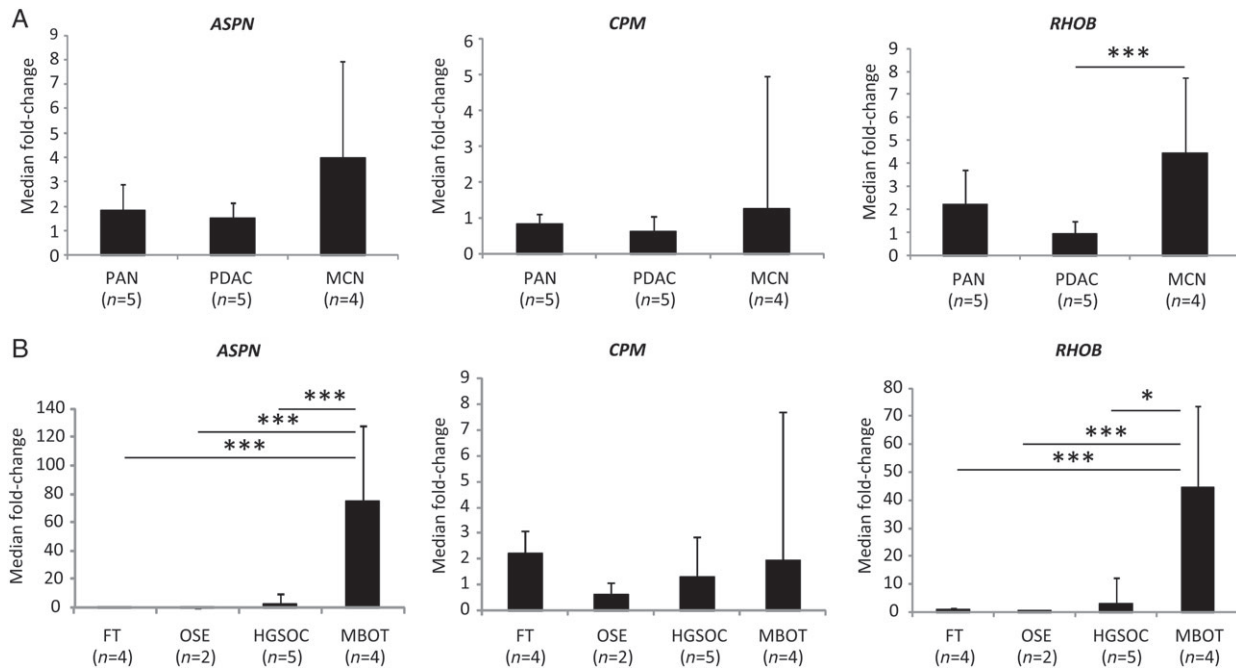


Figure 3. Unsupervised hierarchical clustering of PGCs, and ovarian, Fallopian tube, and MOT samples. (A) Expression of 9626 genes in MOCs, MBOTs, PGCs, HGSOCs, OSE, and FT. Dendrogram of the 67 experimental samples based on hierarchical clustering. MOC and MBOT specimens cluster together and are closely associated with PGCs, whereas high-grade serous ovarian carcinomas (HGSOCs) group with normal Fallopian tube (FT) or ovarian surface epithelium (OSE). (B) Heatmap of the differentially expressed genes in MOCs, MBOTs, PGCs, HGSOCs, OSE, and FT. Blue = high expression; brown = low expression.

common embryologic precursor, PGCs. Approximately 100 PGCs start the journey but by the time they arrive at the gonads, they number about 1700 because they proliferate *en route* [33]. MCNs could arise from some PGCs that stop in the body or tail of the pancreas during their migration to the gonads. Thus, embryological remnants of PGCs that stopped in the body/tail of the pancreas would give rise to MCNs, whereas MOTs

would develop from PGCs that reached the ovaries (Figure 5A,B).

Recent studies suggest that teratoma-associated MOTs are of germ cell origin [3,34]. Using unsupervised clustering of gene expression profiles and RNA sequencing of different ovarian and pancreatic tissues and tumors, we have shown for the first time that gene expression in non-teratoma-associated pancreatic and



**Figure 4.** Expression of *ASPN*, *RHOB*, and *CPM* in ovarian and pancreatic samples. To confirm the increased expression of *ASPN*, *RHOB*, and *CPM* in MBOTs and MCNs, qPCR was performed using cDNA generated from new samples of ovarian and pancreatic tumors and normal tissues. (A) RT-qPCR confirmed an increase of *RHOB* in MCN compared with PDAC. (B) RT-qPCR confirmed the differential expression of *ASPN* and *RHOB* uniquely expressed in MBOT. FT, immortalized Fallopian tube cell lines; OSE, immortalized ovarian surface epithelium cell lines; HGSOCs, high-grade serous ovarian carcinomas; PDACs, pancreatic ductal adenocarcinomas; PAN, normal pancreas; MBOTs, mucinous borderline ovarian tumors; MCNs, mucinous cystic neoplasms of the pancreas. \* $p = 0.01$ ; \*\*\* $p \leq 0.001$ .

ovarian mucinous tumors also resembles PGCs. Validation on independent samples and by RT-qPCR of the microarray data for selected genes further strengthens our microarray analysis.

We acknowledge several limitations of our study. First, while we offer several observations to advance the theory that MOTs and MCNs share a common cell of origin, we cannot exclude convergent evolution of pancreatic and ovarian cells to a common PGC-like phenotype. Second, we have used bulk pancreas as a control. Microdissected pancreatic ductal epithelium would be more ideal, but this is technically challenging as pancreatic enzymes degrade the quality of RNA. Third, we did not investigate the expression of specific PGC markers. This important question needs to be addressed in future work.

This hypothesis can explain many characteristics of MCNs and MOTs: their rarity; their development outside the normal epithelial interfaces; and their clinical, histological, and molecular similarities [30]. Although not profiled in this study, MCNs of the liver and kidney have similar clinical and pathological characteristics of pancreatic MCNs (almost exclusively in young women and the tumor having two components: mucinous epithelium associated with ovarian-like stroma). These could similarly arise from PGCs stopping in the right part of the abdomen (specifically the left lobe of the liver) or retroperitoneum [35–37]. Likewise, another rare tumor that arises mainly in young women and is located on the PGC migration trajectory is the mixed epithelial stromal tumor (MEST). These

tumors develop in the kidney and rarely contain mucinous epithelium, and the epithelial elements are always PAX8-positive; however, like MCNs, MESTs are always associated with ovarian-like stroma and occur almost exclusively in middle-aged females [38]. Nevertheless, several questions remained unanswered: why do MCNs develop only in women since PGCs have the same migration process in male and female embryos? And why are these epithelial tumors mucinous rather than other histological subtypes? It is possible that exposure to female hormones, smoking, and other factors yet to be identified play an important role in the pathogenesis of MCNs.

Our microarray and RT-qPCR data on two independent cohorts suggest that *RHOB* and *ASPN* are common among MOTs, MCNs, and PGCs. Deregulations of these genes have been observed in several types of tumors. *RHOB* codes for Ras homolog B (RhoB) protein, a Rho family GTPase that is itself a subset of the Ras superfamily. RhoB plays an important role in cell migration, membrane trafficking, cell proliferation, and DNA repair. RhoB alteration seems crucial for the response of Ras-transformed cells to farnesyltransferase inhibitors [39]. Because *KRAS* is frequently mutated in MOTs [7] and MCNs [8], it would be interesting to investigate whether *KRAS* mutations correlate with *RHOB* expression.

*ASPN* codes for asporin, a small leucine-rich proteoglycan (SLRP). In the tumor microenvironment, asporin is mainly secreted by cancer-associated fibroblasts [40,41]. Its expression in prostate cancer samples



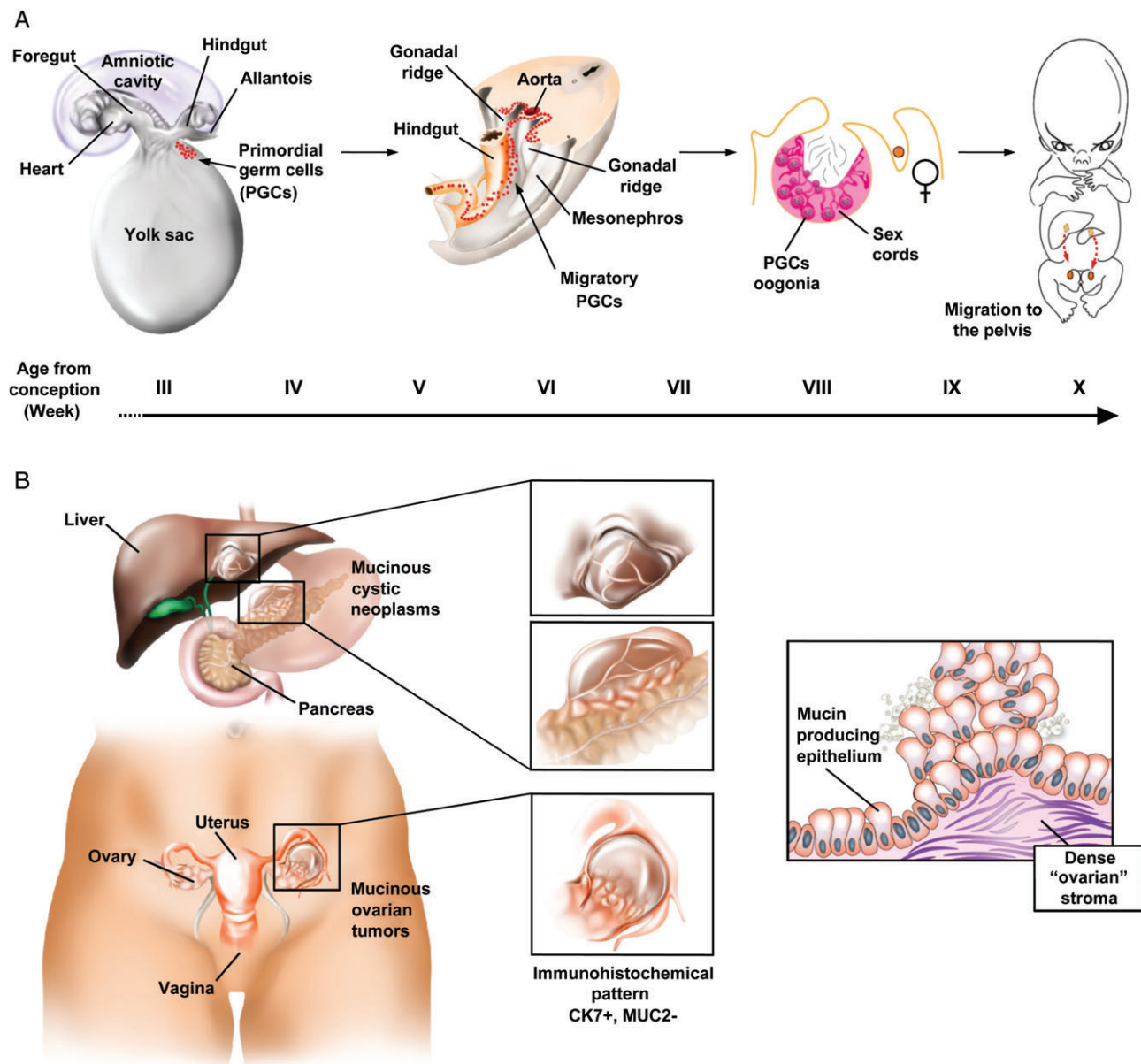


**Figure 5.** Proposed model for the origin of mucinous ovarian tumors and mucinous cystic neoplasms of the pancreas from primordial germ cells. (A) Migration of primordial germ cells (PGCs) in the human embryo starts from the dorsal wall of the yolk sac near the developing allantois (III weeks). At VII weeks, PGCs migrate into the midgut and hindgut, passing through the dorsal mesentery into the gonadal ridges (VIII weeks). At IX weeks, PGCs colonize gonadal ridges [9]. (B) Mucinous cystic neoplasms (MCNs) of the pancreas would arise from left embryological remnant of migrating PGCs that stopped in the body/tail of the pancreas. MCNs of the liver would arise from right embryological remnant of migrating PGCs that stopped in the left lobe of the liver. In the ovaries, MOTs would develop from PGCs that did not develop oogonia. These three mucinous tumors each occur only in women, have CK7<sup>+</sup> MUC2<sup>-</sup> immunohistochemical staining, and are surrounded by ovarian-like stroma.

correlates with disease progression [42]. Certainly, these data need further validation in larger cohorts and at the protein level to elucidate this relationship further.

In conclusion, we present molecular data that may provide a better understanding of the pathogenesis of mucinous ovarian and pancreatic cystic tumors. Our data support the hypothesis that MOTs resemble MCNs of the pancreas at the macroscopic, microscopic, and molecular levels, and share a possible common cell of origin in PGCs. Knowledge of the cell of origin may accelerate translational and clinical research for these rare diseases.

## Acknowledgments

We thank Mrs Laurence Zulianello for iconographic support. We thank the Genomic platform at the Faculty of Medicine of Geneva for technical support. KME and RD are supported by the Honorable Tina Brozman Foundation. KME is supported by the Robert and Deborah First Family Fund, Saltonstall Research Fund, the Minnesota Ovarian Cancer Alliance, and the Reproductive Scientist Development Program from the Eunice Kennedy Shriver National Institute of Child Health and Human Development (NICHD) award

K12-HD000849. RD is supported by the Dr Miriam and Sheldon G Adelson Medical Research Foundation, the Department of Defense, the Claneil Foundation, and the Run & Walk 4 Family & Friends with Cancer Foundation. JH is supported by the Ann and Sol Schreiber Mentored Investigator Award from the Ovarian Cancer Research Fund Alliance (OCRFA) and the Foundation for Women's Wellness. SS is supported by the Ann and Sol Schreiber Mentored Investigator Award from the OCRFA. SILG is supported by the Research Fund of the Department of Internal Medicine of the Hôpitaux Universitaires de Genève and the Faculty of Medicine of Geneva; this fund receives an unrestricted grant from AstraZeneca Switzerland.

### Author contributions statement

KME, RD, and SILG conceived and designed the study. KME, PT, RD, and SILG developed the methodology. KME, PT, JCT, AV, LAD, JLH, DWC, SS, JH, MG, CLK, MB, MSH, RD, and SILG acquired data. KME, PT, AV, LAD, JLH, DWC, MSH, RD, and SILG analyzed and interpreted data. KME, PT, JCT, MG, CLK, MB, MSH, RD, and SILG were responsible for writing, review, and/or revision of the manuscript. KME, PT, JCT, AV, LAD, JLH, GK, LB, DWC, GP, SS, JH, PYD, MG, CLK, MB, MSH, RD, and SILG gave administrative, technical, or material support. RD and SILG supervised the study.

### References

- Siegel RL, Miller KD, Jemal A. Cancer statistics, 2015. *CA Cancer J Clin* 2015; **65**: 5–29.
- Seidman JD, Kurman RJ, Ronnett BM. Primary and metastatic mucinous adenocarcinomas in the ovaries: incidence in routine practice with a new approach to improve intraoperative diagnosis. *Am J Surg Pathol* 2003; **27**: 985–993.
- Kerr SE, Flotte AB, McFalls MJ, et al. Matching maternal isodisomy in mucinous carcinomas and associated ovarian teratomas provides evidence of germ cell derivation for some mucinous ovarian tumors. *Am J Surg Pathol* 2013; **37**: 1229–1235.
- Testini M, Gurrado A, Lissidini G, et al. Management of mucinous cystic neoplasms of the pancreas. *World J Gastroenterol* 2010; **16**: 5682–5692.
- Crippa S, Salvia R, Warshaw AL, et al. Mucinous cystic neoplasm of the pancreas is not an aggressive entity: lessons from 163 resected patients. *Ann Surg* 2008; **247**: 571–579.
- Yamao K, Yanagisawa A, Takahashi K, et al. Clinicopathological features and prognosis of mucinous cystic neoplasm with ovarian-type stroma: a multi-institutional study of the Japan Pancreas Society. *Pancreas* 2011; **40**: 67–71.
- Ryland GL, Hunter SM, Doyle MA, et al. *RNF43* is a tumour suppressor gene mutated in mucinous tumours of the ovary. *J Pathol* 2013; **229**: 469–476.
- Wu J, Jiao Y, Dal Molin M, et al. Whole-exome sequencing of neoplastic cysts of the pancreas reveals recurrent mutations in components of ubiquitin-dependent pathways. *Proc Natl Acad Sci U S A* 2011; **108**: 21188–21193.
- De Felici M. Origin, migration and proliferation of human primordial germ cells. In *Oogenesis*, Coticchio G, Albertini DF, De Santis L (eds). Springer: London, 2013; 19–37.
- Pashai N, Hao H, All A, et al. Genome-wide profiling of pluripotent cells reveals a unique molecular signature of human embryonic germ cells. *PLoS One* 2012; **7**: e39088.
- Guo F, Yan L, Guo H, et al. The transcriptome and DNA methylation landscapes of human primordial germ cells. *Cell* 2015; **161**: 1437–1452.
- Wamunyokoli FW, Bonome T, Lee JY, et al. Expression profiling of mucinous tumors of the ovary identifies genes of clinicopathologic importance. *Clin Cancer Res* 2006; **12**: 690–700.
- Fukushima N, Sato N, Prasad N, et al. Characterization of gene expression in mucinous cystic neoplasms of the pancreas using oligonucleotide microarrays. *Oncogene* 2004; **23**: 9042–9051.
- Tone AA, Begley H, Sharma M, et al. Gene expression profiles of luteal phase fallopian tube epithelium from *BRCA* mutation carriers resemble high-grade serous carcinoma. *Clin Cancer Res* 2008; **14**: 4067–4078.
- Yeung TL, Leung CS, Wong KK, et al. TGF-beta modulates ovarian cancer invasion by upregulating CAF-derived versican in the tumor microenvironment. *Cancer Res* 2013; **73**: 5016–5028.
- Pei H, Li L, Fridley BL, et al. FKBP51 affects cancer cell response to chemotherapy by negatively regulating Akt. *Cancer Cell* 2009; **16**: 259–266.
- R Core Team. *R: A Language and Environment for Statistical Computing*. R Foundation for Statistical Computing: Vienna, 2013. Available from: <https://www.r-project.org>.
- Irizarry RA, Hobbs B, Collin F, et al. Exploration, normalization, and summaries of high density oligonucleotide array probe level data. *Biostatistics* 2003; **4**: 249–264.
- Gautier L, Cope L, Bolstad BM, et al. Affy – analysis of Affymetrix GeneChip data at the probe level. *Bioinformatics* 2004; **20**: 307–315.
- Eisenberg E, Levanon EY. Human housekeeping genes are compact. *Trends Genet* 2003; **19**: 362–365.
- Gagnon-Bartsch JA, Speed TP. Using control genes to correct for unwanted variation in microarray data. *Biostatistics* 2012; **13**: 539–552.
- Ritchie ME, Phipson B, Wu D, et al. *limma* powers differential expression analyses for RNA-seq and microarray studies. *Nucleic Acids Res* 2015; **43**: e47.
- Huang da W, Sherman BT, Stephens R, et al. DAVID gene ID conversion tool. *Bioinformatics* 2008; **2**: 428–430.
- Karst AM, Levanon K, Drapkin R. Modeling high-grade serous ovarian carcinogenesis from the fallopian tube. *Proc Natl Acad Sci U S A* 2011; **108**: 7547–7552.
- Vandesompele J, De Preter K, Pattyn F, et al. Accurate normalization of real-time quantitative RT-PCR data by geometric averaging of multiple internal control genes. *Genome Biol* 2002; **3**: RESEARCH0034.
- Elias KM, Labidi-Galy SI, Vitonis AF, et al. Prior appendectomy does not protect against subsequent development of malignant or borderline mucinous ovarian neoplasms. *Gynecol Oncol* 2014; **132**: 328–333.
- Brown J, Frumovitz M. Mucinous tumors of the ovary: current thoughts on diagnosis and management. *Curr Oncol Rep* 2014; **16**: 389.
- Perets R, Wyant GA, Muto KW, et al. Transformation of the fallopian tube secretory epithelium leads to high-grade serous ovarian cancer in *Brca*/*Tp53*/*Pten* models. *Cancer Cell* 2013; **24**: 751–765.
- Labidi-Galy SI, Papp E, Hallberg D, et al. High grade serous ovarian carcinomas originate in the fallopian tube. *Nat Commun* 2017; **8**: 1093.
- Matthaei H, Schulick RD, Hruban RH, et al. Cystic precursors to invasive pancreatic cancer. *Nat Rev Gastroenterol Hepatol* 2011; **8**: 141–150.

31. Chu PG, Chung L, Weiss LM, *et al.* Determining the site of origin of mucinous adenocarcinoma: an immunohistochemical study of 175 cases. *Am J Surg Pathol* 2011; **35**: 1830–1836.
32. Suzuki Y, Sugiyama M, Abe N, *et al.* Immunohistochemical similarities between pancreatic mucinous cystic tumor and ovarian mucinous cystic tumor. *Pancreas* 2008; **36**: e40–e46.
33. Jones RE and Lopez KH. Sexual differentiation and development. In *Human Reproductive Biology (4th edn)*. Elsevier: London, 2014; Ch 5.
34. Wang Y, Shwartz LE, Anderson D, *et al.* Molecular analysis of ovarian mucinous carcinoma reveals different cell of origins. *Oncotarget* 2015; **6**: 22949–22958.
35. Bosman F, Carneiro F, Hruban R, *et al.* *WHO Classification of Tumours of the Digestive System (4th edn)*. IARC: Lyon, 2010.
36. Matsubara T, Sato Y, Sasaki M, *et al.* Immunohistochemical characteristics and malignant progression of hepatic cystic neoplasms in comparison with pancreatic counterparts. *Hum Pathol* 2012; **43**: 2177–2186.
37. Adsay NV, Eble JN, Srigley JR, *et al.* Mixed epithelial and stromal tumor of the kidney. *Am J Surg Pathol* 2000; **24**: 958–970.
38. Calio A, Eble JN, Grignon DJ, *et al.* Mixed epithelial and stromal tumor of the kidney: a clinicopathologic study of 53 cases. *Am J Surg Pathol* 2016; **40**: 1538–1549.
39. Prendergast GC. Actin' up: RhoB in cancer and apoptosis. *Nat Rev Cancer* 2001; **1**: 162–168.
40. Maris P, Blomme A, Palacios AP, *et al.* Asporin is a fibroblast-derived TGF-beta1 inhibitor and a tumor suppressor associated with good prognosis in breast cancer. *PLoS Med* 2015; **12**: e1001871.
41. Satoyoshi R, Kuriyama S, Aiba N, *et al.* Asporin activates coordinated invasion of scirrhous gastric cancer and cancer-associated fibroblasts. *Oncogene* 2015; **34**: 650–660.
42. Rochette A, Boufaied N, Scarlata E, *et al.* Asporin is a stromally expressed marker associated with prostate cancer progression. *Br J Cancer* 2017; **116**: 775–784.

## SUPPLEMENTARY MATERIAL ONLINE

### Supplementary figure legends

**Figure S1.** Laser-capture microdissection of the epithelium of mucinous tumors

**Figure S2.** Unsupervised hierarchical clustering of PGCs, HGSOCs, Fallopian tube epithelium, ovarian surface epithelium, and MBOT samples

**Figure S3.** Heatmap of differentially expressed genes among MCNs, MBOTs, MOCs, and PGCs versus adnexal and pancreatic samples

**Table S1.** Published datasets used in array expression analysis

**Table S2.** Primers for RT-qPCR

**Table S3.** Gene set enrichment analysis for genes highly expressed by PGCs and mucinous cystic neoplasms of the pancreas

**Table S4.** Gene set enrichment analysis for genes highly expressed by PGCs and mucinous ovarian tumors

**Dataset S1.** Top 1000 genes highly expressed by PGCs and mucinous cystic neoplasms of the pancreas

**Dataset S2.** Top 1000 genes highly expressed by PGCs and mucinous ovarian tumors

**Dataset S3.** Top 411 genes highly expressed by PGCs, mucinous ovarian tumors, and mucinous cystic neoplasms of the pancreas

## **Screening of ovarian cancer: not for tomorrow**

Ovarian cancer is a rare disease with a lifetime risk of 2% for women but it is the leading cause of death from gynecologic cancer. Due to the high mortality to incidence ratio, screening of ovarian cancer has the potential to reduce mortality through early detection and diagnosis. In this article, we review that data of three large screening trials conducted in Japan (Shizuoka), United States (PLCO) and United Kingdom (UKCTOCS) in the last two decades. By combining CA-125 measurements and vaginal ultrasound, the three trials failed to show reduction in mortality from ovarian cancer. A better comprehension of pathogenesis of ovarian cancer could help for developing new methods of screening.

---

# Dépistage du cancer de l'ovaire: ce n'est pas pour demain

Drs AURÉLIE VUILLEUMIER<sup>a</sup> et INTIDHAR LABIDI-GALY<sup>a</sup>

Rev Med Suisse 2017; 13: 1039-41

**L'incidence des cancers ne cesse d'augmenter partout dans le monde. L'une des mesures les plus efficaces pour réduire la mortalité par cancer est le diagnostic précoce, à un stade permettant de proposer un traitement curatif. La colonoscopie ou le frottis du col utérin illustrent la réduction de la mortalité par des méthodes de dépistage efficaces. Première cause de décès par cancer gynécologique en Suisse, le cancer de l'ovaire y est diagnostiqué 600 fois par année, le plus souvent à un stade avancé, synonyme de pronostic réservé. Des mesures de surveillance peuvent-elles le détecter à temps? Trois études randomisées ont démontré l'absence de bénéfice sur la mortalité du dépistage du cancer de l'ovaire avec les méthodes actuellement disponibles. Une meilleure compréhension de la pathogenèse permettrait le développement de nouvelles stratégies.**

## Screening of ovarian cancer: not for tomorrow

*As the worldwide incidence of cancer continuously rises, one of the measures to reduce mortality is early diagnosis while the disease is still curable. Colonoscopy screening and PAP-smears are worthwhile examples illustrating the impact of early diagnosis on mortality. Ovarian cancer is the first cause of mortality by gynecological cancers in Switzerland (incidence of 600 new cases/year), mostly diagnosed at advanced stages with a poor prognosis. Could surveillance measures improve survival? Three large-scale randomized control trials failed to show mortality reduction from ovarian cancer with the methods currently available. A better comprehension of pathogenesis can allow the development of new strategies of screening.*

## INTRODUCTION

L'incidence des cancers ne cesse d'augmenter partout dans le monde, devenant la première cause de mortalité dans les pays développés. Afin de réduire la mortalité liée au cancer, il y a les mesures de prévention, ainsi que la précocité du diagnostic, à un stade permettant d'offrir une prise en charge curative. Première cause de mortalité par cancer gynécologique, le cancer de l'ovaire est nouvellement diagnostiqué chez environ 600 femmes par année en Suisse,<sup>1</sup> le plus souvent à un stade avancé (stades FIGO III ou IV), synonyme de pronostic réservé. L'âge médian au diagnostic est de 63 ans. Grâce à une meilleure prise en charge chirurgicale et à l'utilisation de chimiothérapies combinant les taxanes et les sels de platine, la survie à dix ans s'est améliorée depuis les années 70; elle est actuellement estimée à 40-50% dans les centres de référence.<sup>2</sup> Mais cette maladie reste largement mortelle. Pourrait-on proposer aux femmes de plus de 50 ans un examen simple

permettant le diagnostic du cancer de l'ovaire suffisamment tôt pour qu'un traitement curatif puisse être réalisé? Trois grandes études randomisées ont démontré l'absence de bénéfice sur la mortalité du dépistage du cancer de l'ovaire avec les méthodes actuellement disponibles (ultrason endovaginal ± dosage du CA-125).

## UNE PATHOGENÈSE COMPLEXE

Il n'y a pas un mais des cancers de l'ovaire. Une classification qui prend en compte les données cliniques, histologiques et moléculaires permet de distinguer deux types de tumeurs épithéliales de l'ovaire (les tumeurs germinales et du stroma sont exclues ici). Le type I est d'évolution indolente: il s'agit de carcinomes de bas grade, de sous-types histologiques variés, le plus souvent de stade I au diagnostic, d'évolution lente. Le type II est de haut grade (correspond principalement aux carcinomes séreux de haut grade), diffuse rapidement à la cavité péritonéale et représente à lui seul 90% des décès par cancer de l'ovaire. Cette entité, le type II, est celle qu'il importerait de détecter précocement. Il n'y a pas de progression linéaire entre les types I et II. Ainsi, les carcinomes séreux de bas grade ne se transforment pas en haut grade.<sup>3</sup> Des études récentes suggèrent que les lésions précoces des carcinomes séreux de haut grade de l'ovaire, c'est-à-dire intra-épithéliales, seraient situées dans les trompes de Fallope: il s'agit des carcinomes séreux intra-épithéliaux tubaires ou STIC. Ceux-ci sont indétectables cliniquement ou par échographie et nécessitent un échantillonnage ex vivo extensif des trompes pour les identifier.<sup>4</sup> Les trompes de Fallope, et plus particulièrement le pavillon des trompes, constitueraient donc le site primaire de dégénérescence tumorale, avant l'extension à l'ovaire, raison pour laquelle on s'oriente actuellement vers une reclassification d'une partie des cancers ovariens en cancers des trompes.<sup>5</sup> Selon des études de modélisation, cinq ans s'écouleraient en moyenne entre l'apparition du STIC et les manifestations cliniques.<sup>6</sup>

On estime que 90% des cancers de l'ovaire sont sporadiques. Environ 10-15% des cas peuvent être associés à des prédispositions génétiques constitutionnelles, le plus souvent via des mutations des gènes *BRCA1* ou *BRCA2*<sup>7</sup> ou, plus rarement, dans le cadre d'un syndrome de Lynch.

## GRANDS PRINCIPES DU DÉPISTAGE

Pour qu'un test diagnostique soit proposé comme mesure de dépistage, il doit avoir d'excellentes spécificité, sensibilité et reproductibilité, pour un coût raisonnable, tout en restant acceptable pour la population générale. Il doit concerner une

<sup>a</sup> Service d'oncologie, Département d'oncologie, HUG, 1211 Genève 14  
aurelie.vuilleumier@hcuge.ch | intidhar.labidi-galy@hcuge.ch



pathologie relativement fréquente, responsable d'une mortalité importante. Pour avoir un impact sur celle-ci, le test doit permettre de détecter la maladie à un stade précoce, correspondant à sa phase préclinique, autorisant un traitement efficace. Ce type de stratégie s'applique le mieux en cas de maladie à cinétique lente, avec une progression linéaire entre les stades pré-invasifs et invasifs.

C'est ainsi que le frottis cervical développé par le Dr Papanicolaou a permis de réduire de plus de 60% l'incidence du cancer du col utérin entre 1955 et 1990. Ce test simple consiste en un frottis de la zone de transition cervicale, dont l'analyse cytologique révèle les lésions précancéreuses (CIN), asymptomatiques, qui seront réséquées avant transformation maligne. Pour le cancer colorectal, les lésions invasives, qui se développent à partir de polypes adénomateux, sont détectées avec une excellente sensibilité par la recherche régulière de sang occulte dans les selles ou par des examens endoscopiques.

## PRINCIPAUX ESSAIS SUR LE DÉPISTAGE DU CANCER DE L'OVAIRE

Entre 2008 et 2016, trois grandes études randomisées évaluant l'intérêt du dépistage du cancer de l'ovaire ont été publiées. La première a été menée au Japon (cohorte de Shizuoka; n = 82487),<sup>8</sup> la deuxième aux Etats-Unis (Prostate, Lung, Colorectal and Ovarian Cancer Screening Trial, dite PLCO; n = 78216)<sup>9</sup> et la dernière au Royaume-Uni (UK Collaborative Trial of Ovarian Cancer Screening, dite UKCTOCS; n = 202638)<sup>10</sup> (tableau 1). Toutes trois ciblaient des femmes sans facteur de risque particulier pour le cancer de l'ovaire, sans antécédent d'annexectomie ou de cancer des annexes.<sup>11</sup>

L'étude japonaise a comparé l'absence de surveillance à un bras intervention, combinant l'ultrason endovaginal annuel au dosage sérique du CA-125 (seuil de 35 U/ml) durant cinq ans, chez les femmes ménopausées. Elle n'a pas évalué le bénéfice en termes de mortalité, l'objectif principal consistant dans le nombre de cas dépistés par stade de la maladie. Au total, le nombre de cas détectés dans le groupe intervention était similaire au groupe contrôle (27 vs 32), nombre 9 à 11 fois inférieur aux résultats des études américaines et britanniques (tableau 1). Il y avait une grande proportion de cancers de type I, plus fréquents en Asie qu'en Occident.

L'étude américaine PLCO a également inclus deux groupes de femmes: un groupe contrôle et un groupe intervention, surveillé par ultrason endovaginal et dosage du CA-125 (seuil de 35 U/ml) de manière annuelle chez des femmes âgées entre 55 et 74 ans, s'intéressant à la différence de mortalité entre les deux groupes avec un suivi de douze ans. Franchement négatives en termes de bénéfice sur la mortalité, les courbes tendent même à montrer un effet délétère du dépistage en raison d'un haut taux de complications chirurgicales (15%), y compris dans des situations de faux positifs. Par ailleurs, le nombre de cas diagnostiqués à un stade I était similaire entre le groupe intervention (15%) et le groupe contrôle (10%), de même que pour les stades III et IV, représentant, une fois additionnés, 77 et 78% de l'ensemble des cas diagnostiqués, respectivement.

	Les trois essais randomisés évaluant le dépistage du cancer de l'ovaire		
	TABLEAU 1		
Nom de l'essai (année de publication)	Shizuoka (2008) <sup>8</sup>	PLCO (2011) <sup>9</sup>	UKCTOCS (2016) <sup>10</sup>
Cohorte (n)	82487	78216	202638
Méthode de dépistage (bras contrôle et bras intervention)	<ul style="list-style-type: none"> <li>pas d'intervention (n = 40799)</li> <li>US endovaginal et dosage du CA-125 1 x/an pendant 5 ans (n = 41688)</li> </ul>	<ul style="list-style-type: none"> <li>pas d'intervention (n = 34304)</li> <li>US endovaginal et dosage du CA-125 1 x/an pendant 4 ans (n = 34253)</li> </ul>	<ul style="list-style-type: none"> <li>pas d'intervention (n = 101359)</li> <li>multimodal: US endovaginal 1 x/an pendant 4 ans et dosage du CA-125 1 x/an pendant 6 ans (n = 50640)</li> <li>US endovaginal seul 1 x/an pendant 6 ans (n = 50639)</li> </ul>
Population cible	Femmes ménopausées sans facteur de risque identifié	Femmes entre 55 et 74 ans sans facteur de risque identifié	Femmes entre 50 et 74 ans sans facteur de risque identifié
Suivi médian	9,2 ans	12,4 ans	11,1 ans
Sensibilité	77%	68%	<ul style="list-style-type: none"> <li>85% pour US seul</li> <li>89% pour méthode multimodale</li> </ul>
Nombre de cas dépistés vs cas contrôle	27 (0,06%) vs 32 (0,08%)	212 (0,54%) vs 176 (0,45%)	<ul style="list-style-type: none"> <li>338 dans le bras US + CA-125 (0,67%)</li> <li>314 dans le bras US seul (0,62%)</li> <li>630 dans le bras contrôle (0,62%)</li> </ul>
Impact sur la mortalité	Non disponible	Pas de différence significative	Pas de différence significative quel que soit le groupe d'intervention
Faux positifs	9%	5%	<ul style="list-style-type: none"> <li>1% pour le bras multimodal</li> <li>3,2% pour le bras US seul</li> </ul>

Regroupant plus de 200000 participantes pour un coût de 27 millions de livres sterling, l'étude britannique UKCTOCS avait comme objectif principal l'effet du dépistage sur la mortalité, avec un suivi de onze ans lors de sa publication. Trois bras distincts étaient définis: un premier groupe de femmes n'ayant qu'un ultrason annuel durant six ans, le deuxième groupe (multimodal) ayant à la fois un ultrason annuel durant quatre ans et un dosage du CA-125 durant six ans, comparés à un troisième groupe contrôle. Contrairement aux précédents essais, un algorithme était utilisé pour l'interprétation du CA-125, rapporté au risque en fonction de l'âge et de l'évolution annuelle de la valeur.<sup>12</sup> Cette grande étude ne montre pas de bénéfice du dépistage sur la survie, quelle que soit la méthode, avec une réduction de mortalité non significative de 15% pour le groupe multimodal et de 11% pour le groupe suivi par ultrason endovaginal seul. Suite à ces résultats, les auteurs ont exclu, dans chacun des trois groupes, les cas *prévalents*, c'est-à-dire les cas de cancers ovariens diagnostiqués dans la première année après la randomisation. Ils ont alors mis en évidence une diminution significative de mortalité de 28% pour le groupe multimodal (dosage du CA-125 et ultrason endovaginal) à partir de la septième année d'inclusion. Considérées comme «encourageantes», ces données ne suffisent cependant pas pour recommander une telle surveillance à la population générale.

Au total, aucune de ces trois études n'a montré de bénéfice significatif du dépistage du cancer de l'ovaire sur la mortalité, en comparaison aux groupes contrôles. Bien que le nombre de faux positifs reste faible dans chacune des études, il convient de souligner les répercussions physiques et psychiques d'investigations anxiogènes, d'autant plus lorsque l'intervention chirurgicale est réalisée pour une pathologie s'avérant bénigne.

## QUE RETENIR?

Plusieurs éléments interviennent pour le succès du dépistage populationnel d'un type de cancer, notamment: 1) une bonne connaissance de la pathogenèse de la maladie tumorale; 2) une évolution lente et 3) une situation anatomique accessible aux examens morphologiques. Ainsi, certains organes sont aisément accessibles tels que le col utérin ou le côlon, tandis que d'autres, tels que le pancréas ou les ovaires, sont profonds et difficiles à étudier par des moyens non invasifs. Les caractéristiques du cancer de l'ovaire ne sont malheureusement pas en faveur d'une détection précoce. L'ovaire est un petit organe profond qui «flotte» dans la cavité péritonéale. De plus, il y a plusieurs types de cancer de l'ovaire (type I et type II). Pour les carcinomes séreux de haut grade, qui sont les sous-types les plus graves, les lésions précoces dans les trompes ou STIC ne sont pas détectables par les techniques d'imagerie car elles ne mesurent que 1-2 mm. Il nous manque encore beaucoup de connaissances pour mieux comprendre cette maladie et développer de nouveaux outils de dépistage.

## NOUVEAUX BIOMARQUEURS

Les trois essais que nous avons détaillés démontrent l'échec du dépistage par le dosage sérique du CA-125, combiné à l'ultrason par voie endovaginale. Les études génomiques récentes ont révélé que 99% des carcinomes séreux de haut grade de l'ovaire ont des mutations du gène suppresseur de tumeur *TP53*.<sup>13</sup> Le développement de nouveaux outils d'analyse génomique, tels que le séquençage à haut débit, permet la détection de cellules tumorales circulantes ou l'analyse de l'ADN tumoral dans le sang (biopsies liquides),<sup>14</sup> ouvrant une nouvelle ère de médecine de précision. La mise en évidence de mutations du gène *TP53* dans le sang est possible et pourrait constituer un nouveau test de dépistage pour les cancers

ovariens. Plusieurs études pilotes ont montré la faisabilité de cette stratégie.<sup>15</sup> Reste à démontrer son utilité dans un cadre populationnel, l'objectif ultime étant la réduction de la mortalité par les cancers ovariens.

## CONCLUSION

Bien que rares par rapport à d'autres cancers, les tumeurs malignes épithéliales de l'ovaire restent une pathologie dont le comportement agressif justifie le développement de moyens de dépistage efficaces. Aucune donnée actuelle ne permet de proposer à la population générale un screening systématique tels que l'ultrason endovaginal ou le dosage sérique du CA-125. A noter que les femmes à risque accru, en particulier les femmes portant des mutations constitutionnelles des gènes *BRCA1* ou *BRCA2*, sont encouragées à réaliser une annexectomie prophylactique dès l'âge de 35-40 ans, après le projet parental. Au vu des résultats de l'essai britannique UKCTOCS ayant suivi plus de 200 000 femmes pendant plus de onze ans, il est peu probable qu'un nouvel essai de cette envergure soit entrepris dans un avenir proche: attendons le développement de nouveaux biomarqueurs pour réfléchir à d'inédites procédures!

**Conflit d'intérêts:** Les auteurs n'ont déclaré aucun conflit d'intérêt en relation avec cet article.

## IMPLICATIONS PRATIQUES

- Aucune donnée ne permet actuellement de proposer un dosage du CA-125 ou l'ultrason endovaginal comme mesure de dépistage du cancer de l'ovaire. Même pour les populations à risque (femmes portant des mutations constitutionnelles des gènes *BRCA1* ou *BRCA2*), ces méthodes n'ont pas montré de réduction de la mortalité par cancer de l'ovaire
- Il existe deux types de tumeurs malignes épithéliales de l'ovaire: les cancers de type I, plus fréquents en Asie et dont l'évolution est indolente, et les cancers de type II, dont le carcinome séreux de haut grade, à haut potentiel de dissémination péritonéale
- Les recherches en cours se concentrent notamment sur les biomarqueurs, comme l'ADN tumoral circulant, qui pourraient permettre de détecter des tumeurs infiniment petites, non identifiables par les techniques d'imagerie actuelles

1 Cancer incidence in Switzerland.

Accessible à: [www.nicer.org](http://www.nicer.org).

2 Jelovac D, Armstrong DK. Recent progress in the diagnosis and treatment of ovarian cancer. *CA: a cancer journal for clinicians* 2011;61:183-203.

3 \* Kurman RJ, Shih Ie M. The dualistic model of ovarian carcinogenesis: Revisited, revised, and expanded. *Am J Pathol* 2016;186:733-47.

4 \* Perets R, Drapkin R. It's totally tubular... Riding the new wave of ovarian cancer research. *Cancer Res* 2016;76:10-7.

5 Mutch DG, Prat J. 2014 FIGO staging for ovarian, fallopian tube and peritoneal cancer. *Gynecol Oncol* 2014;133:401-4.

6 Brown PO, Palmer C. The preclinical natural history of serous ovarian cancer:

Defining the target for early detection. *PLoS medicine* 2009;6:e1000114.

7 Norquist BM, Harrell MJ, Brady MF, et al. Inherited mutations in women with ovarian carcinoma. *JAMA Oncol* 2016;2:482-90.

8 Kobayashi H, Yamada Y, Sado T, et al. A randomized study of screening for ovarian cancer: A multicenter study in Japan. *Int J Gynecol Cancer* 2008;18:414-20.

9 \* Buys SS, Partridge E, Black A, et al. Effect of screening on ovarian cancer mortality: The prostate, lung, colorectal and ovarian (plco) cancer screening randomized controlled trial. *JAMA* 2011;305:2295-303.

10 \* Jacobs IJ, Menon U, Ryan A, et al. Ovarian cancer screening and mortality in

the UK Collaborative Trial of Ovarian Cancer Screening (UKCTOCS): A randomised controlled trial. *Lancet* 2016;387:945-56.

11 \* Menon U, Griffin M, Gentry-Maharaj A. Ovarian cancer screening-current status, future directions. *Gynecol Oncol* 2014;132:490-5.

12 Menon U, Ryan A, Kalsi J, et al. Risk algorithm using serial biomarker measurements doubles the number of screen-detected cancers compared with a single-threshold rule in the United Kingdom collaborative trial of ovarian cancer screening. *J Clin Oncol* 2015;33:2062-71.

13 Cancer Genome Atlas Research N. Integrated genomic analyses of ovarian carcinoma. *Nature* 2011;474:609-15.

14 Haber DA, Velculescu VE. Blood-based analyses of cancer: circulating tumor cells and circulating tumor DNA. *Cancer Discov* 2014;4:650-61.

15 Forshew T, Murtaza M, Parkinson C, et al. Non invasive identification and monitoring of cancer mutations by targeted deep sequencing of plasma DNA. *Science Translational Medicine* 2012;4:136ra68.

\* à lire  
\*\* à lire absolument

## Conclusions and perspectives

---

In the current work, we used next-generation sequencing to investigate the pathogenesis of two EOC: the most frequent and lethal one (HGSOC) and the least frequent and studied one (MOC). Identifying the cell of origin will have implications for developing efficient tools for screening and early diagnosis of HGSOC and for new therapies in MOC.

### I. Implications of the fallopian tube as cell of origin of HGSOC

HGSOC is the most common histologic subtype of EOC (22, 162-164). It is diagnosed at advanced stages in the majority of cases. Patients have a median survival of 3 years and did not improve over the last 20 years. Using CA-125 and/or vaginal ultrasound, two large randomized screening trials failed to show reduction in mortality from EOC (reviewed in (165)). A better comprehension of the pathogenesis of HGSOC could help into developing new and effective screening tools.

Accumulated data in the two last decade implicate the fimbria as the potent site of origin of HGSOC. Descriptive molecular pathology and experimental evidence strongly support a serous carcinogenic sequence in the Fallopian tube (166). IHC as well as targeted sequencing analyses have shown that *in situ* fallopian tube lesions (STIC and p53 signatures) harbor the same *TP53* mutation as surrounding invasive carcinomas (5, 9, 41). Additional studies have evaluated clonal intraperitoneal spread of ovarian cancer using whole exome or genome analyses, but this effort did not analyze precursor lesions such as STICs (167, 168).

We analyzed exome-wide sequence and structural analyses of multiple tumor samples from the same individual to examine the origins of HGSOC (13). Specifically, we examined whether the compendium of somatic alterations identified in different lesions may provide insights into the evolutionary relationship between primary fallopian tube lesions, including p53 signatures and STICs, ovarian carcinomas, and intraperitoneal metastases. These results provided a comprehensive evolutionary analysis of sporadic HGSOC in five patients. Our molecular analyses suggest that the fallopian tube tumors are unlikely to be metastatic lesions of ovarian cancer (168, 169). Instead, our results suggest that ovarian cancer originate from the fallopian tubes, with p53 signatures and STICs being the pre-invasive lesions. The subsequent formation of ovarian cancer represents a seeding event from a primary tumor arising in the fallopian tube that contains sequence and structural alterations in key driver genes, mainly *TP53*, *BRCA1/BRCA2* genes and PI3K pathway. A similar work found that STICs are precursor lesions in half of their patient cohort, but also identified STIC as metastases in two patients (44). One limitation of this study is that the authors analyzed only one STIC per patient. In our cohort, four of five patients with advanced stage sporadic HGSOC had multiple STICs. In



particular, case CGOV280 had bilateral STICs. Phylogenetic analysis suggested the lesion in the left fallopian tube which was pathologically determined to be a STIC represented a metastatic lesion of the right ovarian cancer. These observations are consistent with the above model of STIC to ovarian cancer progression, but suggest that in advanced stage HGSOC may also seed metastatic deposits throughout the peritoneum, including to the fallopian tube on the contralateral side (13).

We found that the median time of progression from STICs to ovarian cancer was 6.5 years. It is very likely that seeding of metastatic lesions occurred rapidly thereafter. This timing is consistent with clinical reports showing a difference of 7.7 years in the age of *BRCA* carriers with high-grade tubal intraepithelial neoplasms compared to those with advanced disease (170). A better comprehension of the pathogenesis of HGSOC have implications for screening, early diagnosis and surgical prevention of this lethal cancer in *BRCA* carriers and non-carriers.

### **I.A Screening and early diagnosis**

The majority of EOC are diagnosed at advanced stages (III/IV), largely contributing to the poor prognosis. This results in a high mortality to incidence ratio as survival at one year drops from 90% at stage II to 70% at stage III. As such, screening of EOC has the potential to significantly reduce mortality if detected at earlier stages (171). Annual screening that combines serum CA-125 measurement with transvaginal sonography has been evaluated in the large scale Prostate, Lung, Colorectal and Ovarian (PLCO) Cancer Screening Randomized Trial. Almost 80'000 menopausal women (55-74 years) were assigned to annual screening for 4 years (39'105) or observation (39'111). While screening detected more cancers (212 vs 176), it did not translate into reduction of mortality (172). A second very large trial in the United Kingdom (UK) evaluated a multimodal approach that combined an algorithm based on changes of CA-125 over time coupled with vaginal ultrasound. The UK Collaborative Trial of Ovarian Cancer Screening (UKCTOCS) recruited 202'638 menopausal women who were randomized to a control, ultrasound screening or multimodal screening group. The multimodal screening group showed a stage shift with a higher proportion of detected earlier stages but it did not translate into significant mortality reduction on primary analysis (15% multimodal screening vs 11% ultrasound)(173). Based on the absence of mortality reduction in these two large randomized and well-conducted trials, the US Preventive Services Task Force recommends against screening for ovarian cancer in asymptomatic women (D recommendation)(174).

For cancer screening to be successful, it should primarily detect cancers with lethal potential or their precursors early, leading to therapy that reduces mortality and morbidity (175). Understanding the pathogenesis is an important step toward the development of effective

screening tools in order to detect early stages where treatment will change the outcome and reduce mortality from cancer. Papanicolaou (Pap)-test and colonoscopy are worthwhile examples illustrating the impact of early diagnosis on mortality. The understanding that adenoma is the precancerous lesion that ultimately transform into invasive colon cancers (176, 177) lead to the development and implementation of colonoscopy as an effective screening tool that significantly reduced mortality (178). Similarly, the comprehension that cervical cancer is due to infection by HPV and the identification of cervical intraepithelial neoplasia as a precursor of invasive cervical cancer lead to the development of Pap-test, a screening tool consisting in cytologic examination of cervical brush. Pap-test reduced the incidence of invasive cervical cancer by 60% and mortality by 70% (179). The addition of HPV test to Pap-test further reduces by 42 % the incidence of grade 2 or 3 cervical intraepithelial neoplasia or cancer detected in subsequent screening examinations (180).

Our understanding that HGSOC could originate from the FT has been a revolution in the comprehension of the disease. It is consistent with the observation, through careful review of several hundred cases of HGSOC that stage I, i.e. tumors confined to the ovary according to the past 1988 FIGO classification, virtually does not exist (42). Women diagnosed with isolated STIC have a 5-years specific survival of 97.7% compared to 83.2% in those with early stage invasive serous tubal carcinoma (181). These survival rates are similar to those observed with in situ lesions/early stages of other cancers (182) and suggest that early detection of STICs could potentially reduce mortality from HGSOC. The main limitation is the anatomical location of the FT, a profound and 2 mm-thick organ floating in the peritoneum. Several approaches are investigating the feasibility of FT brushing during abdominal laparoscopy (183) or less invasive transvaginal laparoscopy (184). An alternative to FT brushing are liquid biopsies, i.e. genomic alterations such as gene mutations or copy-number variations that could be detected either in blood (185, 186) or uterine lavage (187). Several trials are currently investigating the feasibility and sensitivity/specificity of liquid biopsies for detecting STIC or early tube carcinomas in high-risk women (NCT03606486, NCT02062697).

### **I.B Surgical prevention in high-risk women**

Prophylactic bilateral salpingo-oophorectomy (BSO) is a very effective method of ovarian cancer risk reduction in high-risk women (188, 189) but leads to significant morbidity caused by iatrogenic early menopause. The understanding that ovarian cancer often arises in the fallopian tube may lead to a two-step risk reducing surgery. After childbearing is completed, *BRCA* carriers will undergo a prophylactic salpingectomy, and only after natural menopause will the women be offered bilateral oophorectomy (10). Such strategy is currently investigated in several trials (NCT02321228; NCT01907789). This approach could have additional

importance in the future, given the earlier age of onset of *BRCA* mutation related cancers in subsequent generations (190, 191). This shift is related to anticipation, a phenomenon observed in genetic disorders of the nervous system such as Fragile X syndrome and Huntington disease. The disease occurs at younger ages or with increased severity in subsequent generations (192) and DNA instability has been identified as the cause of anticipation. In Fragile X syndrome, there is an expanded length of CGG trinucleotide repeats in *FMR1* gene when the gene is passed from a parent to a child, causing the phenotype of the disease more severe (193). According to recent studies, the expected change in age of onset of hereditary breast or ovarian cancer is superior to 8 years (190, 194). The exact molecular mechanism of anticipation in *BRCA* carriers is yet to be identified. Current guidelines recommend prophylactic BSO before the age of 40 in *BRCA1* carriers, and 45 in *BRCA2* carriers, based on the estimated age of diagnosis of EOC (55 years in *BRCA1* and 65 in *BRCA2*)(195). With the phenomenon of anticipation, it is very likely that EOC will develop much earlier in *BRCA* carriers in future generations. If current trials confirm the safety of two-step risk reducing surgery, such strategy would be a good compromise by preserving the fertility of young *BRCA* carriers while reducing their risk of developing EOC.

## **II. Implications of PGCs as cell of origin of MOC**

Mucinous ovarian carcinoma (MOC) is the least frequent EOC and is classified as type I (196). The vast majority of patients with MOC (90% in our series of 156 cases) are diagnosed at stage I (75), typically a large homolateral mucinous cyst of the ovary with a median size of 15 cm (197). Stage I MOCs have an excellent prognosis with 5-years survival exceeding 90%, meaning that they are mostly cured by surgery. However, in case of metastatic spreading to the peritoneum, these tumors are chemoresistant and median survival of stages III/IV is 14 months (198). MOC are poorly infiltrated by TILs and women diagnosed with MOC are excluded from immune checkpoint inhibitor trials (199). Thus, new systemic therapies for metastatic MOC are warranted.

The origin of MOC is still unknown (45). They morphologically resemble mucinous carcinomas of the gastro-intestinal tract. We and others have shown that their IHC pattern is distinct from mucinous appendiceal or colon cancers (75, 200), but similar to an intriguing and rare pancreatic tumors that occur almost exclusively in young women (sex ratio 1:20), are located in the body/tail of the pancreas and are always associated with an ovarian-like stroma: mucinous cystic neoplasm (MCN) of the pancreas (Table 1 and (200, 201)). We found that a possible link between the pancreas and ovaries are primordial germ cells (PGCs) that migrate very early during human embryogenesis (4 to 6 weeks) from the yolk sac to gonadal ridges. During their very long journey (the longest migration of cells in the human embryo), PGCs pass

close to the pancreas. We hypothesize that some embryological remnants could stop in the body/tail of the pancreas and would give rise to MCN in women exposed to certain risk factors such as smoking. To address our hypothesis, we used GEP of different histotype of pancreatic and ovarian tumors, their eutopic tissues (normal pancreas, OSE and FT) and single-cell RNA-sequencing of PGCs. In unsupervised clustering, we observed that MCN or MOT cluster more closely to PGCs to their eutopic tissue of origin. Our work brings a new and plausible explanation of the characteristics of pancreatic MCN, in particular why they develop only in the body/tail of the pancreas and their ovarian-like stroma.

Histologically, MOT are multicystic tumors with large amount of intracellular mucin (present in  $\geq 50\%$  of the cells) in more than 90% of the cells and contain little extracellular mucin (202). This is different from mucinous tumors of the gastrointestinal tract that are characterized by large amount of extracellular mucin (66). The cell of origin of MOT was not defined yet because no mucin secreting cells are described in the ovaries. Oocytes undergo hypertrophy during oogenesis. Just before ovulation, human oocyte has completed its growth, reaching about 100  $\mu\text{m}$  diameter. It is filled with reserve substances, which are mandatory for the proper development of the zygote in the first days of its life. In mature oocytes, the cumulus-corona appear as an expanded and mucified layer, due to active secretion of hyaluronic acid. Morphologically, MOT are very large cyst filled with mucin. They resemble an ovulatory oocyte or egg. We propose that MOT would originate from oocyte at a specific stage of maturation, to be determined.

Our hypothesis is consistent with epidemiologic data. Mucinous borderline ovarian tumors are more frequent than their serous counterparts in the two first decade (45), when the pool of oocytes is the highest. MOC most commonly presents in middle-aged women (39-50 years) and it contrasts with incidence of HGSOE that develop in menopausal women (median age is 65 years). Smoking specifically increase the risk of MOC but has no impact on the other histotypes of EOC (104). This is consistent with the ovotoxicity of cigarette increasing DNA damage and autophagy (203). Statin use is associated with lower risks for EOC with the strongest effect seen for mucinous epithelial subtypes (204). Conversely, statins improve maturation of oocytes. Finally, an increased incidence of MOT was observed in a large case-control study of women undergoing fertility therapy. Five of eleven ovarian tumors were mucinous (two carcinomas, one borderline and two cystadenoma) (142).

There are still unanswered questions that need to be addressed in the future. Our hypothesis did not explain why 1) MCN arise only in women since PGCs have the same migration trajectory in males and females; 2) we did not show whether MCN or MOT express lineage markers of PGCs and 3) we did not investigate at which stage of germ cell maturation

mucinous tumors would arise from. Ongoing work in our lab is investigating the above questions and could bring new pieces to the puzzle in the future.

## References

1. Fathalla MF. Incessant ovulation--a factor in ovarian neoplasia? *Lancet*. 1971;2(7716):163.
2. Casagrande JT, Louie EW, Pike MC, Roy S, Ross RK, Henderson BE. "Incessant ovulation" and ovarian cancer. *Lancet*. 1979;2(8135):170-3.
3. Vercellini P, Crosignani P, Somigliana E, Vigano P, Buggio L, Bolis G, et al. The 'incessant menstruation' hypothesis: a mechanistic ovarian cancer model with implications for prevention. *Hum Reprod*. 2011;26(9):2262-73.
4. Cramer DW, Welch WR. Determinants of ovarian cancer risk. II. Inferences regarding pathogenesis. *J Natl Cancer Inst*. 1983;71(4):717-21.
5. Medeiros F, Muto MG, Lee Y, Elvin JA, Callahan MJ, Feltmate C, et al. The tubal fimbria is a preferred site for early adenocarcinoma in women with familial ovarian cancer syndrome. *Am J Surg Pathol*. 2006;30(2):230-6.
6. Cass I, Holschneider C, Datta N, Barbuto D, Walts AE, Karlan BY. BRCA-mutation-associated fallopian tube carcinoma: a distinct clinical phenotype? *Obstet Gynecol*. 2005;106(6):1327-34.
7. Piek JM, van Diest PJ, Zweemer RP, Jansen JW, Poort-Keesom RJ, Menko FH, et al. Dysplastic changes in prophylactically removed Fallopian tubes of women predisposed to developing ovarian cancer. *J Pathol*. 2001;195(4):451-6.
8. Piek JM, Verheijen RH, Kenemans P, Massuger LF, Bulten H, van Diest PJ. BRCA1/2-related ovarian cancers are of tubal origin: a hypothesis. *Gynecol Oncol*. 2003;90(2):491.
9. Lee Y, Miron A, Drapkin R, Nucci MR, Medeiros F, Saleemuddin A, et al. A candidate precursor to serous carcinoma that originates in the distal fallopian tube. *J Pathol*. 2007;211(1):26-35.
10. Perets R, Drapkin R. It's Totally Tubular....Riding The New Wave of Ovarian Cancer Research. *Cancer Res*. 2016;76(1):10-7.
11. Kindelberger DW, Lee Y, Miron A, Hirsch MS, Feltmate C, Medeiros F, et al. Intraepithelial carcinoma of the fimbria and pelvic serous carcinoma: Evidence for a causal relationship. *Am J Surg Pathol*. 2007;31(2):161-9.
12. Schneider S, Heikaus S, Harter P, Heitz F, Grimm C, Ataseven B, et al. Serous Tubal Intraepithelial Carcinoma Associated With Extraovarian Metastases. *International journal of gynecological cancer : official journal of the International Gynecological Cancer Society*. 2017;27(3):444-51.
13. Labidi-Galy SI, Papp E, Hallberg D, Niknafs N, Adleff V, Noe M, et al. High grade serous ovarian carcinomas originate in the fallopian tube. *Nat Commun*. 2017;8(1):1093.
14. Kurman RJ, Shih le M. Molecular pathogenesis and extraovarian origin of epithelial ovarian cancer--shifting the paradigm. *Hum Pathol*. 2011;42(7):918-31.
15. Wiegand KC, Shah SP, Al-Agha OM, Zhao Y, Tse K, Zeng T, et al. ARID1A mutations in endometriosis-associated ovarian carcinomas. *N Engl J Med*. 2010;363(16):1532-43.
16. Maeda D, Shih le M. Pathogenesis and the role of ARID1A mutation in endometriosis-related ovarian neoplasms. *Adv Anat Pathol*. 2013;20(1):45-52.
17. Jones S, Wang TL, Shih le M, Mao TL, Nakayama K, Roden R, et al. Frequent mutations of chromatin remodeling gene ARID1A in ovarian clear cell carcinoma. *Science*. 2010;330(6001):228-31.
18. Prat J, D'Angelo E, Espinosa I. Ovarian carcinomas: at least five different diseases with distinct histological features and molecular genetics. *Hum Pathol*. 2018;80:11-27.
19. Elias KM, Tsantoulis P, Tille JC, Vitonis A, Doyle LA, Hornick JL, et al. Primordial germ cells as a potential shared cell of origin for mucinous cystic neoplasms of the pancreas and mucinous ovarian tumors. *J Pathol*. 2018.
20. Shih le M, Kurman RJ. Ovarian tumorigenesis: a proposed model based on morphological and molecular genetic analysis. *Am J Pathol*. 2004;164(5):1511-8.
21. Kurman RJ, Shih le M. Pathogenesis of ovarian cancer: lessons from morphology and molecular biology and their clinical implications. *Int J Gynecol Pathol*. 2008;27(2):151-60.

22. Kurman RJ, Shih le M. The origin and pathogenesis of epithelial ovarian cancer: a proposed unifying theory. *Am J Surg Pathol.* 2010;34(3):433-43.
23. Jones S, Wang TL, Kurman RJ, Nakayama K, Velculescu VE, Vogelstein B, et al. Low-grade serous carcinomas of the ovary contain very few point mutations. *J Pathol.* 2012;226(3):413-20.
24. Cancer Genome Atlas Research N. Integrated genomic analyses of ovarian carcinoma. *Nature.* 2011;474(7353):609-15.
25. Singer G, Oldt R, 3rd, Cohen Y, Wang BG, Sidransky D, Kurman RJ, et al. Mutations in BRAF and KRAS characterize the development of low-grade ovarian serous carcinoma. *J Natl Cancer Inst.* 2003;95(6):484-6.
26. Kuo KT, Guan B, Feng Y, Mao TL, Chen X, Jinawath N, et al. Analysis of DNA copy number alterations in ovarian serous tumors identifies new molecular genetic changes in low-grade and high-grade carcinomas. *Cancer Res.* 2009;69(9):4036-42.
27. Ryland GL, Hunter SM, Doyle MA, Rowley SM, Christie M, Allan PE, et al. RNF43 is a tumour suppressor gene mutated in mucinous tumours of the ovary. *J Pathol.* 2013;229(3):469-76.
28. Morgan M, Boyd J, Drapkin R, Seiden MV. *Cancer arising in the ovary.* Abeloff's clinical oncology: Elsevier; 2014. p. 1592-613.
29. Kurman RJ, Shih le M. The Dualistic Model of Ovarian Carcinogenesis: Revisited, Revised, and Expanded. *Am J Pathol.* 2016;186(4):733-47.
30. Alsop K, Fereday S, Meldrum C, deFazio A, Emmanuel C, George J, et al. BRCA mutation frequency and patterns of treatment response in BRCA mutation-positive women with ovarian cancer: a report from the Australian Ovarian Cancer Study Group. *J Clin Oncol.* 2012;30(21):2654-63.
31. Kanchi KL, Johnson KJ, Lu C, McLellan MD, Leiserson MD, Wendl MC, et al. Integrated analysis of germline and somatic variants in ovarian cancer. *Nat Commun.* 2014;5:3156.
32. Ledermann J, Harter P, Gourley C, Friedlander M, Vergote I, Rustin G, et al. Olaparib maintenance therapy in platinum-sensitive relapsed ovarian cancer. *N Engl J Med.* 2012;366(15):1382-92.
33. Mirza MR, Monk BJ, Herrstedt J, Oza AM, Mahner S, Redondo A, et al. Niraparib Maintenance Therapy in Platinum-Sensitive, Recurrent Ovarian Cancer. *N Engl J Med.* 2016;375(22):2154-64.
34. Labidi-Galy SI, Olivier T, Rodrigues M, Ferraioli D, Derbel O, Bodmer A, et al. Location of Mutation in BRCA2 Gene and Survival in Patients with Ovarian Cancer. *Clin Cancer Res.* 2018;24(2):326-33.
35. Wooster R, Neuhausen SL, Mangion J, Quirk Y, Ford D, Collins N, et al. Localization of a breast cancer susceptibility gene, BRCA2, to chromosome 13q12-13. *Science.* 1994;265(5181):2088-90.
36. Miki Y, Swensen J, Shattuck-Eidens D, Futreal PA, Harshman K, Tavtigian S, et al. A strong candidate for the breast and ovarian cancer susceptibility gene BRCA1. *Science.* 1994;266(5182):66-71.
37. De Picciotto N, Cacheux W, Roth A, Chappuis PO, Labidi-Galy SI. Ovarian cancer: Status of homologous recombination pathway as a predictor of drug response. *Crit Rev Oncol Hematol.* 2016.
38. Dubeau L, Drapkin R. Coming into focus: the nonovarian origins of ovarian cancer. *Ann Oncol.* 2013;24 Suppl 8:viii28-viii35.
39. Chen EY, Mehra K, Mehrad M, Ning G, Miron A, Mutter GL, et al. Secretory cell outgrowth, PAX2 and serous carcinogenesis in the Fallopian tube. *J Pathol.* 2010;222(1):110-6.
40. Carcangiu ML, Radice P, Manoukian S, Spatti G, Gobbo M, Pensotti V, et al. Atypical epithelial proliferation in fallopian tubes in prophylactic salpingo-oophorectomy specimens from BRCA1 and BRCA2 germline mutation carriers. *Int J Gynecol Pathol.* 2004;23(1):35-40.

41. Kuhn E, Kurman RJ, Vang R, Sehdev AS, Han G, Soslow R, et al. TP53 mutations in serous tubal intraepithelial carcinoma and concurrent pelvic high-grade serous carcinoma--evidence supporting the clonal relationship of the two lesions. *J Pathol.* 2012;226(3):421-6.
42. Nik NN, Vang R, Shih le M, Kurman RJ. Origin and pathogenesis of pelvic (ovarian, tubal, and primary peritoneal) serous carcinoma. *Annu Rev Pathol.* 2014;9:27-45.
43. Przybycin CG, Kurman RJ, Ronnett BM, Shih le M, Vang R. Are all pelvic (nonuterine) serous carcinomas of tubal origin? *Am J Surg Pathol.* 2010;34(10):1407-16.
44. Eckert MA, Pan S, Hernandez KM, Loth RM, Andrade J, Volchenboum SL, et al. Genomics of Ovarian Cancer Progression Reveals Diverse Metastatic Trajectories Including Intraepithelial Metastasis to the Fallopian Tube. *Cancer Discov.* 2016;6(12):1342-51.
45. Prat J. Pathology of borderline and invasive cancers. *Best Pract Res Clin Obstet Gynaecol.* 2017;41:15-30.
46. Kaldawy A, Segev Y, Lavie O, Auslender R, Sopik V, Narod SA. Low-grade serous ovarian cancer: A review. *Gynecol Oncol.* 2016;143(2):433-8.
47. Bonome T, Lee JY, Park DC, Radonovich M, Pise-Masison C, Brady J, et al. Expression profiling of serous low malignant potential, low-grade, and high-grade tumors of the ovary. *Cancer Res.* 2005;65(22):10602-12.
48. Tsang YT, Deavers MT, Sun CC, Kwan SY, Kuo E, Malpica A, et al. KRAS (but not BRAF) mutations in ovarian serous borderline tumour are associated with recurrent low-grade serous carcinoma. *J Pathol.* 2013;231(4):449-56.
49. Dehari R, Kurman RJ, Logani S, Shih le M. The development of high-grade serous carcinoma from atypical proliferative (borderline) serous tumors and low-grade micropapillary serous carcinoma: a morphologic and molecular genetic analysis. *Am J Surg Pathol.* 2007;31(7):1007-12.
50. Plaxe SC. Epidemiology of low-grade serous ovarian cancer. *Am J Obstet Gynecol.* 2008;198(4):459 e1-8; discussion e8-9.
51. Gershenson DM, Bodurka DC, Coleman RL, Lu KH, Malpica A, Sun CC. Hormonal Maintenance Therapy for Women With Low-Grade Serous Cancer of the Ovary or Peritoneum. *J Clin Oncol.* 2017;35(10):1103-11.
52. Bedard PL, Taberner J, Janku F, Wainberg ZA, Paz-Ares L, Vansteenkiste J, et al. A phase Ib dose-escalation study of the oral pan-PI3K inhibitor buparlisib (BKM120) in combination with the oral MEK1/2 inhibitor trametinib (GSK1120212) in patients with selected advanced solid tumors. *Clin Cancer Res.* 2015;21(4):730-8.
53. Bulun SE. Endometriosis. *N Engl J Med.* 2009;360(3):268-79.
54. Van Gorp T, Amant F, Neven P, Vergote I, Moerman P. Endometriosis and the development of malignant tumours of the pelvis. A review of literature. *Best Pract Res Clin Obstet Gynaecol.* 2004;18(2):349-71.
55. Palacios J, Gamallo C. Mutations in the beta-catenin gene (CTNNB1) in endometrioid ovarian carcinomas. *Cancer Res.* 1998;58(7):1344-7.
56. Madore J, Ren F, Filali-Mouhim A, Sanchez L, Kobel M, Tonin PN, et al. Characterization of the molecular differences between ovarian endometrioid carcinoma and ovarian serous carcinoma. *J Pathol.* 2010;220(3):392-400.
57. Grandi G, Toss A, Cortesi L, Botticelli L, Volpe A, Cagnacci A. The Association between Endometriomas and Ovarian Cancer: Preventive Effect of Inhibiting Ovulation and Menstruation during Reproductive Life. *Biomed Res Int.* 2015;2015:751571.
58. Anglesio MS, Bashashati A, Wang YK, Senz J, Ha G, Yang W, et al. Multifocal endometriotic lesions associated with cancer are clonal and carry a high mutation burden. *J Pathol.* 2015;236(2):201-9.
59. Anglesio MS, Papadopoulos N, Ayhan A, Nazeran TM, Noe M, Horlings HM, et al. Cancer-Associated Mutations in Endometriosis without Cancer. *N Engl J Med.* 2017;376(19):1835-48.
60. Bentivegna E, Fruscio R, Roussin S, Ceppi L, Satoh T, Kajiyama H, et al. Long-term follow-up of patients with an isolated ovarian recurrence after conservative treatment of epithelial ovarian cancer: review of the results of an international multicenter study comprising 545 patients. *Fertil Steril.* 2015;104(5):1319-24.



61. Gemignani ML, Schlaerth AC, Bogomolny F, Barakat RR, Lin O, Soslow R, et al. Role of KRAS and BRAF gene mutations in mucinous ovarian carcinoma. *Gynecologic oncology*. 2003;90(2):378-81.
62. O'Connell JT, Hacker CM, Barsky SH. MUC2 is a molecular marker for pseudomyxoma peritonei. *Modern pathology : an official journal of the United States and Canadian Academy of Pathology, Inc.* 2002;15(9):958-72.
63. Wang Y, Shwartz LE, Anderson D, Lin MT, Haley L, Wu RC, et al. Molecular analysis of ovarian mucinous carcinoma reveals different cell of origins. *Oncotarget*. 2015;6(26):22949-58.
64. Kerr SE, Flotte AB, McFalls MJ, Vrana JA, Halling KC, Bell DA. Matching maternal isodisomy in mucinous carcinomas and associated ovarian teratomas provides evidence of germ cell derivation for some mucinous ovarian tumors. *The American journal of surgical pathology*. 2013;37(8):1229-35.
65. Wang Y, Wu RC, Shwartz LE, Haley L, Lin MT, Shih le M, et al. Clonality analysis of combined Brenner and mucinous tumours of the ovary reveals their monoclonal origin. *The Journal of pathology*. 2015;237(2):146-51.
66. Kelemen LE, Kobel M. Mucinous carcinomas of the ovary and colorectum: different organ, same dilemma. *Lancet Oncol*. 2011;12(11):1071-80.
67. Heinzelmann-Schwarz VA, Gardiner-Garden M, Henshall SM, Scurry JP, Scolyer RA, Smith AN, et al. A distinct molecular profile associated with mucinous epithelial ovarian cancer. *Br J Cancer*. 2006;94(6):904-13.
68. Marquez RT, Baggerly KA, Patterson AP, Liu J, Broaddus R, Frumovitz M, et al. Patterns of gene expression in different histotypes of epithelial ovarian cancer correlate with those in normal fallopian tube, endometrium, and colon. *Clin Cancer Res*. 2005;11(17):6116-26.
69. Wamunyokoli FW, Bonome T, Lee JY, Feltmate CM, Welch WR, Radonovich M, et al. Expression profiling of mucinous tumors of the ovary identifies genes of clinicopathologic importance. *Clin Cancer Res*. 2006;12(3 Pt 1):690-700.
70. Gouy S, Saidani M, Maulard A, Bach-Hamba S, Bentivegna E, Leary A, et al. Characteristics and Prognosis of Stage I Ovarian Mucinous Tumors According to Expansile or Infiltrative Type. *Int J Gynecol Cancer*. 2018;28(3):493-9.
71. Wu J, Jiao Y, Dal Molin M, Maitra A, de Wilde RF, Wood LD, et al. Whole-exome sequencing of neoplastic cysts of the pancreas reveals recurrent mutations in components of ubiquitin-dependent pathways. *Proc Natl Acad Sci U S A*. 2011;108(52):21188-93.
72. Crippa S, Salvia R, Warshaw AL, Dominguez I, Bassi C, Falconi M, et al. Mucinous cystic neoplasm of the pancreas is not an aggressive entity: lessons from 163 resected patients. *Ann Surg*. 2008;247(4):571-9.
73. Yamao K, Yanagisawa A, Takahashi K, Kimura W, Doi R, Fukushima N, et al. Clinicopathological features and prognosis of mucinous cystic neoplasm with ovarian-type stroma: a multi-institutional study of the Japan pancreas society. *Pancreas*. 2011;40(1):67-71.
74. Testini M, Gurrado A, Lissidini G, Venezia P, Greco L, Piccinni G. Management of mucinous cystic neoplasms of the pancreas. *World J Gastroenterol*. 2010;16(45):5682-92.
75. Elias KM, Labidi-Galy SI, Vitonis AF, Hornick JL, Doyle LA, Hirsch MS, et al. Prior appendectomy does not protect against subsequent development of malignant or borderline mucinous ovarian neoplasms. *Gynecol Oncol*. 2014;132(2):328-33.
76. Elias KM, Tsantoulis P, Tille JC, Vitonis A, Doyle LA, Hornick JL, et al. Primordial germ cells as a potential shared cell of origin for mucinous cystic neoplasms of the pancreas and mucinous ovarian tumors. *J Pathol*. 2018;246(4):459-69.
77. Fathalla MF. Incessant ovulation and ovarian cancer - a hypothesis re-visited. *Facts Views Vis Obgyn*. 2013;5(4):292-7.
78. Emori MM, Drapkin R. The hormonal composition of follicular fluid and its implications for ovarian cancer pathogenesis. *Reprod Biol Endocrinol*. 2014;12:60.
79. Espey LL. Ovulation as an inflammatory reaction--a hypothesis. *Biol Reprod*. 1980;22(1):73-106.

80. Espey LL, Stein VI, Dumitrescu J. Survey of antiinflammatory agents and related drugs as inhibitors of ovulation in the rabbit. *Fertil Steril*. 1982;38(2):238-47.
81. Duffy DM. Novel contraceptive targets to inhibit ovulation: the prostaglandin E2 pathway. *Hum Reprod Update*. 2015;21(5):652-70.
82. Bachler M, Menshykau D, De Geyter C, Iber D. Species-specific differences in follicular antral sizes result from diffusion-based limitations on the thickness of the granulosa cell layer. *Mol Hum Reprod*. 2014;20(3):208-21.
83. Bahar-Shany K, Brand H, Sapoznik S, Jacob-Hirsch J, Yung Y, Korach J, et al. Exposure of fallopian tube epithelium to follicular fluid mimics carcinogenic changes in precursor lesions of serous papillary carcinoma. *Gynecol Oncol*. 2014;132(2):322-7.
84. de los Santos MJ, Garcia-Laez V, Beltran D, Labarta E, Zuzuarregui JL, Alama P, et al. The follicular hormonal profile in low-responder patients undergoing unstimulated cycles: Is it hypoandrogenic? *Hum Reprod*. 2013;28(1):224-9.
85. Cavalieri E, Frenkel K, Liehr JG, Rogan E, Roy D. Estrogens as endogenous genotoxic agents--DNA adducts and mutations. *J Natl Cancer Inst Monogr*. 2000(27):75-93.
86. Savage KI, Matchett KB, Barros EM, Cooper KM, Irwin GW, Gorski JJ, et al. BRCA1 deficiency exacerbates estrogen-induced DNA damage and genomic instability. *Cancer Res*. 2014;74(10):2773-84.
87. Hall OJ, Limjunyawong N, Vermillion MS, Robinson DP, Wohlgemuth N, Pekosz A, et al. Progesterone-Based Therapy Protects Against Influenza by Promoting Lung Repair and Recovery in Females. *PLoS Pathog*. 2016;12(9):e1005840.
88. Di Renzo GC, Giardina I, Clerici G, Brillo E, Gerli S. Progesterone in normal and pathological pregnancy. *Horm Mol Biol Clin Investig*. 2016;27(1):35-48.
89. Lydon JP, DeMayo FJ, Funk CR, Mani SK, Hughes AR, Montgomery CA, Jr., et al. Mice lacking progesterone receptor exhibit pleiotropic reproductive abnormalities. *Genes Dev*. 1995;9(18):2266-78.
90. Kim J, Bagchi IC, Bagchi MK. Control of ovulation in mice by progesterone receptor-regulated gene networks. *Mol Hum Reprod*. 2009;15(12):821-8.
91. Widschwendter M, Rosenthal AN, Philpott S, Rizzuto I, Fraser L, Hayward J, et al. The sex hormone system in carriers of BRCA1/2 mutations: a case-control study. *Lancet Oncol*. 2013;14(12):1226-32.
92. Nolan E, Vaillant F, Branstetter D, Pal B, Giner G, Whitehead L, et al. RANK ligand as a potential target for breast cancer prevention in BRCA1-mutation carriers. *Nat Med*. 2016;22(8):933-9.
93. Sigl V, Owusu-Boaitey K, Joshi PA, Kavirayani A, Wirnsberger G, Novatchkova M, et al. RANKL/RANK control Brca1 mutation-driven mammary tumors. *Cell Res*. 2016;26(7):761-74.
94. Brisken C, Hess K, Jeitziner R. Progesterone and Overlooked Endocrine Pathways in Breast Cancer Pathogenesis. *Endocrinology*. 2015;156(10):3442-50.
95. Tone AA, Begley H, Sharma M, Murphy J, Rosen B, Brown TJ, et al. Gene expression profiles of luteal phase fallopian tube epithelium from BRCA mutation carriers resemble high-grade serous carcinoma. *Clin Cancer Res*. 2008;14(13):4067-78.
96. George SH, Milea A, Shaw PA. Proliferation in the normal FTE is a hallmark of the follicular phase, not BRCA mutation status. *Clin Cancer Res*. 2012;18(22):6199-207.
97. Tone AA, Virtanen C, Shaw P, Brown TJ. Prolonged postovulatory proinflammatory signaling in the fallopian tube epithelium may be mediated through a BRCA1/DAB2 axis. *Clin Cancer Res*. 2012;18(16):4334-44.
98. Risch HA, Marrett LD, Howe GR. Parity, contraception, infertility, and the risk of epithelial ovarian cancer. *Am J Epidemiol*. 1994;140(7):585-97.
99. Booth M, Beral V, Smith P. Risk factors for ovarian cancer: a case-control study. *Br J Cancer*. 1989;60(4):592-8.
100. Gwinn ML, Lee NC, Rhodes PH, Layde PM, Rubin GL. Pregnancy, breast feeding, and oral contraceptives and the risk of epithelial ovarian cancer. *J Clin Epidemiol*. 1990;43(6):559-68.

101. Collaborative Group on Epidemiological Studies of Ovarian C, Beral V, Doll R, Hermon C, Peto R, Reeves G. Ovarian cancer and oral contraceptives: collaborative reanalysis of data from 45 epidemiological studies including 23,257 women with ovarian cancer and 87,303 controls. *Lancet*. 2008;371(9609):303-14.
102. Whittemore AS, Harris R, Itnyre J. Characteristics relating to ovarian cancer risk: collaborative analysis of 12 US case-control studies. II. Invasive epithelial ovarian cancers in white women. Collaborative Ovarian Cancer Group. *Am J Epidemiol*. 1992;136(10):1184-203.
103. Bodelon C, Wentzensen N, Schonfeld SJ, Visvanathan K, Hartge P, Park Y, et al. Hormonal risk factors and invasive epithelial ovarian cancer risk by parity. *Br J Cancer*. 2013;109(3):769-76.
104. Wentzensen N, Poole EM, Trabert B, White E, Arslan AA, Patel AV, et al. Ovarian Cancer Risk Factors by Histologic Subtype: An Analysis From the Ovarian Cancer Cohort Consortium. *J Clin Oncol*. 2016;34(24):2888-98.
105. Jordan SJ, Siskind V, A CG, Whiteman DC, Webb PM. Breastfeeding and risk of epithelial ovarian cancer. *Cancer Causes Control*. 2010;21(1):109-16.
106. Titus-Ernstoff L, Rees JR, Terry KL, Cramer DW. Breast-feeding the last born child and risk of ovarian cancer. *Cancer Causes Control*. 2010;21(2):201-7.
107. Luan NN, Wu QJ, Gong TT, Vogtmann E, Wang YL, Lin B. Breastfeeding and ovarian cancer risk: a meta-analysis of epidemiologic studies. *Am J Clin Nutr*. 2013;98(4):1020-31.
108. Jordan SJ, Cushing-Haugen KL, Wicklund KG, Doherty JA, Rossing MA. Breast-feeding and risk of epithelial ovarian cancer. *Cancer Causes Control*. 2012;23(6):919-27.
109. Havrilesky LJ, Moorman PG, Lowery WJ, Gierisch JM, Coeytaux RR, Urrutia RP, et al. Oral contraceptive pills as primary prevention for ovarian cancer: a systematic review and meta-analysis. *Obstet Gynecol*. 2013;122(1):139-47.
110. Doufekas K, Olaitan A. Clinical epidemiology of epithelial ovarian cancer in the UK. *Int J Womens Health*. 2014;6:537-45.
111. McLaughlin JR, Risch HA, Lubinski J, Moller P, Ghadirian P, Lynch H, et al. Reproductive risk factors for ovarian cancer in carriers of BRCA1 or BRCA2 mutations: a case-control study. *Lancet Oncol*. 2007;8(1):26-34.
112. Modan B, Hartge P, Hirsh-Yechezkel G, Chetrit A, Lubin F, Beller U, et al. Parity, oral contraceptives, and the risk of ovarian cancer among carriers and noncarriers of a BRCA1 or BRCA2 mutation. *N Engl J Med*. 2001;345(4):235-40.
113. Friebel TM, Domchek SM, Rebbeck TR. Modifiers of cancer risk in BRCA1 and BRCA2 mutation carriers: systematic review and meta-analysis. *J Natl Cancer Inst*. 2014;106(6):dju091.
114. Kotsopoulos J, Lubinski J, Gronwald J, Cybulski C, Demsky R, Neuhausen SL, et al. Factors influencing ovulation and the risk of ovarian cancer in BRCA1 and BRCA2 mutation carriers. *Int J Cancer*. 2014.
115. Lacey JV, Jr., Brinton LA, Leitzmann MF, Mouw T, Hollenbeck A, Schatzkin A, et al. Menopausal hormone therapy and ovarian cancer risk in the National Institutes of Health-AARP Diet and Health Study Cohort. *J Natl Cancer Inst*. 2006;98(19):1397-405.
116. Trabert B, Wentzensen N, Yang HP, Sherman ME, Hollenbeck A, Danforth KN, et al. Ovarian cancer and menopausal hormone therapy in the NIH-AARP diet and health study. *Br J Cancer*. 2012;107(7):1181-7.
117. Riman T, Dickman PW, Nilsson S, Correia N, Nordlinder H, Magnusson CM, et al. Hormone replacement therapy and the risk of invasive epithelial ovarian cancer in Swedish women. *J Natl Cancer Inst*. 2002;94(7):497-504.
118. Yang HP, Anderson WF, Rosenberg PS, Trabert B, Gierach GL, Wentzensen N, et al. Ovarian cancer incidence trends in relation to changing patterns of menopausal hormone therapy use in the United States. *J Clin Oncol*. 2013;31(17):2146-51.
119. Rizzuto I, Behrens RF, Smith LA. Risk of ovarian cancer in women treated with ovarian stimulating drugs for infertility. *Cochrane Database Syst Rev*. 2013;8:CD008215.
120. Stewart LM, Holman CD, Finn JC, Preen DB, Hart R. In vitro fertilization is associated with an increased risk of borderline ovarian tumours. *Gynecol Oncol*. 2013;129(2):372-6.

121. Bjornholt SM, Kjaer SK, Nielsen TS, Jensen A. Risk for borderline ovarian tumours after exposure to fertility drugs: results of a population-based cohort study. *Hum Reprod.* 2015;30(1):222-31.
122. Choi JH, Wong AS, Huang HF, Leung PC. Gonadotropins and ovarian cancer. *Endocr Rev.* 2007;28(4):440-61.
123. Simoni M, Gromoll J, Nieschlag E. The follicle-stimulating hormone receptor: biochemistry, molecular biology, physiology, and pathophysiology. *Endocr Rev.* 1997;18(6):739-73.
124. Mandai M, Konishi I, Kuroda H, Fukumoto M, Komatsu T, Yamamoto S, et al. Messenger ribonucleic acid expression of LH/hCG receptor gene in human ovarian carcinomas. *Eur J Cancer.* 1997;33(9):1501-7.
125. Chu S, Rushdi S, Zumpfe ET, Mamers P, Healy DL, Jobling T, et al. FSH-regulated gene expression profiles in ovarian tumours and normal ovaries. *Mol Hum Reprod.* 2002;8(5):426-33.
126. Wang J, Lin L, Parkash V, Schwartz PE, Lauchlan SC, Zheng W. Quantitative analysis of follicle-stimulating hormone receptor in ovarian epithelial tumors: a novel approach to explain the field effect of ovarian cancer development in secondary mullerian systems. *Int J Cancer.* 2003;103(3):328-34.
127. Feng Z, Wen H, Ju X, Bi R, Chen X, Yang W, et al. Expression of hypothalamic-pituitary-gonadal axis-related hormone receptors in low-grade serous ovarian cancer (LGSC). *J Ovarian Res.* 2017;10(1):7.
128. Chen X, Aravindakshan J, Yang Y, Sairam MR. Early alterations in ovarian surface epithelial cells and induction of ovarian epithelial tumors triggered by loss of FSH receptor. *Neoplasia.* 2007;9(6):521-31.
129. Danilovich N, Roy I, Sairam MR. Ovarian pathology and high incidence of sex cord tumors in follitropin receptor knockout (FORKO) mice. *Endocrinology.* 2001;142(8):3673-84.
130. Chen T, Surcel HM, Lundin E, Kaasila M, Lakso HA, Schock H, et al. Circulating sex steroids during pregnancy and maternal risk of non-epithelial ovarian cancer. *Cancer Epidemiol Biomarkers Prev.* 2011;20(2):324-36.
131. Schock H, Surcel HM, Zeleniuch-Jacquotte A, Grankvist K, Lakso HA, Fortner RT, et al. Early pregnancy sex steroids and maternal risk of epithelial ovarian cancer. *Endocr Relat Cancer.* 2014;21(6):831-44.
132. Barthelmeß EK, Naz RK. Polycystic ovary syndrome: current status and future perspective. *Front Biosci (Elite Ed).* 2014;6:104-19.
133. Harris HR, Terry KL. Polycystic ovary syndrome and risk of endometrial, ovarian, and breast cancer: a systematic review. *Fertil Res Pract.* 2016;2:14.
134. Harris HR, Babic A, Webb PM, Nagle CM, Jordan SJ, Risch HA, et al. Polycystic Ovary Syndrome, Oligomenorrhea, and Risk of Ovarian Cancer Histotypes: Evidence from the Ovarian Cancer Association Consortium. *Cancer Epidemiol Biomarkers Prev.* 2018;27(2):174-82.
135. Makanji Y, Zhu J, Mishra R, Holmquist C, Wong WP, Schwartz NB, et al. Inhibin at 90: from discovery to clinical application, a historical review. *Endocr Rev.* 2014;35(5):747-94.
136. Tournier I, Marlin R, Walton K, Charbonnier F, Coutant S, Thery JC, et al. Germline mutations of inhibins in early-onset ovarian epithelial tumors. *Hum Mutat.* 2014;35(3):294-7.
137. Matzuk MM, Finegold MJ, Su JG, Hsueh AJ, Bradley A. Alpha-inhibin is a tumour-suppressor gene with gonadal specificity in mice. *Nature.* 1992;360(6402):313-9.
138. Kumar TR, Wang Y, Matzuk MM. Gonadotropins are essential modifier factors for gonadal tumor development in inhibin-deficient mice. *Endocrinology.* 1996;137(10):4210-6.
139. Kumar TR, Palapattu G, Wang P, Woodruff TK, Boime I, Byrne MC, et al. Transgenic models to study gonadotropin function: the role of follicle-stimulating hormone in gonadal growth and tumorigenesis. *Mol Endocrinol.* 1999;13(6):851-65.
140. Nagaraja AK, Agno JE, Kumar TR, Matzuk MM. Luteinizing hormone promotes gonadal tumorigenesis in inhibin-deficient mice. *Mol Cell Endocrinol.* 2008;294(1-2):19-28.
141. Willemssen W, Kruitwagen R, Bastiaans B, Hanselaar T, Rolland R. Ovarian stimulation and granulosa-cell tumour. *Lancet.* 1993;341(8851):986-8.

142. Rossing MA, Daling JR, Weiss NS, Moore DE, Self SG. Ovarian tumors in a cohort of infertile women. *N Engl J Med.* 1994;331(12):771-6.
143. Chakravarti S, Collins WP, Forecast JD, Newton JR, Oram DH, Studd JW. Hormonal profiles after the menopause. *Br Med J.* 1976;2(6039):784-7.
144. Cramer DW, Xu H. Epidemiologic evidence for uterine growth factors in the pathogenesis of ovarian cancer. *Ann Epidemiol.* 1995;5(4):310-4.
145. Halme J, Hammond MG, Hulka JF, Raj SG, Talbert LM. Retrograde menstruation in healthy women and in patients with endometriosis. *Obstet Gynecol.* 1984;64(2):151-4.
146. Vercellini P, Vigano P, Somigliana E, Fedele L. Endometriosis: pathogenesis and treatment. *Nat Rev Endocrinol.* 2014;10(5):261-75.
147. Giudice LC. Clinical practice. Endometriosis. *N Engl J Med.* 2010;362(25):2389-98.
148. Lee WL, Chang WH, Wang KC, Guo CY, Chou YJ, Huang N, et al. The Risk of Epithelial Ovarian Cancer of Women With Endometriosis May be Varied Greatly if Diagnostic Criteria Are Different: A Nationwide Population-Based Cohort Study. *Medicine (Baltimore).* 2015;94(39):e1633.
149. Muzii L, Di Tucci C, Achilli C, Di Donato V, Musella A, Palaia I, et al. Continuous versus cyclic oral contraceptives after laparoscopic excision of ovarian endometriomas: a systematic review and metaanalysis. *Am J Obstet Gynecol.* 2016;214(2):203-11.
150. Modugno F, Ness RB, Allen GO, Schildkraut JM, Davis FG, Goodman MT. Oral contraceptive use, reproductive history, and risk of epithelial ovarian cancer in women with and without endometriosis. *Am J Obstet Gynecol.* 2004;191(3):733-40.
151. Pearce CL, Templeman C, Rossing MA, Lee A, Near AM, Webb PM, et al. Association between endometriosis and risk of histological subtypes of ovarian cancer: a pooled analysis of case-control studies. *Lancet Oncol.* 2012;13(4):385-94.
152. Kurman RJ, Shih Ie M. Seromucinous Tumors of the Ovary. What's in a Name? *Int J Gynecol Pathol.* 2016;35(1):78-81.
153. King CM, Barbara C, Prentice A, Brenton JD, Charnock-Jones DS. Models of endometriosis and their utility in studying progression to ovarian clear cell carcinoma. *J Pathol.* 2016;238(2):185-96.
154. Oral E, Olive DL, Arici A. The peritoneal environment in endometriosis. *Hum Reprod Update.* 1996;2(5):385-98.
155. Giudice LC, Kao LC. Endometriosis. *Lancet.* 2004;364(9447):1789-99.
156. Lebovic DI, Mueller MD, Taylor RN. Immunobiology of endometriosis. *Fertil Steril.* 2001;75(1):1-10.
157. Purdie D, Green A, Bain C, Siskind V, Ward B, Hacker N, et al. Reproductive and other factors and risk of epithelial ovarian cancer: an Australian case-control study. Survey of Women's Health Study Group. *Int J Cancer.* 1995;62(6):678-84.
158. Cornelison TL, Natarajan N, Piver MS, Mettlin CJ. Tubal ligation and the risk of ovarian carcinoma. *Cancer Detect Prev.* 1997;21(1):1-6.
159. Falconer H, Yin L, Gronberg H, Altman D. Ovarian cancer risk after salpingectomy: a nationwide population-based study. *J Natl Cancer Inst.* 2015;107(2).
160. Sieh W, Salvador S, McGuire V, Weber RP, Terry KL, Rossing MA, et al. Tubal ligation and risk of ovarian cancer subtypes: a pooled analysis of case-control studies. *Int J Epidemiol.* 2013;42(2):579-89.
161. Rice MS, Hankinson SE, Tworoger SS. Tubal ligation, hysterectomy, unilateral oophorectomy, and risk of ovarian cancer in the Nurses' Health Studies. *Fertil Steril.* 2014;102(1):192-8 e3.
162. Karst AM, Drapkin R. Ovarian cancer pathogenesis: a model in evolution. *J Oncol.* 2010;2010:932371.
163. Levanon K, Crum C, Drapkin R. New insights into the pathogenesis of serous ovarian cancer and its clinical impact. *J Clin Oncol.* 2008;26(32):5284-93.
164. Bowtell DD, Bohm S, Ahmed AA, Aspuria PJ, Bast RC, Jr., Beral V, et al. Rethinking ovarian cancer II: reducing mortality from high-grade serous ovarian cancer. *Nat Rev Cancer.* 2015;15(11):668-79.

165. Vuilleumier A, Labidi-Galy I. [Screening of ovarian cancer : not for tomorrow]. *Rev Med Suisse*. 2017;13(563):1039-41.
166. Crum CP, Herfs M, Ning G, Bijron JG, Howitt BE, Jimenez CA, et al. Through the glass darkly: intraepithelial neoplasia, top-down differentiation, and the road to ovarian cancer. *J Pathol*. 2013;231(4):402-12.
167. McPherson A, Roth A, Laks E, Masud T, Bashashati A, Zhang AW, et al. Divergent modes of clonal spread and intraperitoneal mixing in high-grade serous ovarian cancer. *Nat Genet*. 2016;48(7):758-67.
168. Bashashati A, Ha G, Tone A, Ding J, Prentice LM, Roth A, et al. Distinct evolutionary trajectories of primary high-grade serous ovarian cancers revealed through spatial mutational profiling. *J Pathol*. 2013;231(1):21-34.
169. McDaniel AS, Stall JN, Hovelson DH, Cani AK, Liu CJ, Tomlins SA, et al. Next-Generation Sequencing of Tubal Intraepithelial Carcinomas. *JAMA Oncol*. 2015;1(8):1128-32.
170. Conner JR, Meserve E, Pizer E, Garber J, Roh M, Urban N, et al. Outcome of unexpected adnexal neoplasia discovered during risk reduction salpingo-oophorectomy in women with germ-line BRCA1 or BRCA2 mutations. *Gynecologic oncology*. 2014;132(2):280-6.
171. Gupta KK, Gupta VK, Naumann RW. Ovarian cancer: screening and future directions. *Int J Gynecol Cancer*. 2019;29(1):195-200.
172. Buys SS, Partridge E, Black A, Johnson CC, Lamerato L, Isaacs C, et al. Effect of screening on ovarian cancer mortality: the Prostate, Lung, Colorectal and Ovarian (PLCO) Cancer Screening Randomized Controlled Trial. *JAMA*. 2011;305(22):2295-303.
173. Jacobs IJ, Menon U, Ryan A, Gentry-Maharaj A, Burnell M, Kalsi JK, et al. Ovarian cancer screening and mortality in the UK Collaborative Trial of Ovarian Cancer Screening (UKCTOCS): a randomised controlled trial. *Lancet*. 2016;387(10022):945-56.
174. Force USPST, Grossman DC, Curry SJ, Owens DK, Barry MJ, Davidson KW, et al. Screening for Ovarian Cancer: US Preventive Services Task Force Recommendation Statement. *JAMA*. 2018;319(6):588-94.
175. Srivastava S, Koay EJ, Borowsky AD, De Marzo AM, Ghosh S, Wagner PD, et al. Cancer overdiagnosis: a biological challenge and clinical dilemma. *Nat Rev Cancer*. 2019.
176. Bos JL, Fearon ER, Hamilton SR, Verlaan-de Vries M, van Boom JH, van der Eb AJ, et al. Prevalence of ras gene mutations in human colorectal cancers. *Nature*. 1987;327(6120):293-7.
177. Fearon ER, Hamilton SR, Vogelstein B. Clonal analysis of human colorectal tumors. *Science*. 1987;238(4824):193-7.
178. Nishihara R, Wu K, Lochhead P, Morikawa T, Liao X, Qian ZR, et al. Long-term colorectal-cancer incidence and mortality after lower endoscopy. *N Engl J Med*. 2013;369(12):1095-105.
179. Landy R, Pesola F, Castanon A, Sasieni P. Impact of cervical screening on cervical cancer mortality: estimation using stage-specific results from a nested case-control study. *Br J Cancer*. 2016;115(9):1140-6.
180. Naucler P, Ryd W, Tornberg S, Strand A, Wadell G, Elfgren K, et al. Human papillomavirus and Papanicolaou tests to screen for cervical cancer. *N Engl J Med*. 2007;357(16):1589-97.
181. Trabert B, Coburn SB, Mariani A, Yang HP, Rosenberg PS, Gierach GL, et al. Reported Incidence and Survival of Fallopian Tube Carcinomas: A Population-Based Analysis From the North American Association of Central Cancer Registries. *J Natl Cancer Inst*. 2018;110(7):750-7.
182. Serati M, Siesto G, Carollo S, Formenti G, Riva C, Cromi A, et al. Risk factors for cervical intraepithelial neoplasia recurrence after conization: a 10-year study. *Eur J Obstet Gynecol Reprod Biol*. 2012;165(1):86-90.
183. Chui MH, Vang R, Wang TL, Shih IM, VandenBussche CJ. Cytomorphologic and molecular analyses of fallopian tube fimbrial brushings for diagnosis of serous tubal intraepithelial carcinoma. *Cancer Cytopathol*. 2019;127(3):192-201.

184. Gordts S, Campo R, Bogers JP, Tanos V, Segaeert I, Valkenburg M, et al. Transvaginal laparoscopy: A minimally invasive approach to obtain brush cytology of the Fallopian tube. *Eur J Obstet Gynecol Reprod Biol.* 2017;212:80-4.
185. Cohen JD, Li L, Wang Y, Thoburn C, Afsari B, Danilova L, et al. Detection and localization of surgically resectable cancers with a multi-analyte blood test. *Science.* 2018;359(6378):926-30.
186. Cristiano S, Leal A, Phallen J, Fiksel J, Adleff V, Bruhm DC, et al. Genome-wide cell-free DNA fragmentation in patients with cancer. *Nature.* 2019.
187. Maritschnegg E, Wang Y, Pecha N, Horvat R, Van Nieuwenhuysen E, Vergote I, et al. Lavage of the Uterine Cavity for Molecular Detection of Mullerian Duct Carcinomas: A Proof-of-Concept Study. *J Clin Oncol.* 2015;33(36):4293-300.
188. Kauff ND, Satagopan JM, Robson ME, Scheuer L, Hensley M, Hudis CA, et al. Risk-reducing salpingo-oophorectomy in women with a BRCA1 or BRCA2 mutation. *N Engl J Med.* 2002;346(21):1609-15.
189. Kauff ND, Domchek SM, Friebel TM, Robson ME, Lee J, Garber JE, et al. Risk-reducing salpingo-oophorectomy for the prevention of BRCA1- and BRCA2-associated breast and gynecologic cancer: a multicenter, prospective study. *J Clin Oncol.* 2008;26(8):1331-7.
190. Litton JK, Ready K, Chen H, Gutierrez-Barrera A, Etzel CJ, Meric-Bernstam F, et al. Earlier age of onset of BRCA mutation-related cancers in subsequent generations. *Cancer.* 2012;118(2):321-5.
191. King MC, Marks JH, Mandell JB, New York Breast Cancer Study G. Breast and ovarian cancer risks due to inherited mutations in BRCA1 and BRCA2. *Science.* 2003;302(5645):643-6.
192. Sherman SL, Jacobs PA, Morton NE, Froster-Iskenius U, Howard-Peebles PN, Nielsen KB, et al. Further segregation analysis of the fragile X syndrome with special reference to transmitting males. *Hum Genet.* 1985;69(4):289-99.
193. Verkerk AJ, Pieretti M, Sutcliffe JS, Fu YH, Kuhl DP, Pizzuti A, et al. Identification of a gene (FMR-1) containing a CGG repeat coincident with a breakpoint cluster region exhibiting length variation in fragile X syndrome. *Cell.* 1991;65(5):905-14.
194. Noh JM, Choi DH, Baek H, Kim MJ, Park H, Huh SJ, et al. Genetic anticipation of familial breast cancer with or without BRCA mutation in the Korean population. *Cancer Genet.* 2014;207(4):160-3.
195. Practice Bulletin No. 182 Summary: Hereditary Breast and Ovarian Cancer Syndrome. *Obstet Gynecol.* 2017;130(3):657-9.
196. Kobel M, Kalloger SE, Huntsman DG, Santos JL, Swenerton KD, Seidman JD, et al. Differences in tumor type in low-stage versus high-stage ovarian carcinomas. *Int J Gynecol Pathol.* 2010;29(3):203-11.
197. Morice P, Gouy S, Leary A. Mucinous Ovarian Carcinoma. *N Engl J Med.* 2019;380(13):1256-66.
198. Mackay HJ, Brady MF, Oza AM, Reuss A, Pujade-Lauraine E, Swart AM, et al. Prognostic relevance of uncommon ovarian histology in women with stage III/IV epithelial ovarian cancer. *Int J Gynecol Cancer.* 2010;20(6):945-52.
199. Matulonis UA, Shapira-Frommer R, Santin AD, Lisyanskaya AS, Pignata S, Vergote I, et al. Antitumor Activity and Safety of Pembrolizumab in Patients with Advanced Recurrent Ovarian Cancer: Results from the Phase 2 KEYNOTE-100 Study. *Ann Oncol.* 2019.
200. Chu PG, Chung L, Weiss LM, Lau SK. Determining the site of origin of mucinous adenocarcinoma: an immunohistochemical study of 175 cases. *Am J Surg Pathol.* 2011;35(12):1830-6.
201. Suzuki Y, Sugiyama M, Abe N, Fujioka Y, Atomi Y. Immunohistochemical similarities between pancreatic mucinous cystic tumor and ovarian mucinous cystic tumor. *Pancreas.* 2008;36(1):e40-6.
202. Ricci F, Affatato R, Carrassa L, Damia G. Recent Insights into Mucinous Ovarian Carcinoma. *Int J Mol Sci.* 2018;19(6).

203. Budani MC, Tiboni GM. Ovotoxicity of cigarette smoke: A systematic review of the literature. *Reprod Toxicol.* 2017;72:164-81.
204. Akinwunmi B, Vitonis AF, Titus L, Terry KL, Cramer DW. Statin therapy and association with ovarian cancer risk in the New England Case Control (NEC) study. *Int J Cancer.* 2019;144(5):991-1000.